POST-MIOCENE DEFORMATION OF THE AREA BETWEEN ALİBEY (KIZILCAHAMAM) AND KARALAR (KAZAN) VILLAGES, NW ANKARA (TURKEY)

A THESIS SUBMITTED TO
THE GRADUATE SCHOOL OF NATURAL AND APPLIED SCIENCES
OF
MIDDLE EAST TECHNICAL UNIVERSITY

BY

AYKUT KARACA

IN PARTIAL FULFILLMENT OF THE REQUIREMENTS
FOR
THE DEGREE OF MASTER OF SCIENCE

IN

GEOLOGICAL ENGINEERING

SEPTEMBER 2004

Approval of the Graduate School of Natural and Applied Sciences

Prof. Dr. Canan ÖZGEN
Director

I certify that this thesis satisfies all the requirements as a thesis for the degree of Master of Science.

Prof. Dr. Asuman G. TÜRKMENOĞLU
Head of Department

This is to certify that we have read this thesis and that in our opinion it is fully adequate, in scope and quality, as a thesis for the degree of Master of Science.

Assoc. Prof. Dr. Bora ROJAY
Supervisor

Examining Committee Members (first name belongs to the chairperson of the jury and the second name belongs to supervisor)

Prof. Dr. Vedat TOPRAK	(METU, GEOE)	
Prof. Dr. Erdin BOZKURT	(METU, GEOE)	
Assoc. Prof. Dr. Kadir DİRİK	(HU, GEOE)	
Assoc. Prof. Dr. Bora ROJAY	(METU, GEOE)	
Asst. Prof. Dr. İ. Ömer YILMAZ	(METU, GEOE)	

I hereby declare that all information in this document has been obtained and presented in accordance with academic rules and ethical conduct. I also declare that, as required by these rules and conduct, I have fully cited and referenced all material and results that are not original to this work.

Name, Last name : Aykut Karaca

Signature :

ABSTRACT

POST-MIOCENE DEFORMATION OF THE AREA BETWEEN
ALİBEY (KIZILCAHAMAM) AND KARALAR (KAZAN) VILLAGES,
NW ANKARA (TURKEY)

Karaca, Aykut
M.Sc., Department of Geological Engineering
Supervisor: Assoc. Prof. Dr. Bora Rojay

September 2004, 100 pages

The study area is located within the Neogene-Quaternary sequences on top of the Mesozoic accreted mass at the northwest of Kazan (40 km NW of Ankara) between Karalar and Alibey villages. The research deals with the post-Miocene deformational history of an area situated at the southern edge of Galatian Volcanic Province.

Two main Neogene rock sequences are cropped out; 1) Late Miocene Pazar Formation, 2) Plio-Quaternary Sinap Formation. The Pazar Formation has a succession composed mainly of clastics at the bottom and, cherts and limestones to the top of the sequence representing a fresh water lake environment. Sedimentation seems to be affected by the intense volcanism going on in the Galatian Volcanic Province. Location of a mammalian fossil found in the Pazar Formation yielded a possible time interval between MN-9 to MN-13 (Middle to Late Miocene). Sinap Formation overlies the Pazar Formation unconformably and it is dominantly represented by fluvial clastics.

The post-Miocene deformational studies based on the analysis of the structural data collected from bedding planes and fault planes. Totally 213 dip-strike measurements from the Neogene units and 204 slip lineation data from the fault planes were taken. Fold analysis of dip and strike measurements taken from the Pazar Formation gave a common fold axis trending in N43^{0}E direction. Similarly fold analysis for the Sinap Formation resulted N40^{0}E striking trend for the fold axis. Stress analysis was performed by processing slip lineation data using Angelier direct inversion method. In the analysis, no reliable results for the post-Miocene compressional phase could be obtained. But the results of the post-Plio-Quaternary extensional regime are strongly reliable. It clearly gives an extension in NW-SE direction.

Stress analysis together with the field observations show that the area has been structurally evolved in several phases of deformation. The NW-SE to N-S-directed post-Miocene compressional event is followed by a regional extension operating since Plio-Quaternary.

Keywords: Galatian, paleo-stress analysis, neotectonics.

ÖZ

ALİBEY (KIZILCAHAMAM) VE KARALAR (KAZAN) KÖYLERİ ARASINDAKİ BÖLGENİN MİYOSEN SONRASI DEFORMASYONU KB ANKARA (TÜRKİYE)

Karaca, Aykut
Y.Lisans, Jeoloji Mühendisliği Bölümü
Tez Yöneticisi: Doç. Dr. Bora Rojay

Eylül 2004, 100 sayfa

Çalışma alanı Kazan ilçesinin kuzeybatısında (Ankara’nın 40 km kuzeybatısı), Karalar ve Alibey köyleri arasında Mezozoik yığışım kütlesi üzerinde gelişen Neojen-Kuvaterner birimleri içerisinde yeralmaktadır. Bu araştırma Galatyan Volkanik Bölgesinin güney kenarındaki bu alanın Miyosen sonrası deformasyon tarihçesini incelemektedir.

Alanda iki ana Neojen kaya birimi yüzeylenmektedir; (1) Geç Miyosen Pazar Formasyonu; (2) Pliyosen-Kuvaterner Sinap Formasyonu. Pazar Formasyonu tatlı su gölsel ortamı temsil eden, altta kalstikler ve üstte çört ve kireçtaşlarından oluşan bir kayaç serisine sahiptir. Ortamdaki sedimentasyonun Galatyan Volkanik Bölgesinde gelişen volkanizmadan yoğun bir şekilde etkilendiği görülmektedir. Pazar Formasyonu içinde bulunan memeli fosilinin lokasyonu muhtemel MN-9 ile MN-13 (Orta-Geç Miyosen) zamanları arasında bir yaş vermiştir. Alanda ana olarak akarsu sistemi klastik kayaçlarla temsil edilen Sinap Formasyonu, Pazar Formasyonunu uyumsuzluk ile örtmektedir.

Miyosen sonrası deformasyonu çalışmaları tabakalardan ve fay düzlemlerinden toplanan yapısal verileri temel almaktadır. Toplam olarak Neojen yaşlı birimlerden 213 adet doğrultu-eğim ölçümü ve faylarda 204 adet kayma (slip) lineasyon verisi toplanmıştır. Pazar Formasyonundan alınan doğrultu eğim ölçümleri ile yapılan kıvrım analizi, N43^{0}E yönünde doğrultusu olan bir kıvrım ekseninin varlığını ortaya koymuştur. Benzer şekilde Sinap Formasyonu için yürütülen kıvrım analizi, N40^{0}E yönünde bir kıvrım ekseni vermiştir. Slip lineasyon verilerinin Angelier'in "direct inversion" metodu ile işlenerek stres analizi yürütülmüştür. Yapılan analiz sonucunda Miyosen sonrası sıkışma evresi ile ilgili güvenilir sonuçlar elde edilememiştir. Fakat Pliyo-Kuvaterner sonrası gerilme ile ilgili olarak bulunan sonuçlar oldukça güvenilirdir. Sonuçlar açıkça KB-GD yönünde bir gerilme evresi vermiştir.

Yapılan stres analizi ve arazi çalışmaları alanın birkaç evrede yapısal olarak geliştiğini ortaya koymuştur. Miyosen sonrası KB-GD – K-G yönündeki sıkışma tektoniğini Pliyo-Kuvaterner' den başlayarak bir gerilme evresi izlemiştir.

Anahtar sözcükler: Galatyan , Paleo-stres analizi, neotektonik.

To my niece Merve,

ACKNOWLEDGMENTS

First of all, I would like to express my gratitude to my supervisor Bora Rojay for his clear guidance, valuable criticism and continuous support during every stage of this thesis. Without any hesitation, he shared his vast geological knowledge with me generously. His friendly and humorous manner towards me always encouraged me to complete this study.

Secondly I would like to express my highest gratitude to my family. Every member in my family showed extreme patience and gave unlimited encouragement during this study. Mom, thanks for bringing my meal to my desk when I was working on the thesis.

I would like to express that I am grateful to my boss Cengiz Y. Demirci for his support on the processing of the slip data by using the TENSOR software. His continuous encouragement and high degree of tolerance made this study possible.

I am indebted to my collogues in the company, Atilla Ömerbeyoğlu, Mert Ertuğrul and Burcu Öztürk for their help in my office studies about the thesis and for their continuous support. I must not forget to thank the summer student Kerem Atik for entering the data on the computer for me.

I would also like to thank Nuretdin Kaymakçı for his help and comments on the age of the mammalian fossil that is found in the study area.

I would like to thank Baki Varol for making the petrographical analysis for the study. His results and comments added a new insight to the interpretations.

Lastly, I would like to thank the company I work for, Rio Tinto, for the financial support and letting me to conduct this study and to reserve some of my time.

“*One’s ideas must be as broad as Nature if they are to interpret Nature”*

Sir Arthur Conan Doyle

(*From his novel,* Sherlock Holmes – A Study in Scarlet**)**

TABLE OF CONTENTS

LIST OF FIGURES

LIST OF TABLES

LIST OF PLATES

CHAPTER 1

INTRODUCTION

1.1. Purpose and Scope

The selected area is a part of geologically important terrain which is one of the major volcanic provinces of Turkey, Galatian volcanic province, where important geological and tectonic events were recorded in the complex tectonic history of Anatolia. Neogene units cover spatially extensive areas at the north and northwest of Ankara closely associated with the Galatian volcanics. Those units, whose stratigraphy has been subject of many previous tectonostratigraphic researches, are intensely deformed during post-Miocene tectonism.

The area is located within an economically important terrain as well since it is surrounded by economical mineral deposits, namely, Kazan trona deposit at south, Beypazarı trona deposit and Çayırhan coal deposit at southwest, and Çeltikçi coal deposit at northwest. Another reason to choose such an area is the good control in the stratigraphy. Radiometrically well-dated volcanism and associated paleontologically well-dated stratigraphic sequences will ease the analysis on the deformation history. Collectively, the area chosen for the subject of this thesis is situated within a geologically and economically important region where the stratigraphy is already set.

Therefore this thesis aims to analyze the deformational structures developed during post-Miocene – Quaternary period in an area between Çeltikçi and

Kazan (NW of Ankara). For this purpose, i) the stratigraphy of the area was studied to differentiate the unconformities and depositional settings, and ii) structural data (strike/dip measurements of the beddings and faults, and slip-lineation data from the fault planes) were collected for structural analysis.

1.2. Geographic Location

The thesis carried out in an area between Çeltikçi and Kazan districts of Ankara province, where extensive Neogene units are exposed. It is an area trending in southeast to northwest direction and covers an area of 62 km^2 (Figure 1.1 and Figure 1.2). It is located at 40 km northwest of Ankara province, 13 km southeast of Çeltikçi and 9 km northwest of Kazan. More specifically, the study area is limited by Alibey village at the northwest and Karalar village at the southeast where Ankara-Bolu-İstanbul highway (TEM-E80) cross-cuts the study area. The study area is included within the 1:25000-scale topographic H29-D1 and H29-A4 sheets.

1.3. Previous Studies

There are several previous studies basically on the stratigraphy of the region including the study area. They are mainly focused on the geological evolution of the Galatian Volcanic Province (GVP) and stratigraphy of the north of Ankara region. Additions to those surveys, economic potential and paleontological surveys are extensively searched. However, the studies on the deformation of the terrain are limited.

Since 1950's, geological surveys extensively carried out in the terrain and some of them are summarized as below;

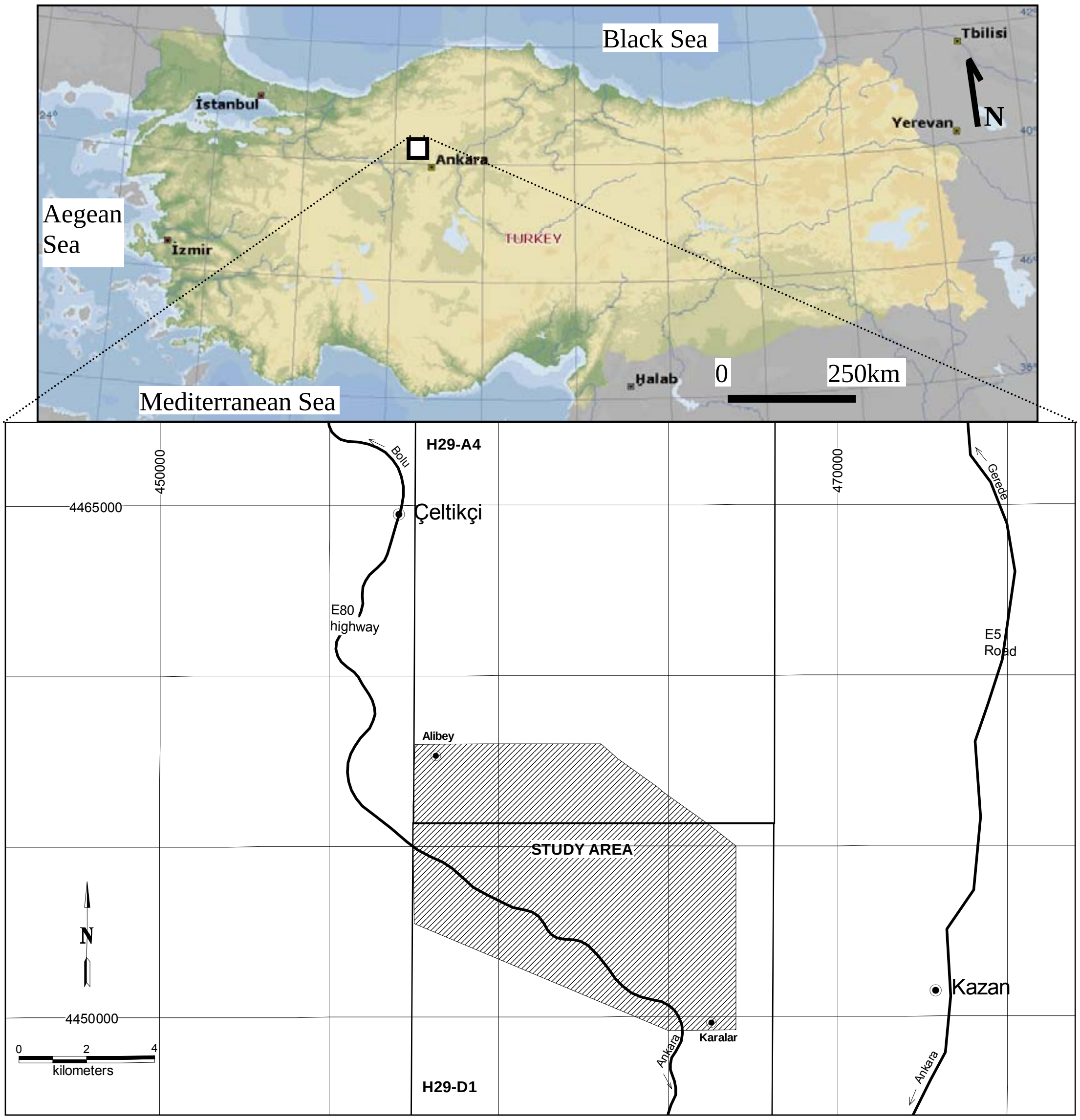

Figure 1.1. Location map of the study area.

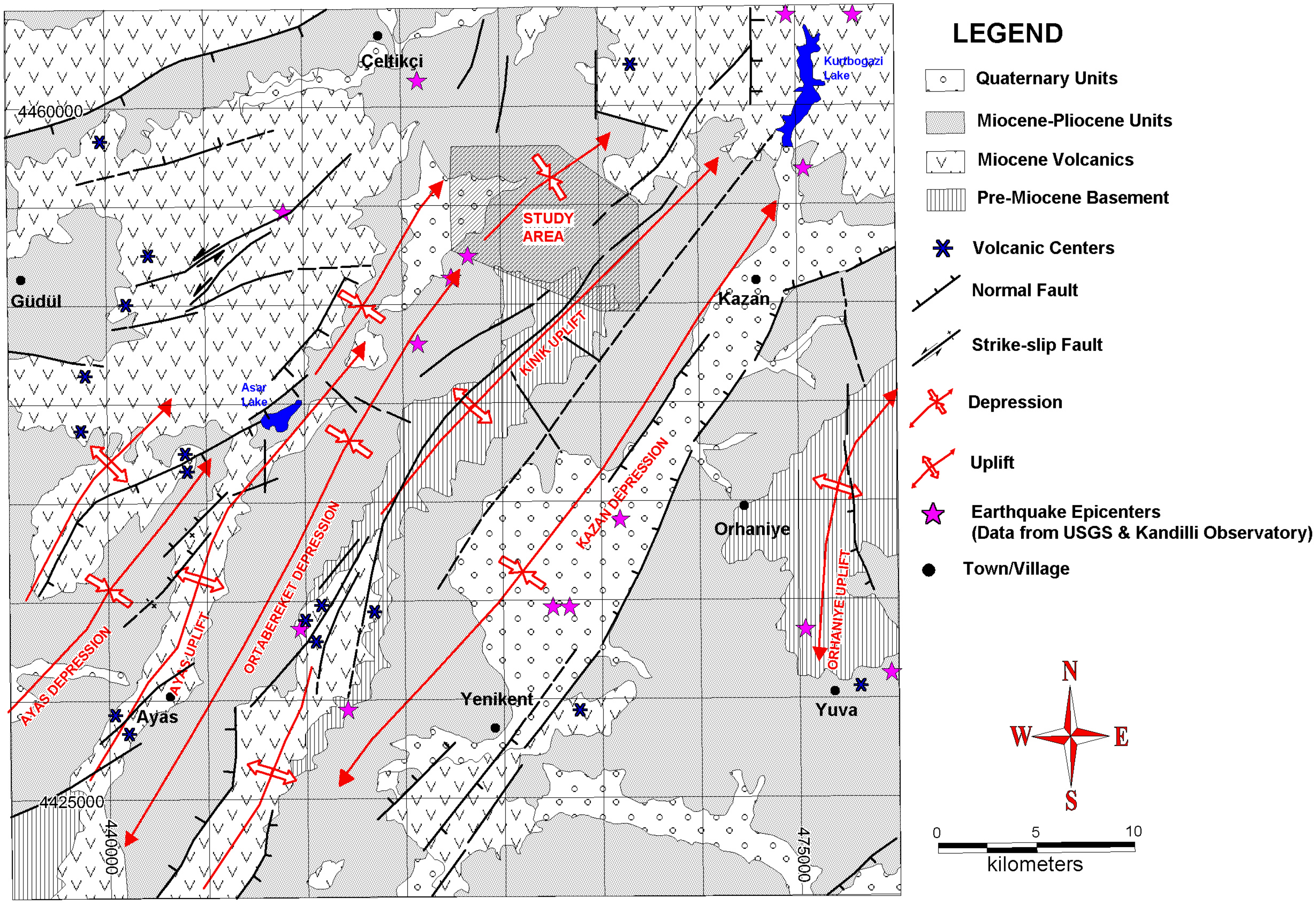

Figure 1.2. Simplified geological map of the area surrounding the study area with the geological structures and earthquake epicenters overlaid. Map was created by aerial photographical interpretations (1:60000). 1:500000 scale geological maps of MTA were also utilized.

The study by Erol (1955) is among the pioneering geological studies in the region. He studied the geology of the Neogene basin between Köroğlu and Işık volcanic mountains of GVP, and by Beypazarı and Ayaş towns. He defined the Neogene series, ranging in age from Miocene to Late Pliocene, as composed of lacustrine units intercalated with volcanic material from contemporaneous volcanism. It is said that the effect of volcanism vanishes upwards in the section indicating that the volcanism was chiefly active during the Neogene. He indicated that the gypsum content of the sediments decreases and they become deltaic towards northeast along the Kirmir creek (NE of Beypazarı). The Neogene lacustrine series near Pecenek town are found to be composed of diatomaceous sediments interbedded with volcaniclastics and green to light green colored marls. He correlates light green colored marls in the upper levels with the marls overlying gypsum beds at the southwest along Kirmir creek. He assigned Late Pliocene age to sandy-pebbly clastics that are quite widespread around Çeltikçi town. He points out that the faults and folds generally have WSW to ENE trends at the west and SW to NE trends at the east.

Erol (1961) –who is the first interpreting the tectonism of Neogene series around Ankara- worked on the orogenic phases of Ankara region. The Alpine orogenic movements have gradually weakened in Neogene and Quaternary. Some foldings and vertical movements have occurred in the Miocene. But in the Pliocene, vertical movements are also important and broad “upfolds and downfolds” formed produced a chain of sedimentary basins. The relative movements between the mountains and the basin blocks are very slight during Quaternary uplift.

Akyol (1968) worked on the coal occurrences in the area around Kızılcahamam and Çeltikçi. He summarizes the general geology of the area as being composed of tuffs, tuffites and agglomerates intercalated with coal bearing, occasionally silicified marls. According to the palynological analysis on spores and pollens from the coal layers, The Middle Miocene age is given to the coal deposits that are deposited in the same paleo-lake. He also mentions about E-W folding in the sequences.

Öngür (1973) studied the geology of the region around Kızılcahamam, Çamlıdere, Çeltikçi and Kazan and evaluated the geothermal energy potential. He mainly focused on the volcanic rock units (mainly lava flows) and classified them into different members. The Miocene sedimentary units, whose estimated thickness is around 200 m, overlie the lower volcanics of calc-alkaline composition. The sedimentary units interpreted as lacustrine units are overlain by volcanics and pyroclastics of calc-alkaline composition.

Tatlı (1975) studied the geology and geothermal potential of the area at the east of Kızılcahamam town. He named the Miocene lacustrine units as Pazar Formation, which is widespread near Pazar town. The lacustrine units are interbedded with volcanics/volcaniclastics. The fossils found in the formation reveal an age of Miocene. He also assigns the name Sinap Formation to the units that unconformably overlies the Pazar Formation dated as the Early Pliocene. On the structural geology of the area, the folding and faulting in the Pazar Formation is interpreted as a result of volcanic activity. The overlying Sinap Formation is less deformed with dip amounts less than 5^0 and with no definite folding.

Turgut (1978) studied the lignite bearing Neogene basins in Kızılcahamam, Çeltikçi and Çamlıdere. He lists the lithostratigraphic units observed in the area as; 1) Oligocene andesitic volcanics, 2) Miocene clastics and carbonates with lignite and 3) Pliocene clastics. As a result of conducting palynological analysis on the coal seams, Middle Miocene age is assigned. He comments that the tectonism was active after deposition of Miocene clastics but gets weaker by the deposition of Pliocene sediments.

Yağmurlu et al. (1988) studied the Neogene basin extending along E-W direction from Beypazarı to Nallıhan. The Beypazarı Basin is thought to be developed as an asymmetric depression during the first deformational phase during Miocene. Nearly N-S trending extension in this phase caused a subsidence in the basin and the formation of ENE-trending growth faults at the northern margin of the basin, which controlled the deposition. The second tectonic regime is interpreted to be NW-SE compression that affected the upper Miocene sediments in the basin. This phase is indicated by monoclines, reverse faults and asymmetric folds. As a result, it was concluded that a major change in the tectonic regime occurred after Late Miocene related to the movements along the North Anatolian Fault and Eskişehir fault.

Türkecan et al. (1991) worked in two areas within GVP; Seben-Gerede (Bolu) to Güdül-Beypazarı (Ankara) and Çerkeş-Orta-Kurşunlu (Çankırı). The Lower Miocene lacustrine units intercalated with the volcaniclastics/volcanics around the town Beypazarı are named as Hırka Formation. Age dating analysis on tuff samples yielded an age interval of 21 Ma to 25 Ma (Early Miocene). On the other hand, they named Miocene lacustrine units at the east of their study area around Orta town as Hüyükköy Formation. By using a palynological analysis, Middle to Late Miocene age is assigned to Hüyükköy Formation. The uppermost Neogene unit in their area, the Uruş Formation, is composed of clastics with carbonates and gypsum levels. They assign Late Miocene age to the Uruş Formation obtained by a paleontological analysis on mammalian fossils. They further comment that roughly NNW-SSE directed compressional forces were active till Late Miocene as evidenced by anticlines and synclines. They proposed an initiation age of Late Miocene-Early Pliocene to the North Anatolian Fault Zone that caused extensional deformation in the area forming Çeltikçi graben.

Gökten et al. (1996) in their study about the volcanic and tectonic evolution of the Ayaş-Güdül-Çeltikçi region stated that the Middle Miocene lacustrine units overlie the first two phase of volcanic activity (Karaçamtepe volcanics and Hacılar volcanics) in the study area. According to the authors, these two volcanics of GVP are in calc-alkaline composition and are related to subduction and continental collision in the northern branch of Neotethys. The last phase of volcanism, which is related to the extensional tectonism in the area, is represented by Early Pliocene basaltic volcanics. So the authors conclude that the area was under the effect of pure-shear stress (compression in NW-SE direction) from Oligocene (?) until the end of Early Pliocene. The Early Pliocene is interpreted as the time of transition of the stress regime from pure-shear to simple-shear. And after Early Pliocene time, active tension in a N30^{0}W direction was predominant in the area.

Süzen (1996) studied the geology and mineralogy of the Neogene lacustrine facies of a basin near Pelitçik town. Based on dolomite stoichiochemistry and mineral paragenesis found in Pelitçik Basin, he infers that the depositional conditions of the lake were perennial, shallow and quite lacustrine environment with fresh to slightly saline and slightly alkaline water chemistry.

Toprak et al. (1996) identified nine volcanic complexes within the GVP with numerous parasitic cones scattered around these main centers in their extensive study on GVP. The informal name “Galatian Volcanic Province” is proposed in this study

Wilson et al. (1997) on the Tertiary volcanism of the GVP said that the main phase of volcanism in the region, whose composition ranges from alkali basalt to trachyandesite and trachydacite with rare dacite and rhyolite, occurred during the Early Miocene (17-19 Ma). After a major hiatus in volcanic activity, eruption of a cover sequence of alkali basalts began in the Late Miocene (<10 Ma). They interpret the magma in the first volcanism in the GVP as sourced from lithospheric mantle modified by earlier subduction in the northern Neotethys, and the more mafic magma of the latest phase was sourced from asthenospheric mantle. The authors accept that progressive lithospheric thinning was involved in the magma generation throughout the Miocene. And they support the idea saying extensional tectonics in the Galatian Volcanic Province date back to at least the Early Miocene.

Tankut et al. (1998) about the volcanics in Güvem area (NE of Kızılcahamam) said that parental magmas of the Early Miocene volcanism in the Galatian province were generated in a post-collisional tectonic setting from a previously subduction-modified mantle source. They stress that the Mid-Miocene hiatus in volcanic activity in the area, after which the eruptive style and geochemical characteristics of the volcanics changed, strongly suggests a major change in the geodynamic setting. They state that the hiatus could mark onset of transtensional tectonics associated with the North Anatolian Fault Zone.

Demirci (2000) studied the structural geology of the Neogene units present in an area extending from Çayırhan at west to Çeltikçi at east. He differentiated five Neogene units ranging from Early Miocene to Late Miocene. Their environment of deposition is thought to be fluvial to lacustrine. Among those, early Miocene-aged Hırka formation is known to host economical trona deposit around Beypazarı town. Results of his structural geology analysis show that there were three main deformational phases operated during the Miocene; 1) E-W compression, 2) N-S compression, 3) E-W extension. Relative order of the events was determined by using the overprinting slickenlines and cross-cutting faults. The first (oldest) deformation, E-W compression, has a principal stress in 096^0, 17^0. The second deformation, N-S compression has a principal stress direction at 189^0, 17^0. And the last deformation characterized by E-W extension has maximum stress direction acted at 308^0, 88^0. Although no definitive age of the phases could be given except the second one, probable age intervals were given by using the ages of the units they had affected. Age of the first phase (E-W compression) is considered as Early Tortonian or younger. Tortonian to Late Tortonian age is assigned to the second phase (N-S compression) by using a radiometric age dating (7.7 Ma) from the rock units that were deformed syn-depositionally. Then it is said that the third deformational phase, which is E-W extension, must have an age of post 7.7 Ma. Well-known monoclines in the Beypazarı area are thought to be as a result of the second deformational phase. Finally, it is concluded that all three phases identified are found to be present in almost every region in the study area.

Adıyaman et al. (2001) described the Late Cenozoic tectonism in the Galatian Volcanic Province and tried to evaluate the evolution of magmatism in the area by geochemical methods. They concluded that there are two successive volcano-tectonic events in the region. The first one, which is Early to Middle Miocene, corresponds to a NE-SW oriented extension responsible for the opening of NW-striking tensional fractures through which the first phase of Galatian volcanics erupt. The second event, which is Late Miocene (or earlier), corresponds to a E-W trending extension creating N-striking tensional fractures through which the second phase of more alkali volcanics erupt. Authors relate the first tectonic event as the backward retreat of the Hellenic slab and the second extensional event as the result of the strike-slip motion along North Anatolian Fault Zone.

The paleontological surveys are one of the important parts of the stratigraphy surveys carried out in the study area where international Neogene –especially the uppermost Late Miocene to Pliocene- calibration is set (Ozansoy 1961; Tekkaya 1973; 1974; Şen and Rage 1974; Gürbüz 1981). The calibration and paleo-environmental evolution of the terrain well-described and addressed. The geological time scale of the top stages of the Neogene is set according to European time scale.

On the other hand, the radiometric dating and geodynamic-volcanic evolution of the GVP is discussed extensively by various previous papers that are mainly based on the radiometric dating and geochemistry. The age range is from Paleocene to Neogene (Koçyiğit et al., 2003) or solely in Miocene (Keller et al., 1992, Türkecan et al., 1991; Tankut et al., 1993; Wilson et al., 1997). Two stages volcanism in the GVP is proposed by various researchers (Türkecan et al., 1991; Tankut et al., 1993; Wilson et al., 1997; Adıyaman et al., 2001; Koçyiğit et al., 2003). The volcanism is interpreted as being generating from a subducting slab and a rifting processes related to subduction in two intermittent or successive stages.

1.4. Methods of Study

This thesis involves a series of steps taken professionally from the beginning to the completion of the study.

Before the initiation of any fieldwork to the study area, preliminary office studies were performed. First a literature survey about the geology of the area and its vicinity was carried out in order to set a basic knowledge. Then, prior to field studies, aerial photographs of the area at 1:60000 scales were examined to get some information on major structures of the region. Later, extensive field studies were conducted and 1:25000 scale geological map of the area with the geological structures (faults, folds and monoclines) was done. Types of the faults were determined by using their slickenlines and/or field observations. Numerous striae data from the faults with dip-strike measurements from the faults and the dip-strike measurements of beds were collected over the study area for structural analysis.

Bidirectional rose diagrams of the strike data at 10^0 class intervals were created by Rockworks 2002 software for the analysis of bedding planes. The same program was also used for creating contoured stereonet diagrams of the bedding data for the fold analysis. For this purpose, Schmidt net (equal-area net), which is commonly preferred in structural analyses to prevent preferred alignment of the data, was used.

For the analysis of the slip data, the software Tensor v.5.42 (Angelier Inversion Method) was used (Angelier 1979; 1984; 1991). Different deformational phases affected the study area were recognized by using that software and by field observations. Principal paleo-stress directions of those deformational stages were calculated by using the software.

CHAPTER 2

REGIONAL GEOLOGY

Turkey, which is located just on the tremendous Alpine-Himalayan orogenic belt, has quite complicated regional geology. Its tectonic structure is composed of several pre-Alpine and Alpine microcontinents of different origin and characteristics. Complex geological history of Turkey involves interactions of those microcontinents, and opening and closure of the oceans separating them at different geological times. The mentioned oceanic basins are collectively known as Tethys Ocean. It is a triangular shaped, gigantic embayment (basin), which narrows down from east to west, and separates Laurasia and Gondwana continents of Permo-Triassic Pangea (Şengör and Yılmaz, 1981). The mentioned microcontinents, from north to south, are pre-Alpine İstanbul terrane and the Alpine continents; Sakarya Continent and Tauride-Anatolide platform. The İstanbul terrane in the north was probably located, during the Paleozoic, at the passive margin of an isolated continental fragment within a Paleozoic ocean to the north of Gondwana. The Alpine Sakarya Continent is generally accepted as an isolated carbonate platform in the Tethys during Middle-Late Mesozoic time. The Tauride-Anatolide units represent the Gondwana continental platform, which was isolated in the Alpine Tethys (Göncüoğlu et al, 2000).

Numerous authors studied the geology of Turkey, tried to define the tectonic units of Turkey and evaluated the tectonic evolution by using different models dating from 1800s to 1900s. Pioneering studies have been published before establishing today's mostly accepted history of Turkey, although there are still disagreements going on about the timing of those tectonic events. Among those valuable studies, Ketin (1966) was crucial that differentiates clearly the tectonic units of Turkey. Although he gave no suture interpretation, he has found for the first time that Anatolides are not pre-Cambrian but Alpine. Moreover he stated that there is no double vergency but only south-vergent structures in Anatolia. He named the tectonic units, from north to south, as follows:

- North and northwest Anatolia ranges, or Pontids in a broader sense
- Inner Anatolian ranges, or Anatolids, in a limited sense
- South and East Anatolia ranges, or Taurids, in a broader sense
- Southeast Anatolian ranges, or region of Border folds

According to his explanations, the tectonic-orogenic evolution of Anatolia proceeded gradually from north to south. The first stronger and effective orogenic movements began in the northern ranges, then passed to the Central-Anatolia, afterwards to the Taurus, and at last to the Border-folds region (Ketin, 1966). The legendary paper by Şengör and Yılmaz (1981) forms a turning point in the history of this rival to interpret the tectonic evolution of Turkey in a global tectonic view.

2.1. Tectonic Evolution of Turkey

The main tectonic events in the complex geological history of Turkey during Paleozoic to Mesozoic times can be summarized as simultaneous convergent and divergent movements of microcontinents within the Paleo-ocean, Tethys. Paleotethys designates the Paleozoic Tethys Ocean that separates the Laurasia and Gondwana at that time. By continuous movement of Gondwana towards north caused the southward subduction and final closure of Paleotethys underneath the Gondwana. This southward subduction of the Paleotethyan oceanic crust, which lasted till Early-Mesozoic times, is believed to initiate back-arc spreading in the northern margin of Gondwana (Şengör and Yılmaz, 1981). This spreading event gave way to the formation of another oceanic basin (Mesozoic Tethys), named as Neotethys. It continued to evolve during Middle Mesozoic after the total consumption of Paleotethys under Gondwana. Neotethys Ocean was embracing the isolated continental fragments; microcontinent Sakarya Continent and Tauride-Anatolide carbonate platform. There were two main branches of Neotethys; northern Neotethys (also known as İzmir-Ankara ocean or Vardar ocean), which is surrounded by Sakarya continent at north and Tauride-Anatolide platform at south, and southern Neotethys at the south of Tauride-Anatolide platform. Indeed northern Neotethys had further branches that had coexisted independently in Turkey during Mesozoic. Those are called as Intra-Pontide and Inner Tauride oceans (Şengör and Yılmaz, 1981). Continuing northward drift of Gondwana triggered a northward subduction in northern Neotethyan oceanic crusts during Cretaceous. Total consumption of the oceanic crust in the northern Neotethys and collision of Sakarya Continent to Tauride-Anatolide platform took place diachronously from Late Mesozoic to Early Paleogene (Şengör and Yılmaz, 1981; Koçyiğit, et al., 1988; 1991b). After the collision, continental to shallow marine deposition in fault controlled basins was predominated in the region (Şengör and Yılmaz, 1981). Because of the incessant movement of the continents, tectonic slices of both the oceanic crust of the northern Neotethys and the accretionary complex have been transported toward the south for many kilometers (Koçyiğit, et al., 1988; 1991b). While the ophiolites and mélange of the closed İzmir-Ankara ocean were being obducted on the Tauride-Anatolide platform, which was also being internally deformed due to the compressional tectonism, the southern Neotethys remained open. Shallow to deep marine deposition and arc volcanism during Paleocene age, which was positioned at north of the ocean and resulted from northward subduction in the oceanic crust, were predominant especially at the southeastern Anatolia. Because of the continuing northward movement of the Arabian plate towards Anatolian plate, which was composed of amalgamated continents; İstanbul Fragment, Sakarya Continent and Tauride-Anatolide platform, the southern Neotethys is thought to be totally closed in Middle Miocene (Şengör and Yılmaz, 1981). This distinctive collisional event marks the beginning of a new tectonic era, neotectonic period in the area where proto-Anatolia was located (Şengör et al., 1985). Şengör et al. (1985) defines a neotectonic period as the time that elapsed since the last major wholesale tectonic reorganization in a region of interest. So he thinks that the collision of Arabian plate with Anatolia in Middle Miocene, which is accepted as the last major tectonic event in the evolutionary history of Turkey, is drastic enough forming a land-mark to separate the country's neotectonic development from its paleotectonic development. He supports a tectonic escape model in which the Anatolian block escapes westward along the major strike-slip faults, North Anatolian and East Anatolian Fault Zones due to the post-collisional convergence of Arabian platform and Eurasia. Although initiation time of movement along the famous North Anatolian Fault Zone is debated, it is proposed as Late Miocene-Pliocene (please see Bozkurt 2001). Further westerly motion of Anatolian block is obstructed at eastern Mediterranean which results in an N-S extensional regime in the western Turkey (Şengör et al., 1985).

After the Late Miocene, the present tectonic regime of Turkey was established with the formation of above tectonic provinces that have been operating till present. By the end of Miocene, all of the oceans were already closed completely and all microcontinents were already amalgamated. Limited marine invasions occurred again and molassic to fluvial to lacustrine deposition have been dominating throughout the Anatolian landmass. Turkey acquired its today's geography, and as a result of its complicated geological history, it is a complex mixture of different amalgamated microcontinents, remnants of consumed oceans (ophiolites, mélanges) in the form of belts, magmatic arcs produced by subduction zones, massifs (Menderes Massif, Kırşehir Massif) and finally a vast collection of tectonically formed Tertiary basins filled by shallow marine to molassic to fluvial to lacustrine deposits mostly interbedded with volcanics/volcaniclastics.

2.2. Tertiary Paleogeography of Turkey

When the Tertiary paleogeography of Turkey is examined, it becomes quite easy to understand the geologic evolution of the study area and its close vicinity around Ankara province. Before the total closure of İzmir-Ankara ocean and Intra-Pontide ocean, Paleocene paleogeographical setting around Ankara is represented by shallow to deep marine environment that are mainly characterized by reefal, platform limestones and flyschoidal sediments extending from Polatlı-Haymana to Kırıkkale-Çankırı. Terrestrial sequences consisting mainly of fluvial and lacustrine environments in Paleocene age occur along a NE-SW trending belt covering northwest of Ankara extending towards Nallıhan-Göynük where marine sequences of Intra-Pontide ocean are present. Paleocene volcanics and volcaniclastics rocks, with numerous volcanic centers which are interpreted as members of a magmatic-arc formed by northward subduction of İzmir-Ankara Ocean, also occur on that belt. Interbedded sequences of volcanics/volcaniclastics and terrestrial sediments imply that the paleogeographic setting is composed of a continental deposition with small lakes around the terrestrial volcanic vents. So it can be deduced that both terrestrial sediments and volcanics/volcaniclastics were deposited in an inter-arc depositional system at the north of İzmir-Ankara Ocean (Kazancı and Gökten, 1988). After the entire consumption of the northern Neotethys and consequent collision during post-Paleocene-Eocene period, paleogeography of the Ankara and its vicinity has changed considerably. The land area of western and central Anatolia including Ankara was uplifted due to collision and formed highlands relative to its surroundings. During Early Miocene, these highlands were surrounded by shallow seas in the north, east and south (especially in the east and south) as evidenced by presence of widespread reefal limestones. Marine waters from east and south occasionally invaded small areas in central Anatolia and evaporite deposits of limited extent were formed (Şengör et al., 1985). Once again continental deposition in fluvial to lacustrine environments became predominant in the central Anatolia.

Especially alkaline to fresh water lakes covered quite large areas at the northwest of Ankara. A volcanic activity of mainly calc-alkaline composition has started to give its first products and affected entire northwestern Anatolia. The deposition in the lakes during their entire existence was interfered by this Miocene volcanism. This well-known volcanism created one of the most important volcanic provinces of Turkey, Galatian volcanic province. Since the study area is located within this volcanic province, which covers large areas and is thought to be crucial in determining the Neogene evolution, geology of the Galatian Volcanic Province will be given in detail in a separate section below.

2.3. Galatian Volcanic Province

Galatian Volcanic Province (GVP) occupies a more or less triangular area covering approximately an area of 6500 km^2 at northwest central Anatolia. It is truncated and bounded at the north by North Anatolian Fault Zone (Toprak et al., 1996).

Volcanic/volcaniclastic products of this well-known volcanism were called as “Kızılcahamam volcanics” or “Köroğlu volcanics” in previous studies. But later studies believed that those names can be used to refer only certain parts of the province and do not represent the entire belt (Toprak et al., 1996). Therefore the informal name “Galatian Volcanic Province” is preferred in this study.

Two distinctly identified eruption cycles of volcanic activity occurred throughout the GVP during Miocene (Türkecan et al., 1991; Tankut et al., 1993; Wilson et al., 1997; Adıyaman et al., 2001; Koçyiğit et al., 2003). With the help of age-dating data from previous studies in this well-studied province, the older volcanic cycle is known to have taken place between 25 Ma and <10 Ma (Early-Late Miocene) (Türkecan et al., 1991; Wilson et al.,

1997) even with much older initiation age (since Paleocene) (Koçyiğit et al., 2003). Approximately 1500 m thick products of this earlier volcanism, which is the major phase, are calc-alkaline in character ranging in composition from K-rich basaltic trachyandesite to rhyolite with minor occurrences of alkali-basalts. There are several successive lava flows usually underlain by associated widespread volcanic breccias and pyroclastics. Some lava horizons have manifestations that indicate sub-aqueous flow, which most probably occurred through the shallow lakes surrounding the calderas. The latest cycle, whose age is constraint between 8.5 Ma and 11 Ma, consists of small volume of alkali basalt flows capping the older volcanic sequences. Previous suggest that the basaltic rocks are restricted to certain parts of the GVP, particularly in close proximity to the North Anatolian Fault Zone (Türkecan et al., 1991; Toprak et al., 1996; Wilson et al., 1997; Tankut et al., 1998; Adıyaman et al., 2001).

Earlier works on GVP have long considered the older (Early-Middle Miocene) intermediate to felsic volcanic activity as characterizing a volcanic arc related to the subduction of northern branch of Neotethys (Tankut et al., 1990; Gökten et al., 1996). However, with the well-constrained radiometric age data from the volcanics and new geochemical data supported by recent studies, it is now possible to better evaluate the tectonic setting and genesis of the GVP. New geochemical data and Sr-Nd isotope data suggest that the parental magmas in this earlier phase were generated in a post-collisional tectonic setting from a previously subduction modified mantle source (Tankut et al., 1998). Source magma coming from the lower lithospheric mantle is believed to have been modified by flux of fluids originating from the earlier formed Tethyan subduction system. This magma generation within lower lithospheric mantle was resulted from progressive lithospheric thinning that occurred throughout the Miocene. However the reason for this onset of regional extension that was effective during Miocene and caused lithospheric thinning is controversial. It might be related to orogenic collapse causing localized extensional tectonics. Alternatively, it might be related to the backward retreat of the subducting South Aegean slab towards north under the Anatolian Plate. The Upper Miocene alkaline basalts of the latest phase in GVP simply correspond to typical rift-type basalts related to extensional tectonics, which were possibly transtensional forces associated with initiation of movement along the North Anatolian Fault Zone.

It is also crucial to mention about the Neogene sedimentary sequences in sedimentary basins in GVP. There are two types of sedimentary basins in GVP. The first one with a thick lacustrine sequence is exposed at the south of the province and it is thought to be a continuous belt, on which the study area of this thesis is located, extending from Beypazarı at west to Çubuk at east. The sedimentary sequence intercalated with volcaniclastics/volcanics in this area accumulated in a time interval from Early Miocene to Late Miocene as mentioned by previous studies in the region (Erol, 1955; Akyol, 1968; Tatlı, 1975; Turgut, 1978; Yağmurlu et al., 1988; Türkecan, 1991; Toprak et al., 1996). The second types of basins are composed of sedimentary sequences completely located in GVP. Examples of those basins are Pelitçik, Güvem and Orta basins, which are completely surrounded by volcanic complexes and separated from one another (Toprak et al., 1996).

CHAPTER 3

STRATIGRAPHY

Stratigraphy and depositional settings of the rock units are well-documented in order to understand the deformational history of the study area. Stratigraphy of the study area is classified into three major groups of rock units (Plate 1; Figure 3.1); (1) Pre-Miocene basement rocks; (2) Neogene rock units; and (3) Quaternary units. Among those, Neogene rock units are the most widespread ones cropping out in the area and will be the main focus of this chapter.

3.1. Pre-Miocene Basement Rocks

Pre-Miocene rocks are classified as the basement rocks in the study area and will be described briefly since they are not the main concern of this study. Basement rocks unconformably underlying the Neogene units crop out in limited areas at the west and north of Karalar village, and at the north of İneköy village (Figure 3.2). They have an unconformable boundary with the overlying units except one locality where they are juxtaposed with younger units along faulted contact at the north of Karalar village.

The basement is composed of schist, calc-schist, quartzite, phillite, Jurassic limestones, Eocene conglomerates and nummulitic limestones (Öngür, 1976). Eocene limestones containing abundant nummilite fossils crop out at the north of İneköy village. Eocene conglomerates, which were observed at just the north Karalar village, have a faulted contact with the older basement and are unconformably overlain by Neogene clastics at the west of Sivri Hill.

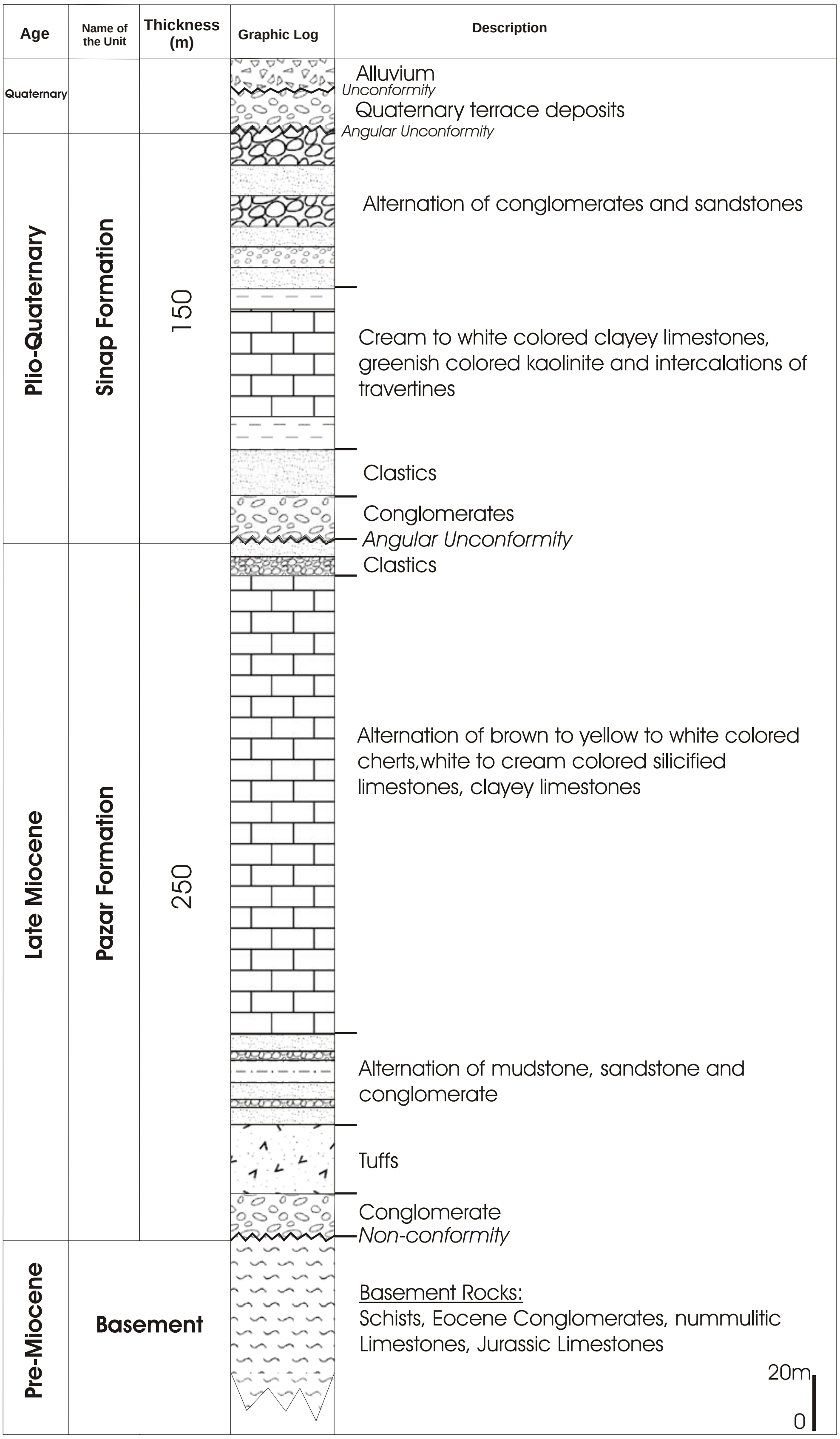

Figure 3.1. Generalized stratigraphic section of the study area.

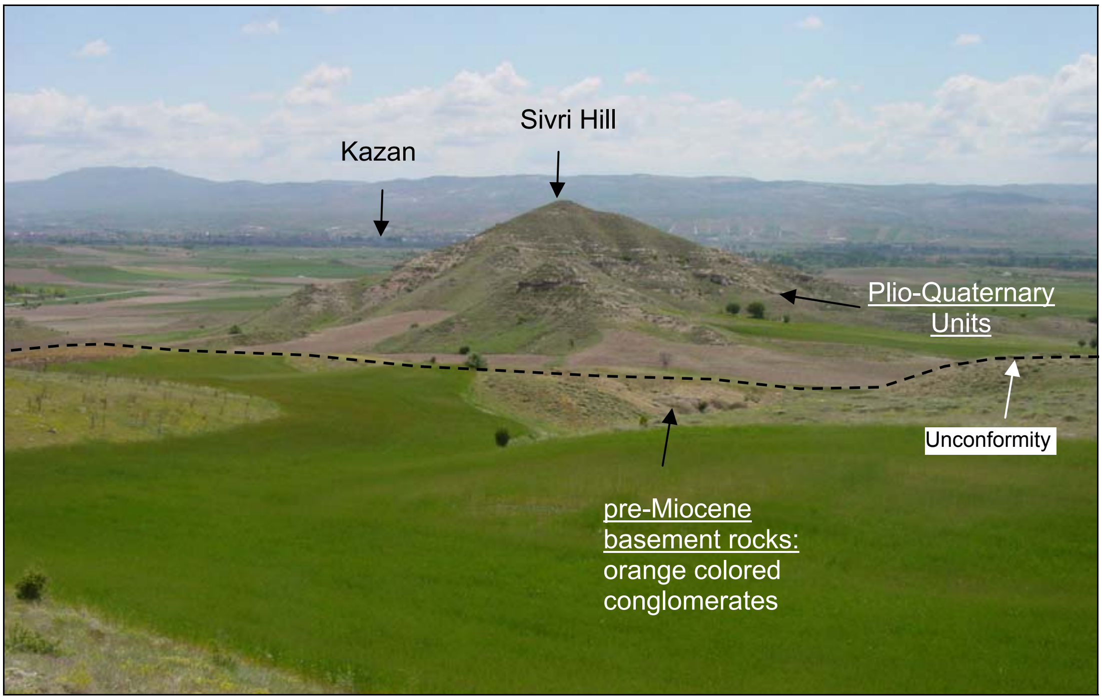

Figure 3.2. Pre-Miocene basement rocks unconformably overlain by the Plio-Quaternary units, at 1.5 km N of Karalar village (photo towards SE).

3.2. Neogene Units

Neogene units are divided into two distinctive groups; (1) Miocene unit (Pazar Formation); and (2) Plio-Quaternary unit (Sinap Formation).

Table 3.1. Stratigraphic nomenclature chart of the study area.

Age		Tatlı (1975)	Gökten et al. (1988)	Türkecan et al. (1991)	Süzen (1996)	Gökten et al. (1996)	This Study (2004)
PLIOCENE	Late	GAP	Memlik Fm.				Sinap Fm.
	Early	Sinap Fm.					
MIOCENE	Late			Uruş Fm.	Pazar Fm.	Uruş Fm.	Pazar Fm.
	Middle	Pazar Fm.		Hüyükköy Fm.		Hüyükköy Fm.	
	Early						

3.2.1. Miocene Pazar Formation

Miocene units cropping out in the study area and in the Çeltikçi basin were named differently by various authors (Table 3.1). Among those Tatlı (1975) was first to name Miocene units as Pazar Formation that he finds them quite widespread around the town Pazar at the 18 km northeast of the study area. Süzen (1996) also follows the same nomenclature in Peçenek basin. On the other hand, Türkecan et al. (1991) and Gökten et al. (1996) give the name Hüyükköy formation to the Middle to Late Miocene lacustrine units, which are composed dominantly of tuffs, tuffites, limestones and cherts at Hüyükköy village near Orta town (Çankırı). Due to priority, the Pazar Formation proposed by Tatlı (1975) is found to be suitable nomenclature for the Miocene units.

The units are widely exposed at; Alibey and Gölköy villages, a NE-SW trending area at the southeast of Çalta village, a NE-SW trending area at the north of İneköy village and at the southeast of Sarılar village, an area at the southern border of the study area between Evci and İneköy villages (Plate 1).

The units are dated as Late Miocene with mammalian fossils (Ozansoy, 1961; Gürbüz, 1981). A mammalian fossil was found at around 1.2 km northwest of Karalar village, at a stratigraphic level very close to its lower boundary with the basement rocks (Figure 3.3). The fossil was collected from a red brown colored massive mudstone/sandstone unit (>1 m thick) overlain by a 1.7 m thick white colored clayey/sandy limestone with a sharp stratigraphic contact (See stratigraphic section-1). Most probably the mudstones and sandstones were deposited in a flood-plain environment, which were then flooded by transgressing waters burying and preserving the vertebrate fossils within the units. Sample site of the fossil was correlated with the paleontological and lithologically equivalent levels at type locality. Age of the sample is determined to be situated in MN-9 to MN-13 time interval in the mammalian time scale for Europe (oral communication with N. Kaymakçı, 2004). It corresponds to Middle-Late Miocene age (11.1 Ma to 6.8 Ma; Agusti et al., 2001). The units in Çeltikçi basin are dated as Middle Miocene (Akyol, 1968; Turgut, 1978) according to the palynological analyses on spores and pollens from the coal layers. Although the coal bearing units are not present in the study area, lithostratigraphically they are well-correlative with the units cropping out in the study area. Furthermore, the studies concerning mainly the volcanics in the region conducted extensive age dating analyses on the volcanic rocks and dated the units as Early Miocene to Late Miocene.

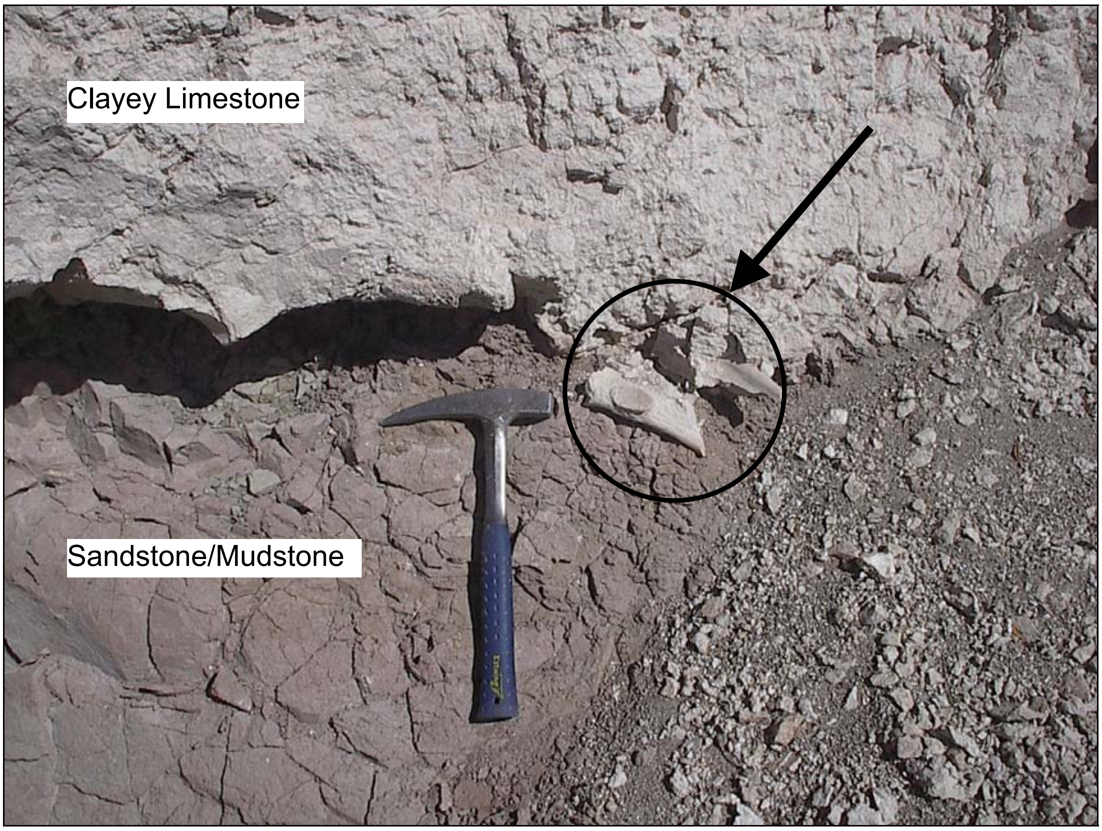

Figure 3.3. Mammalian fossils (shown by an arrow) found within the units of the Pazar Formation. Hammer for scale is 33-cm-long (E: 464974, N: 4450645, ~750 m NE of İneköy village).

Dominant lithologies representing the Miocene succession in the study area are chert beds, silicified clayey limestones, silicified mudstones, greenish colored fine clastics, pyroclastics tuffs, conglomerates, volcanogenic conglomerates and tuffaceous sandstones.

Chert beds are very characteristic in the area and they form extensive outcrops at some localities (Figure 3.4), such as; at the east of Evci village, around Sarılar village, around Çalta and Çırpan villages and around Alibey and Gölköy villages (Plate 1). Thickness of the chert beds may reach up to 14 m. They are yellow brown/reddish brown colored mostly opaque, crudely bedded with a mottled, patchy texture. In some places, they are yellowish to white to gray colored and opaque to semi-transparent. They usually form resistant ridges on the topography (Figure 3.5). Clayey limestones are observed at the north of İneköy village, around Çalta village, at the northwest of Çırpan village and around Gölköy village. Limestones are mostly clayey but sometimes silty to sandy. Their colors range from white-cream to yellowish cream to gray. They are silicified at some levels. Silicified levels, which sometimes include chert and inclusions of non-silicified limestone, form ridges similar to bedded cherts. Limestone levels not suffering from silicification may sometimes have mesh structures and vugs, which may have been imparted by a hydrothermal alteration (oral communication with B. Varol). Mudstones are seen at the northwest of Çırpan village. They are distinctively white colored and partly silicified. Silicified mudstones have opaque glassy appearance and concoidal fractures. Greenish colored fine clastics are exposed near İneköy village and at the southeast of Sarılar village. They are composed of yellowish green colored, very thin to thin bedded, sometimes cross-bedded/laminated mudstones and sandstones. Pyroclastic tuffs are observed near İneköy, at the southeast of Sarılar village

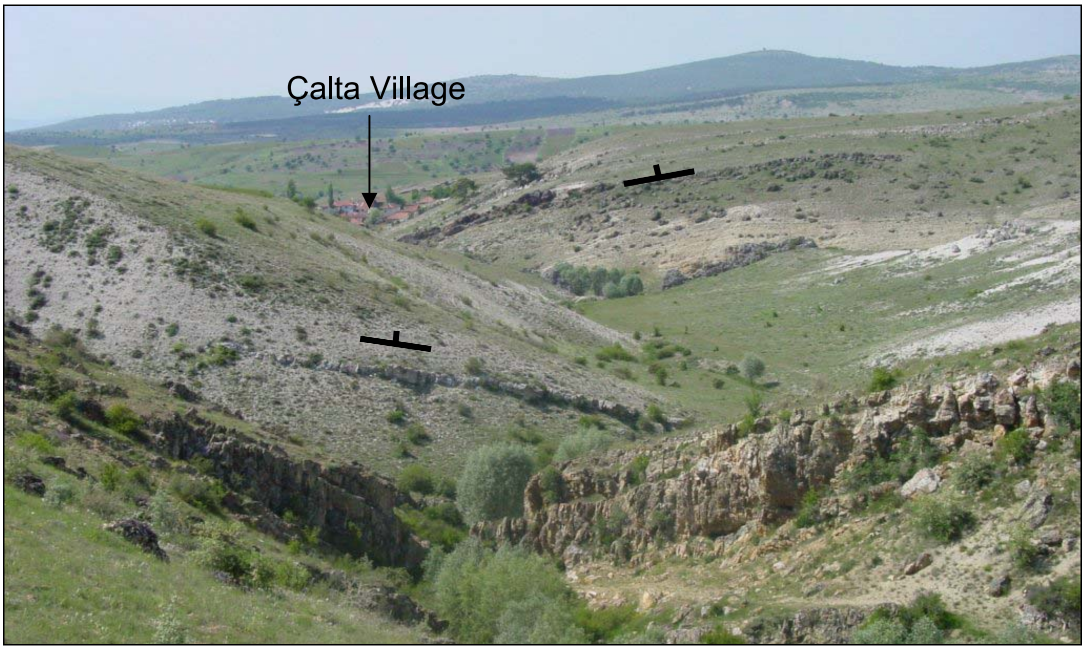

Figure 3.4. General view of the chert beds in Pazar Formation. They dip towards Çalta village (towards NW) in the photo. View is towards NNW.

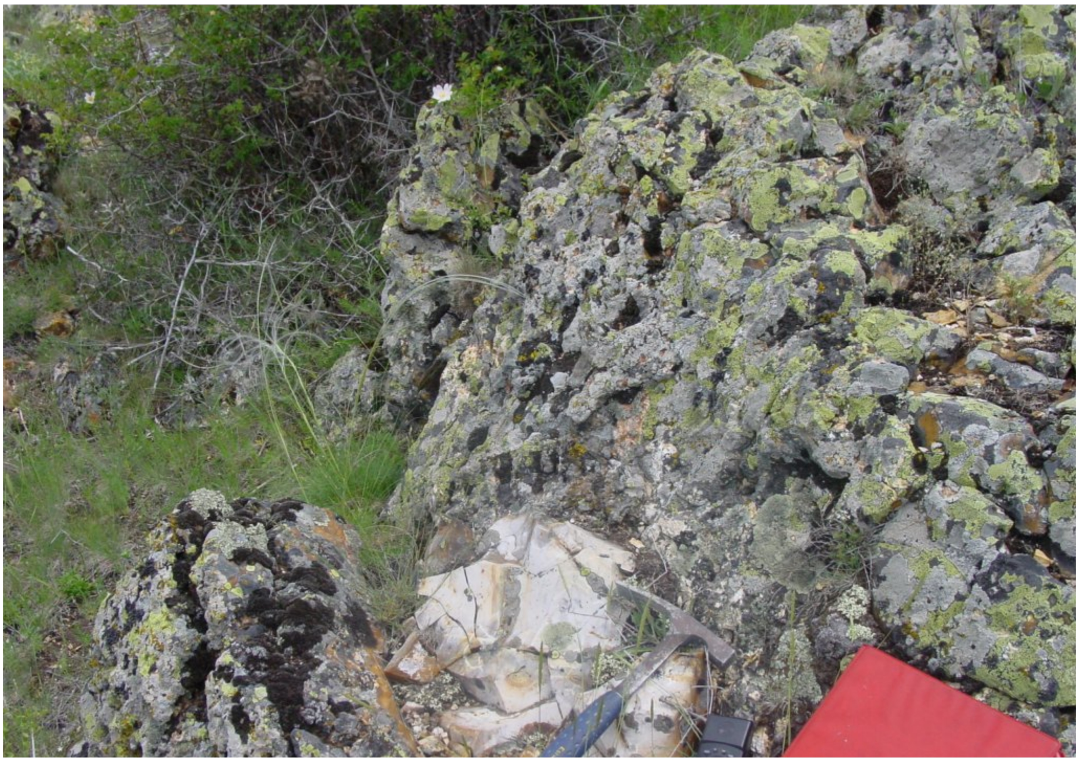

Figure 3.5. Close-up view of the resistant chert beds. As seen they typically display resistant ridges.. Location is at SE of Çalta village, view is towards NE. Hammer for scale is 33-cm-long.

and at the northeast of Evci village on the highway (in an outcrop where Miocene units have a faulted contact with the overlying pinkish clastics along a roadcut). White to yellow to orange colored tuffs are fresh to altered (altered to clay). They are usually coarse grained, pumice rich and contain dark colored biotite crystals.

Polygenic conglomerates are observed locally near Çalta village in a section above the chert beds. They are gray to cream colored, well-consolidated, moderately to well sorted and matrix to clast supported. Clasts in the unit are subangular to subrounded chert, metamorphic and limestone (max. ~2 cm) derived from the basement. There is no imbrication of pebbles. Grading is poorly developed and bedding is obscure. Volcanogenic conglomerates and sandstones are also locally exposed near Gölköy above a section of cherts and silicified limestones. They are white to gray colored, poorly to moderately sorted conglomerates/sandstones consisting of angular to subangular gray colored volcanic and cream to white colored pumice clasts (<2 cm). All of the above properties imply that they may have been formed as a result of volcanogenic mass flows. Tuffaceous sandstones and other volcaniclastics varieties are mostly exposed around Evci village. Minor exposures exist at the southeast of Sarılar village. They are cream to greenish to pinkish colored tuffaceous sandstones and volcaniclastics. They occasionally contain gastropod fossils and pumice pebbles replaced and filled completely by white lime.

Miocene units unconformably overlie the older basement rocks as observed at the north of İneköy village. They are overlain unconformably by Plio-Quaternary units.

Measured stratigraphic section-1 is located at the north of İneköy village (Figure 3.6). Total measured thickness of the units in this section is 144.4 m, while the thickness of the Miocene part of the section is 100 m. The Miocene lithologies unconformably overlie the basement schists. The stratigraphy

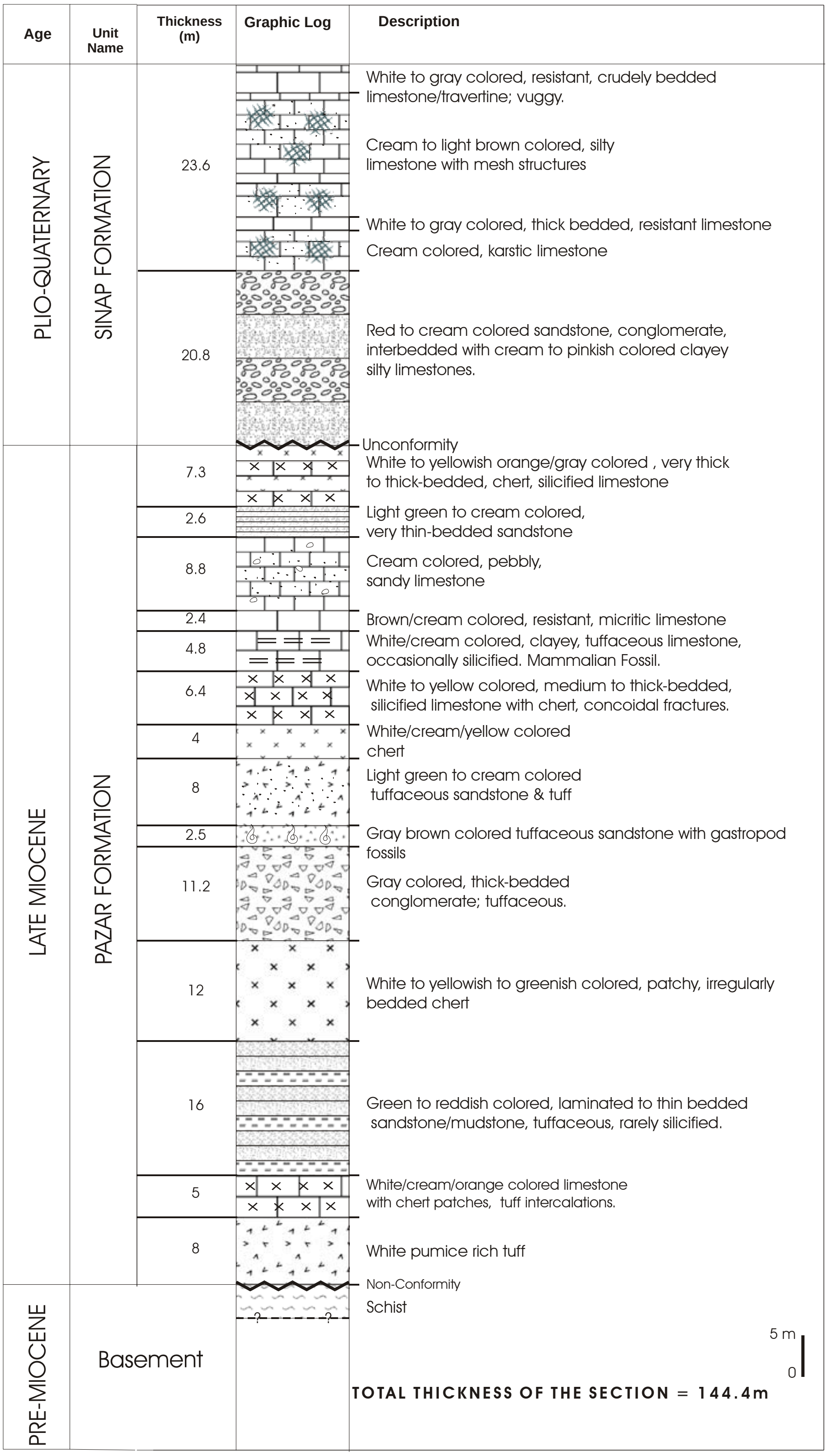

Figure 3.6. Stratigraphic section-1 measured between İneköy and Karalar villages. (Starting point = E: 463900, N: 4451150; End point = E:465162, N: 4450896).

from bottom to top is; 1) 8 m-thick, white colored, pumice-bearing, pyroclastics tuff with faint laminations; 2) 5 m-thick, white to cream to orange colored, medium to thick bedded and brecciated silicified limestone with chert patches and green to red orange colored altered tuff intercalations; 3) 16 m-thick, mudstone/sandstone; green to reddish colored, laminated to thin bedded, rarely silicified; 4) 12 m-thick, chert; white to yellowish to greenish colored, irregularly patchy; 5) 11.2 m-thick, conglomerate; gray colored, tuffaceous, non-calcareous, matrix supported and contains dark green schist clasts in form of angular flakes; 6) 2.5 m-thick tuffaceous sandstone; grayish brown colored, with white pumice clasts and gastropod fossils; 7) 8 m-thick, tuffaceous sandstone, tuff and altered tuff; light green to cream colored; 8) 4 m-thick, chert, white to cream to yellow colored, resistant and internally patchy; 9) 6.4 m-thick, white to yellow colored, medium to thick bedded silicified limestone; with concoidal fractures. It contains chert inclusions; 10) 4.8 m-thick, white to cream colored, occasionally silicified clayey tuffaceous limestone; 11) 2.4 m-thick, resistant, brown to cream colored micritic limestone; 12) 8.8 m-thick, cream colored, pebbly-sandy limestone; 13) 3.6 m-thick, light green to cream colored, very thin bedded sandstone; 14) 7.3 m-thick, white to yellow to orange to gray colored, very thick to thick bedded and resistant, chert and silicified limestone;. At the top of the section, the Miocene units are overlain unconformably by 44.4 m-thick Pio-Quaternary conglomerates.

Stratigraphic section-2 (Figure 3.7) was measured at around 750 m northwest of Çırpan village. Total measured thickness is 86.5 m. The upper 14 m of the section is represented by unconformably overlying Plio-Quaternary sediment. The following Miocene units were encountered in the section, starting from bottom to top; 1) greater than 5 m-thick, white colored mudstone, occasionally silicified; 2) 1 m-thick, white to gray colored completely silicified mudstone. It is resistant and has iron-oxide coating, porcelaneous texture and concoidal fractures; 3) 1.6 m-thick, yellowish to brownish to cream colored mudstone; 4) 1.3 m-thick, white to gray colored

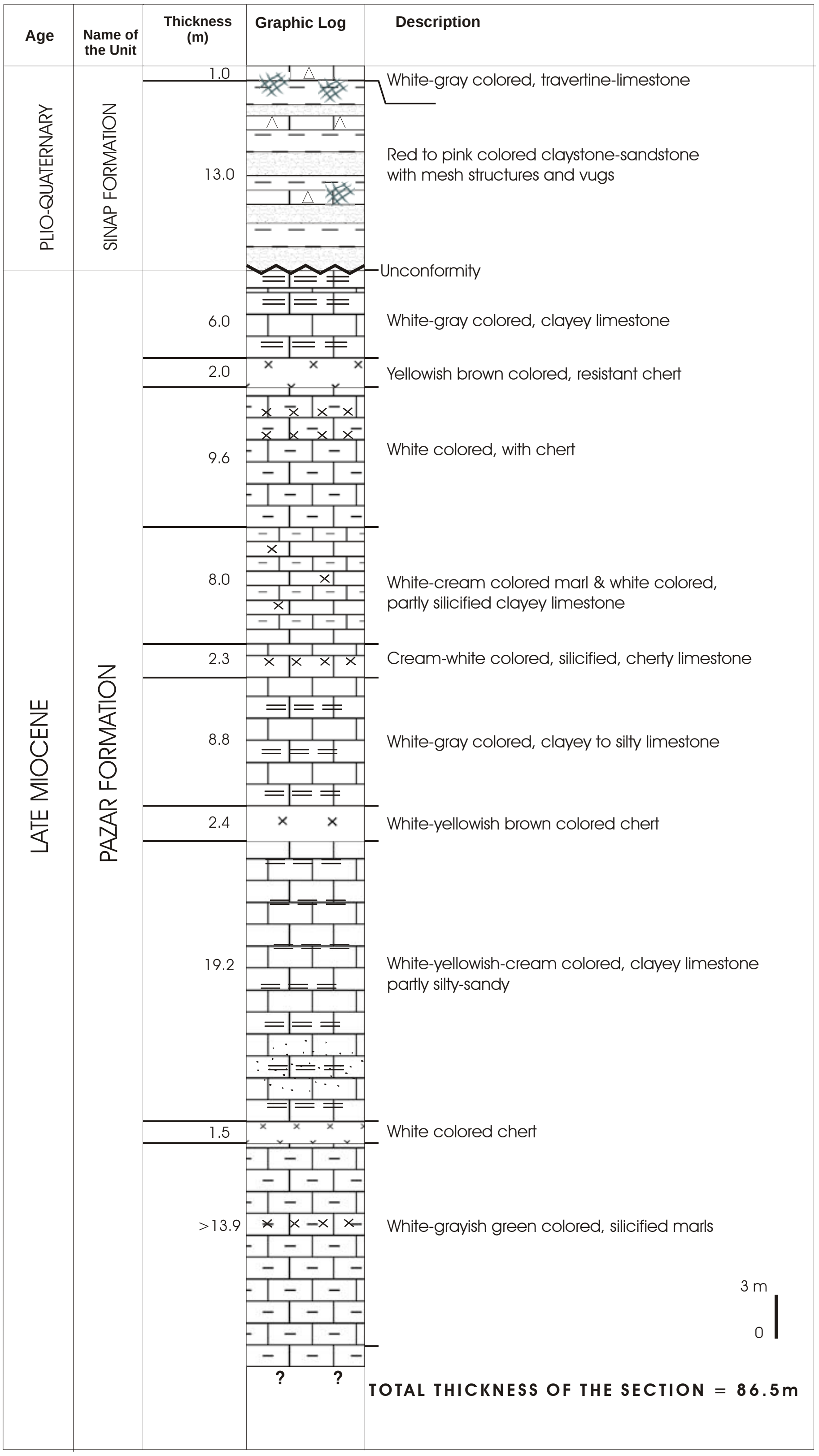

Figure 3.7. Stratigraphic section-2 measured near Çırpan village (Starting point = E: 461015, N: 4457239; End point = E: 460581, N: 4456714).

silicified mudstone; 5) 5 m-thick, white to cream colored mudstone; 6) 1.5 m-thick resistant, chert and silicified mudstone; 7) 8 m-thick, white to gray to cream colored clayey to silty to sandy limestone with chert pebbles; 8) 11.2 m-thick, white-cream to yellowish, silicified clayey limestone. It is basically non-resistant; 9) 2.4 m-thick, white to yellowish brown colored, resistant chert. It has patchy and brecciated appearance; 10) 8.8 m-thick white to gray colored, occasionally silicified clayey to silty limestone; 11) 2.3 m-thick completely silicified cherty limestone, cream to white colored. It is in resistant character. It contains spherical nodules up to 2cm, which are filled by white colored powdery lime; 12) 8 m-thick alternation of white to cream colored mudstone and white colored clayey limestone, which is resistant and partly silicified; 13) 4.8 m-thick white colored mudstone with chert alternations; 14) 4.8 m-thick white to cream to yellowish colored, completely silicified mudstone having a resistant character; 15) 2 m-thick yellowish to brown colored, resistant bedded chert; 16) 4.8 m-thick clayey limestone; 17) 1.2 m-thick, white to gray colored, bedded, resistant, clayey limestone with a brecciated appearance. The remaining 14 m of the section is composed of Plio-Quaternary sediments.

A stratigraphic reference section was measured at around 750 m southeast of Çalta village that displays a gradational boundary relationship between overlying 24 m thick white-grayish green-cream clayey limestones and underlying 13.2 m thick cream-orange-yellowish brown colored cherts. Total thickness of the units measured is 37.2 m.

By using the information from the measured stratigraphic sections and observations during the fieldwork, the thickness of Miocene units in the study area can be estimated as around 250 m. It is known by previous studies that Miocene units intercalated with volcanics/volcaniclastics have a thickness more than 200 m in the region.

Although no specific fossils depicting a certain environment found, presence of clayey limestones, mudstones and claystones that are completely devoid of any marine fossils indicates a fresh water lacustrine environment (Boggs, 1995). Presence of volcaniclastics, pyroclastics and tuffaceous sediments shows that the lake was under high influence of volcanic activity coeval with the deposition. Moreover, the existence of travertine-like features (wavy laminations, karstic vugs etc.) in limestones and chert beds/bands also points out that a hydrothermal activity was present during the deposition of the sediments.

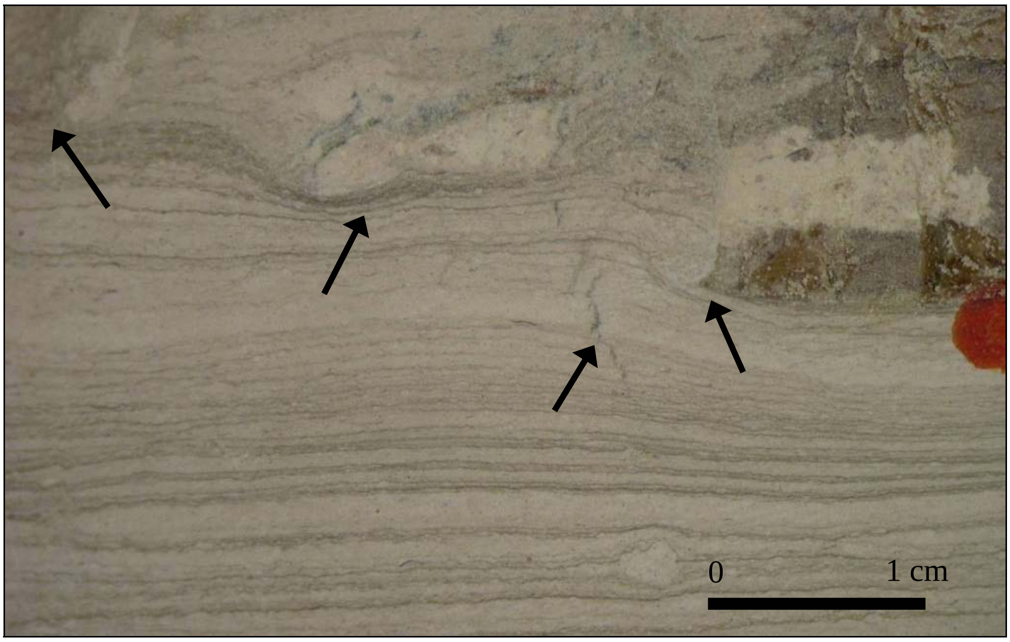

Figure 3.8. Polished section of a clayey limestone sample. Darker colored thinner interlaminae are composed of amorphous silica. Arrows indicate the soft sedimentary deformations.

It is most probable that, later on, a post-depositional hydrothermal activity, manifested by widespread silicification in the units and mesh structures, also affected the sediments. Petrographical analysis of one clayey limestone sample from the study area (Figure 3.8) was performed by Dr. Baki Varol from Geological Engineering Department of Ankara University. He also concluded that the depositional environment must be lacustrine due to the lack of any fossils reflecting marine life. Laminae in the sample, which are mainly made up of amorphous silica, are likely resulted from a hydrothermal activity in the lake environment. The soft sedimentary deformational structures, such as slumps, growth faults, are quite evident in the sample. Those kinds of syn-depositional structures are quite characteristic in lacustrine systems (Boggs, 1995).

3.2.2. Plio-Quaternary Sinap Formation

The Plio-Quaternary units, unconformably overlying the Miocene sequences, are named as Sinap Formation by Tatlı (1975) (Table 3.1). Type locality is quite close to the study area at the northwestern continuation of the Plio-Quaternary units cropping out in the study area (located at 5.5 km northwest of Kazan town near a hill called Sinap that gives its name to the formation). Lithologically equivalent rock sequences in the study area are named as Sinap Formation. Gökten et al. (1988) named Pliocene clastics in their study as Memlik Formation. Although the ages somewhat differs, Türkecan et al. (1991) and Gökten et al (1996) called late Miocene gypsum bearing possible equivalent clastics unconformably overlying Middle to Late Miocene units as the Uruş Formation. But it is not clear whether those units are equivalents of the Plio-Quaternary units with the Kazan area or not. The Plio-Quaternary units in Kazan area are free from gypsum bearing levels.

The Plio-Quaternary units crop out in; a NE-SW trending area between Çalta and Sarılar villages, at the north and northwest of Karalar village, the area near to eastern boundary of the study area, between Evci and Çalta villages, between Çalta and Alibey villages and at the southwest of Sarılar village (Plate 1).

The unit is dated as Early Pliocene with mammalian fossils at west of Çalta village and its type locality near Sinap hill in Yassıören village (Kazan) (Ozansoy, 1961; Tekkaya, 1973; 1974; Şen and Rage, 1974; Tatlı, 1975).

However, there is not any suitable volcanic rock for radiometric age dating within the sequence. They overlie the Middle Miocene units with an angular unconformity and have clasts derived from the underlying Miocene units, thus the age of the units is anticipated to be post-Miocene, as Plio-Quaternary. Semi-consolidated nature of the lithologies supports the above interpretation. Demirci (2000) assigned Late Miocene (7.7 ± 0.4Ma) age to gypsum-bearing clastics overlying Miocene sequences in Beypazarı region by performing K-Ar age dating analysis on a tuff sample. The sample is from a sequence of similar clastics just below the massive gypsum beds in Ayaş area. But it is questionable if those units from which the age dating was conducted are simply the equivalents with the units cropping out in the study area or not.

The Plio-Quaternary units can easily be recognized in the field as they represent soft morphologies mostly with gentle dip amounts except the areas where highly deformed due to faulting. They are generally reddish to pinkish to cream in color, generally semi-consolidated and hardly give bedding planes except for more resistant conglomeratic layers (Figure 3.9). The dominant lithologies are; pinkish to reddish to grayish colored, coarse to fine grained polygenic conglomerates, red to pink to cream colored, fine to coarse grained siltstones/sandstones, cream to green colored claystones, white to cream colored clayey/silty limestones and white colored, resistant limestones.

Conglomerates vary in character from place to place. For example in the area at the north of Karalar village, they are pinkish brown to gray colored and semi-consolidated. They contain clasts of various origin, such as volcanics (pink, gray brown and purple colored), igneous (gray colored) and chert (brown and orange colored) clasts, which are sub-rounded and moderately to poorly sorted (Figure 3.10). Between Çalta and Evci villages, steeply dipping loose conglomerates interfingering with cream to brown

Figure 3.9. General view of the Sinap Formation unconformably overlying the Pazar Formation, at ~500 m southwest of Sarılar village (photo towards NNE).

Figure 3.10. Close-up view of the conglomerate layers composed dominantly of chert clast. Location is ~1.5 km east of Gölköy village. Hammer is 33-cm-long.

colored, clayey siltstones/sandstones were observed. Conglomerates at this spot are composed of rounded to sub-rounded volcanic clasts and chert pebbles. Pebble imbrication developed parallel to bedding is quite evident within individual beds. Also at the southwest of Sarılar village, poorly sorted, clast-supported, semi-resistant conglomerates, which are underlain by pinkish white colored fine sandstones, contain dominantly volcanic pebbles and minor chert pebbles. Similar conglomerates dominated by volcanic clasts are also present at the upper levels of the section between Sarılar and Çalta villages. But they are coarser grained (up to 40cm clasts), more poorly sorted (see measured stratigraphic section-3). Another type of conglomerate with less or no volcanic clasts was also seen in the study area. They are creamish to gray colored, relatively resistant, clast to matrix supported and poorly to moderately sorted. Their matrix is made up of an argillaceous and calcareous material. Clasts range varies from sand to boulder and are composed of sub-angular to angular cherts (yellow, orange and brown colored) and sub-rounded silicified clayey limestones (cream colored). Those conglomerates are widespread especially in the area between Çalta and Gölköy villages. Sandstones, siltstones and claystones are the dominant and extensive rock units within the Plio-Quaternary outcrops in the study area. They are cream to pinkish to light brown colored, semi-consolidated and clayey. Sometimes sandstones form resistant ridges. They often possess cross-laminations or cross-beds (Figure 3.11). Claystones are cream to green colored and kaolinitic. They are mainly present in the lower levels of the section at the area between Sarılar and Çalta villages. They are recognized easily by their distinctive white colors. Limestones are cream to pinkish colored, clayey to silty and sometimes sandy. They are usually soft and altered by post-depositional hydrothermal alteration (mesh structures, Figure 3.12). Resistant limestones are white colored. They are generally suffering from internal brecciation and possess travertine properties (wavy beddings, lenticular vugs etc.). Those limestone lithologies are widely observed unconformably overlying the Miocene units in an area at the north of Karalar village (see measured stratigraphic section-1).

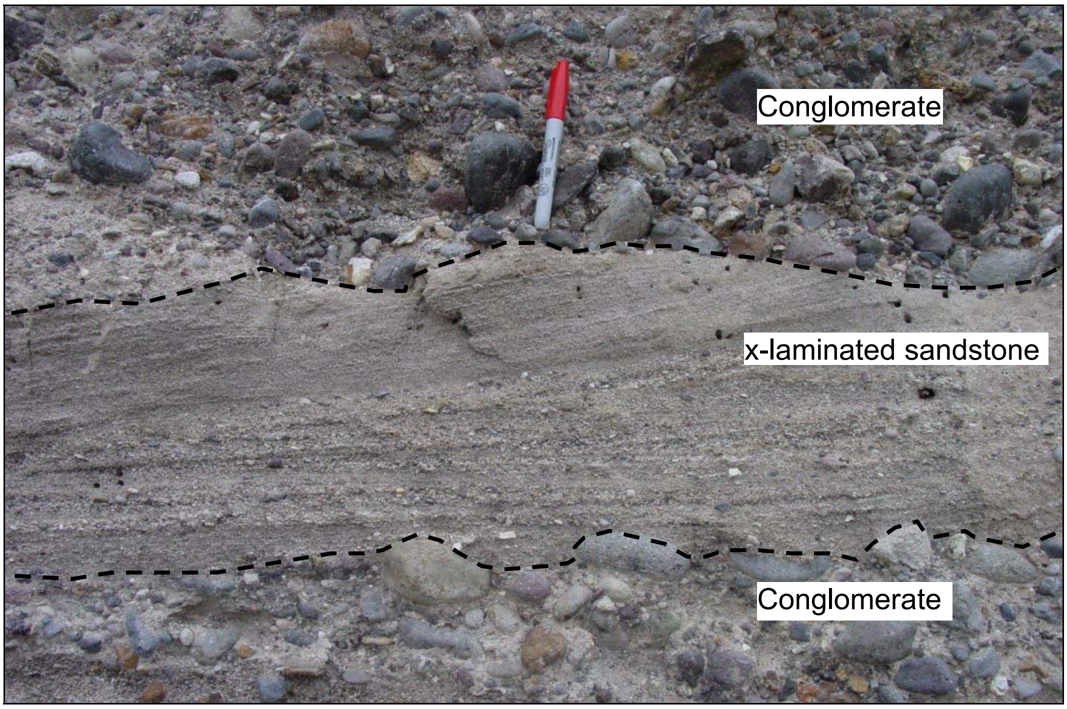

Figure 3.11. Cross-laminations commonly observed in the sandstones of Sinap Formation. The pencil is 13-cm-long.

Figure 3.12. Common mesh structures caused by hydrothermal alteration in clayey limestones of the Sinap Formation. Hammer is 33-cm-long.

Plio-Quaternary units unconformably overlie Miocene units all throughout the study area. Only in one area, at the north of Karalar village, they are observed to overlie the basement rocks with an unconformity (around Sivri hill). They also have faulted contacts with Miocene units in many places. The best localities where the angular unconformity with the underlying Miocene units is evident are; at the west of Çırpan village and at around 2 km north of Karalar village (Plate 1). Plio-Quaternary units are unconformably overlain by Quaternary terrace deposits and alluvium.

Measured stratigraphic section-1 (Figure 3.6), whose location is described in section 3.2.1., continues with 44.4 m-thick Plio-Quaternary units unconformably overlying the 100 m-thick Miocene units. The following Plio-Quaternary lithologies were encountered in the section, from bottom to top; 1) 20.8 m-thick conglomerate and sandstone; red to cream colored and interbedded with cream to pinkish colored clayey/silty limestones. Conglomerates are moderately sorted, clast-supported with chert, quartz and limestone clasts (up to 15 cm) in a calcareous sandy matrix; 2) 4.8 m-thick silty limestone; cream colored, often possesses mesh structures with occasional chert infilling; 3) 1.6 m-thick resistant limestone; white to gray colored, brecciated; 4) 4 m-thick silty/sandy limestone; cream to pinkish colored, fragile; 5) 1.2 m-thick resistant limestone; white colored; 6) 9.6 m-thick silty limestone; cream to light brown colored, mesh textured; 7) 2.4 m-thick resistant limestone/travertine; white to gray colored, vuggy and obscured (highly disturbed) bedding.

The last 14 meters of the measured stratigraphic section-2 (Figure 3.7) also ends with Plio-Quaternary units unconformably overlying the Miocene units. The lithologies from bottom to top are; 1) 13 m-thick claystone and sandstone; red to pink colored and interbedded with pinkish cream colored sandy limestone, which has mesh structures and vugs. 2) 1 m-thick resistant travertine limestone; white to gray colored, occasionally brecciated and contains vugs.

Stratigraphic section-3 (Figure 3.13) was measured at the west of Sarılar village. This section, whose total thickness is 105.2 m, represents the whole area between Sarılar and Çalta villages. The lithologies measured in this section are as follows, from bottom to top; 1) 11 m-thick kaolinitic claystone; green to cream colored. 2) 12.8 m-thick alternation of green colored kaolinitic claystone; gray colored, thin bedded travertine and creamish colored clayey limestone; 3) 0.8 m-thick resistant travertine limestone; gray colored, highly vuggy with mesh structures; 4) 3.6 m-thick clayey limestone; greenish colored (non-resistant); 5) 1.2 m-thick resistant travertine-limestone; gray-cream colored, fine crystalline. Karstic vugs and brecciation are common structures; 6) 8.8 m-thick non-resistant claystone; olive brown colored, slightly calcareous. It is usually interbedded with thin bedded very clayey limestone; 7) 8 m-thick claystone and limy claystone; pinkish brown colored; 8) 8 m-thick conglomerate and sandstone. Conglomerates are resistant, gray to cream colored, moderately sorted, mostly matrix supported. Clasts are dominantly sub-angular chert clasts. Grading is obscure and there are no other sedimentary structures. Sequence is fining upward; 9) 4.8 m-thick sandstone; cream to white colored, resistant, medium to thick bedded and calcareous; 10) 8 m-thick alternation of claystone and sandstone; pinkish brown to cream colored and limy; 11) 1 m-thick conglomerate; resistant, gray colored, moderately sorted and clast supported. It is composed of sub-rounded volcanic and sub-angular chert clasts (max. ~5 cm). There is no obvious imbrication of clasts; 12) 2.4 m-thick cream colored, pebbly sandstone; 13) 5.6 m-thick alternation of reddish brown colored claystone and sandstone; 14) 9.6 m-thick coarse conglomerate; poorly sorted and matrix supported. Rounded boulders (up to 40 cm) of volcanic origin (dominantly basaltic composition) float in a pinkish colored sandy matrix; 15) 9.6 m-thick reddish brown to cream colored clayey sandstone; 16) 10 m-thick coarse conglomerate; boulder-size fragments, poorly sorted and matrix supported but it contains more chert clasts.

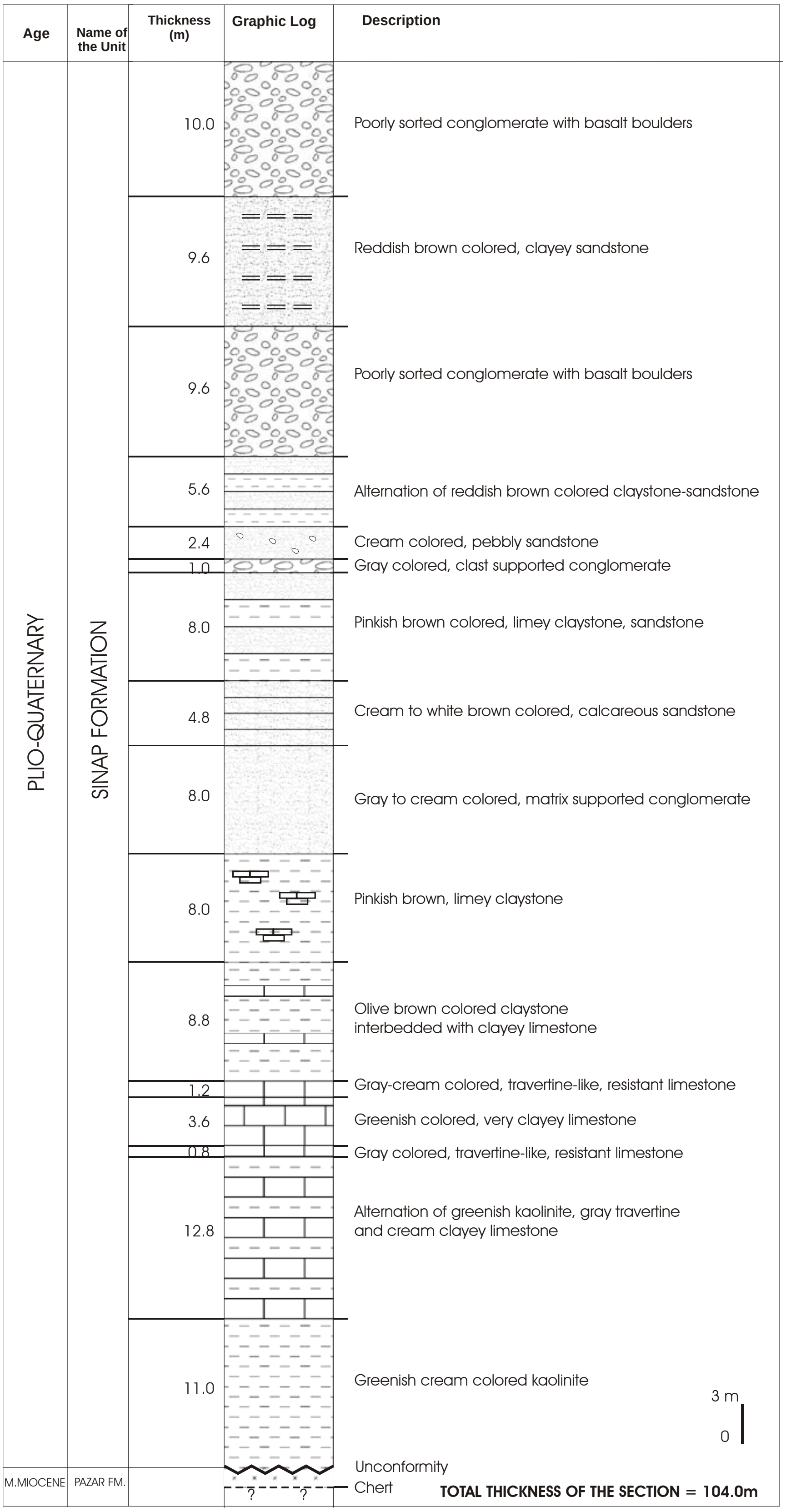

Figure 3.13. Stratigraphic section-3 measured near Sarılar village. (Starting point = E: 462987, N: 4453537; End Point = E: 463338, N: 4453867).

By using the information gathered from the measured stratigraphic sections and observations during the fieldworks, the thickness of Plio-Quaternary units in the study area can be estimated as around 150 m.

Although no specific fossils depicting a certain environment found, by looking at the properties of widespread red to pinkish colored coarse clastics, it is obvious that the environment of deposition of the units is a continental environment. More specifically, presence of cross-beds in the sandstones, channel type conglomerates, imbrication of the pebbles and poorly to moderately sorted conglomerates with hardly distinctive gradation (indistinct fining upward deposition) indicates an alluvial-fan to fluvial environment (Boggs, 1995). In addition, existence of kaolinitic clays and limestones at some localities means that a fresh-water lacustrine environment had prevailed for some time in the area.

3.3. Quaternary Units

This group of sedimentary units includes; (1) Quaternary aged products of recent deposition in stream channels and creeks throughout the study area and (2) relatively older terrace deposits (Erol, 1961). Young unconsolidated sediments occupy large areas mainly at the northwestern portion of the study area between Gölköy and Çalta villages (Plate 1). They are composed of loosely consolidated to unconsolidated conglomerates and sandstones containing clasts of variable sizes from all other underlying units.

Quaternary terrace deposits include nearly horizontal beds of terrace conglomerates and sandstones very well observed at the southwest of Çalta village near İnönü hill and at the northwest of Çırpan village. Conglomerates are dark gray colored and composed dominantly of sand to boulder-size (max. ~30 cm) basaltic and volcanic clasts, which might have been derived from Galatian volcanics. They are poorly sorted and clast supported. Clasts are sub-rounded to rounded and cemented in an argillaceous and calcareous matrix. There are also rare sub-angular chert pebbles (Figure 3.14).

Age of these units is assumed as Quaternary since they overlie the Plio-Quaternary units with a clear unconformity and they represent gently dipping plains at the hill tops and valley floors (Figure 3.14). Observed thickness of the unit is about 10 meters. Environment of deposition of the units is most probably fluvial.

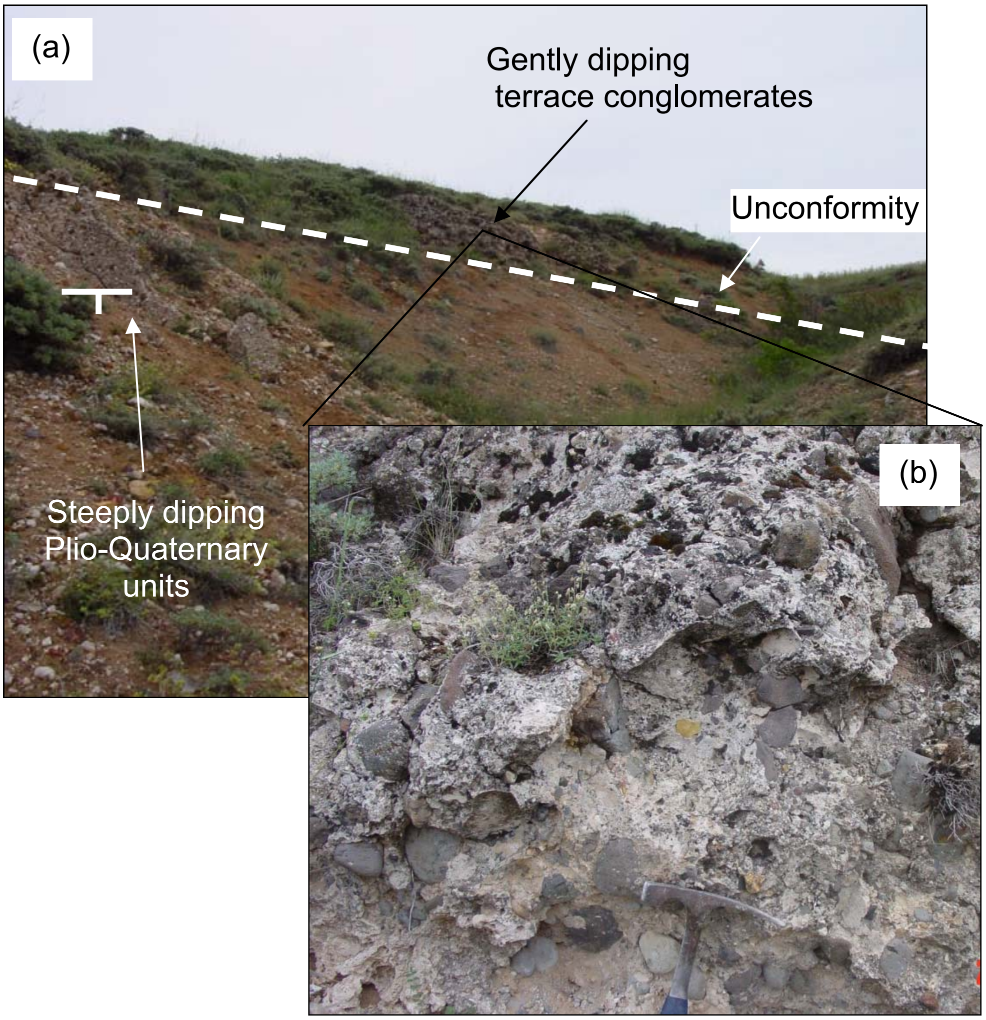

Figure 3.14. (a) The unconformity between Plio-Quaternary units and gently dipping terrace conglomerates. Location is ~200m SW of Çalta village. Photo is towards SE. **(b)** Typical appearance of terrace conglomerates at ~750 m southwest of Çalta village near İnönü hill. Pebbles are dominantly composed of basalt.

CHAPTER 4

STRUCTURAL GEOLOGY

Description of the observed geological structures together with analysis and interpretation of the structural data gathered during the extensive field studies will constitute the main subject of this chapter. Principally, two types of structural data were collected: (i) dip-strike measurements of bedding planes and (ii) slip-lineation data from the fault planes. The description and analysis of the geological structures, - bedding planes, folds, faults and unconformities -, will be given in the following sections.

4.1. Bedding Planes

Totally 213 dip-strike measurements of the bedding planes from the different units were taken. 157 measurements out of 213 were collected from the Miocene units and 55 measurements out of 213 are from the Plio-Quaternary units.

For the analysis of bedding planes, rose diagrams are prepared by using RockWorks-2002 software (www.rockware.com) for rocks of the same age and for the whole data. In order to have a better understanding of bedding attitudes, dip-strike data is elaborated for each formation. Since the Quaternary terrace units crop out in a very limited area, there is not enough number of measurements to conduct a bedding plane analysis. So they will be skipped. Similarly, the analysis for other Quaternary units is not performed as they do not display any bedding planes.

If a generalization is made by looking at the rose diagram of all strike measurements, it can be said that all of the units in the area tend to have a strike at NE-SW (average N55^{0} E) (Figure 4.1). Dip amounts measured have a broad range of values varying from gentle dips (05^{0}) to vertical (90^{0}) while the dip directions are either due to NW or SE.

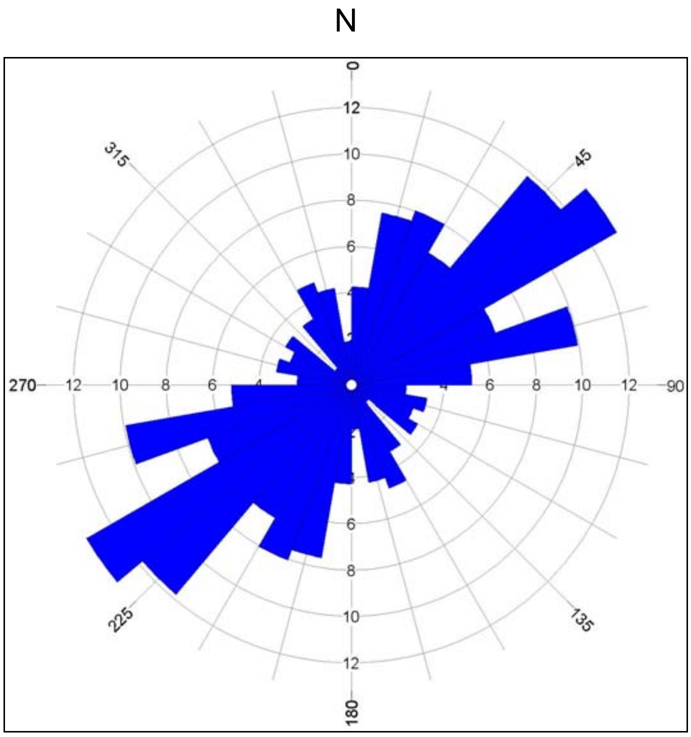

Figure 4.1. Rose diagram showing the strike measurements of bedding planes from Miocene-Plio-Quaternary units (n=213).

4.1.1. Miocene Units

157 measurements out of 213 were taken from the Miocene units over the study area. Since the Miocene units are older and undergone more deformation than younger units, larger number of measurements collected from these units in order to understand the bedding attitudes with a better accuracy. Folding, which will be studied in the next section, is quite common in the Miocene units throughout the study area. The attitude of bedding is

variable due to the later effect of folding and faulting. Bedding planes of the units were measured quite easily and it is also very easy to find bedding planes of the units in the field since they are mostly resistant and give good beddings in the outcrops throughout the study area. Only measurement of thick chert beds is problematic because their surfaces can be fairly irregular and this makes the bedding plane attitudes difficult to understand in the field. The cherts cover large areas the areas between Evci and İneköy villages, at the south of Sarılar village and at the east of Alibey village without giving a definite bedding plane. So in those specific areas, only a few measurements from the Miocene units are taken.

The rose diagram of the bedding plane measurements from the Miocene units drawn at 10^0 class intervals indicates that the most prominent strike trend is at an interval from N50^0E to N60^0E directions (average N55^0E) (Figure 4.2). It constitutes around 14.6% of the 157 measurements taken. The second most common strike trend with 10% of abundance and being close to the most prominent one is at an interval between N40^0E to N50^0E. There are also some other minor directions as indicated by the diagram. One is in the interval from N10^0E to N20^0E and the other is in the interval from N70^0E to N80^0E.

Dip directions of above mentioned trends are either NW or SE, which are the prominent dip directions in the study area. When basic statistics of dip amounts of the beddings are investigated, it is seen that they range from 05^0 minimum to 90^0 maximum. Especially in the areas where the deformation is evident (e.g., near Çalta village) bedding planes are steeply dipping with amounts reaching up to 90^0 (Figure 4.3). The average dip amount is around 32^0 and it has a standard deviation of 15.8 degrees (Table 4.1).

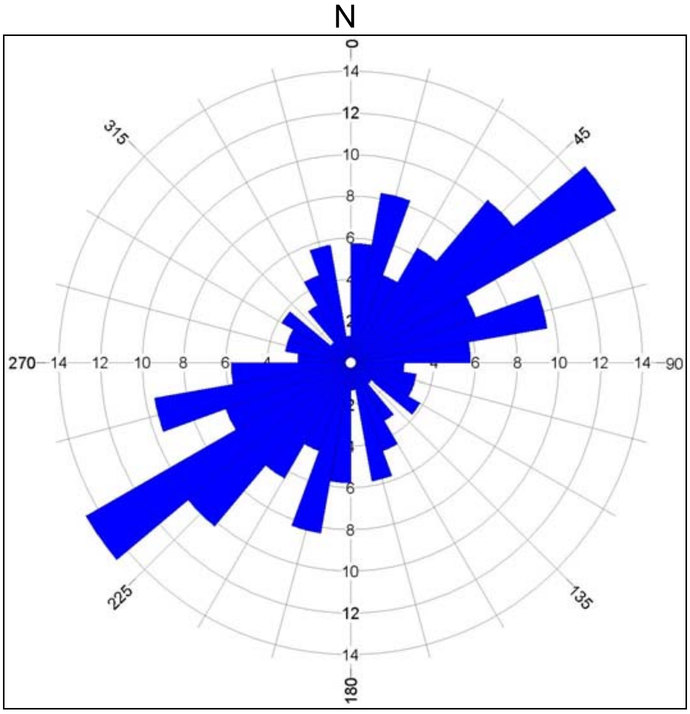

Figure 4.2. Rose diagram showing strike measurements taken from bedding planes of the Miocene units (n=157).

Figure 4.3. Steeply dipping (nearly vertical) silicified limestones of the Miocene Pazar Formation, at around 250 m northeast of Çalta village (photo towards NE), note the poles for scale (~10m).

4.1.2. Plio-Quaternary Units

55 measurements out of 213 were taken from the Plio-Quaternary units over the study area. The units are relatively less deformed thus the bedding planes seem to be more consistent throughout the study area. But at some places, especially at the northwestern part of the study area (around Çalta, Çırpan and Evci villages), bedding attitudes are variable due to intense deformation. Measurement of bedding planes is difficult in the field because they are usually semi-consolidated and do not give bedding planes in most of their outcrops. The units have soft morphologies where the bedding is quite indistinct. Only relatively more resistant conglomerates and silty-clayey limestones are suitable for bedding plane measurements.

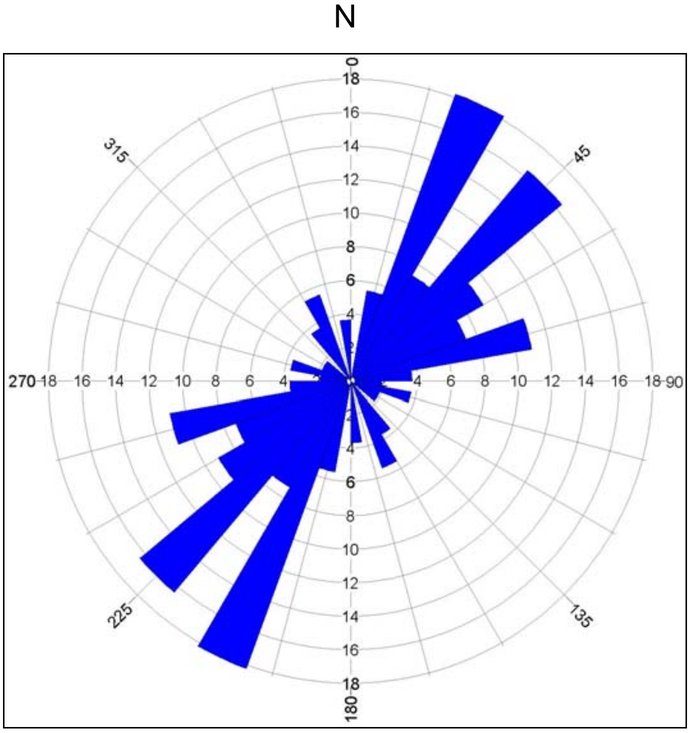

Figure 4.4. Rose diagram showing strike measurements taken from the Plio-Quaternary Sinap Formation (n=55).

When the rose diagram of the bedding plane measurements from Plio-Quaternary units is examined, it is seen that there are two prominent strike directions (Figure 4.4). The first (the most dominant) one is in an interval from N20^{0}E to N30^{0}E (N25^{0}E). It constitutes around 18.2% of 55 measurements. The second most dominant trend is in an interval from N40^{0}E to N50^{0}E (N45^{0}E) with a slightly lower abundance of around 16.2%. This gives a more or less NE-SW trend. There is another minor strike trend in an interval from N70^{0}E to N80^{0}E (N75^{0}E) having 11% abundance. Overall, statistical results point out that the dominant strike trend will be N40^{0}E to N50^{0}E.

Dip directions of above mentioned trends are either NW or SE, which are the most prominent dip directions of those units in the study area. When basic statistics of dip amounts of the beddings are investigated, it is seen that they range from 05^0 minimum to 87^0 maximum. Especially in the areas where the deformation is evident (e.g., at the southwest of Çalta village, near İnönü hill) bedding planes are steeply dipping with amounts reaching up to 87^0 (Figure 4.5). The average dip amount is around 28^0 and it has a standard deviation of 18.8 degrees (Table 4.1).

Table 4.1. Summary of the results obtained by rose diagrams together with the basic statistics on dip amounts.

	Dominant Strike Trend	**Abundance**	**Average Dip Amount**	**Maximum Dip**	**Minimum Dip**
Miocene	N50^0-60^{0}E	14.6%	32^0	90^0	05^0
Plio-Quaternary	N40^0-50^{0}E	16.2%	28.4^0	87^0	05^0

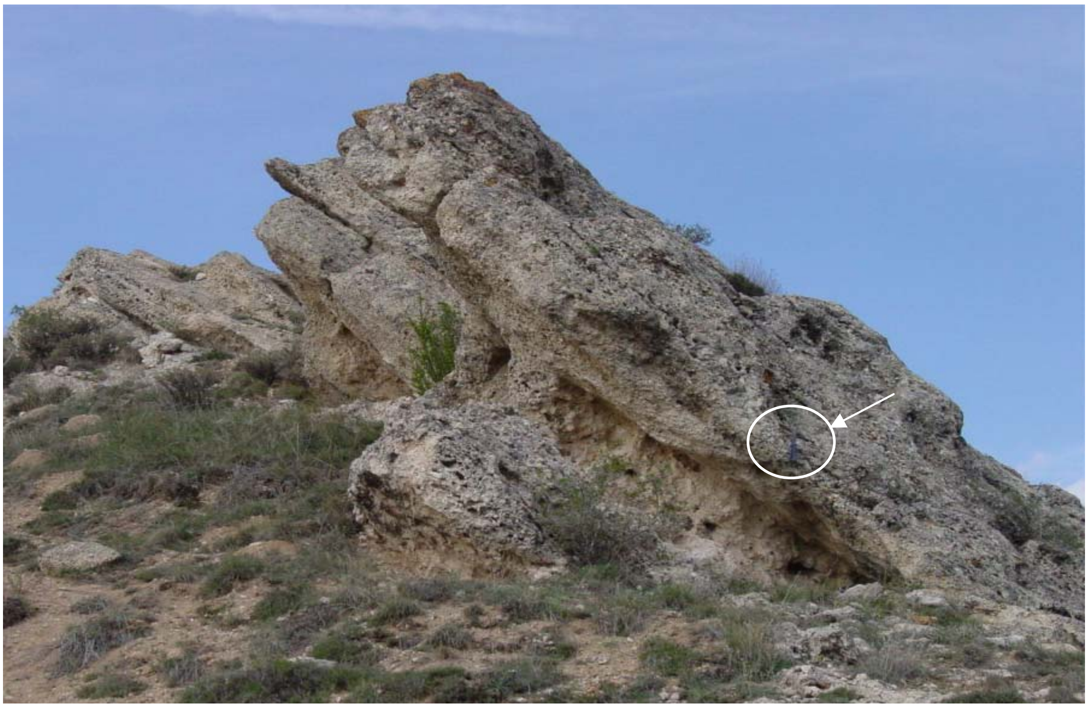

Figure 4.5. Conglomerates of the Plio-Quaternary Sinap Formation dipping (~47^0) towards SE, at ~1.5 km east of Gölköy village. Note the arrow pointing out the hammer for scale (33-cm-long).

4.2. Folding

Folds are one of the most distinguishing geological structures deforming the Post-Miocene units in the study area. Mainly anticlines and synclines, and rarely monoclines of variable sizes from outcrop-scale to mappable-scale can often be observed throughout the study area. To get a better understanding of folding in the area, folds in the post-Miocene units will be examined in two groups; (i) folds developed in the Miocene units and (ii) folds developed in Plio-Quaternary units. Firstly the major fold structures observed in the study area will be described seperately for each formation. Then the results of fold analysis conducted for each formation will be explained and interpreted. Fold analysis is a statistical analysis performed by plotting bedding plane data (dip-strike measurements) on a stereonet.

Fold analysis principally aims to find out the attitude of the fold axis of a large structure present in a region. It is also used to calculate the average bedding attitudes of units in a region. For performing a fold analysis, Schmidt net (equal-area net) is preferred. It maintains the proportion of the lower hemisphere surface projected to the plane of the net. In other words, no preferred alignment of data will be apparent if the data are truly random. For the plotting of a large number of structural data elements, the equal area net is used to remove any bias when interpreting the average trend of the data. It is also necessary to contour the data rather than plot individual points or great circles since if a large number of data is plotted on a net, the diagram may become overwhelmed by the number of plotted data, making it difficult to interpret for structural trends. Moreover, it is generally more convenient to plot the poles to the planes (beddings), rather than the planes themselves, because the diagram becomes very crowded when there are a large number of planar data. This diagram is called as π-diagram. The plotted points (poles to planes) tend to line up along a great circle and the vectors representing the plotted points tend to lie within a plane. The vector that is perpendicular to the plane defined by this great circle, which is also called as best fit circle or girdle, gives us the fold axis.

4.2.1. Miocene Units

Miocene units are intensely folded within the limits of the study area. They are relatively more folded and deformed than the Plio-Quaternary units in the study area. Size of the structures ranges from outcrop-scale to mappable-scale. The reason for presence of relatively more folding in Miocene units is most probably that they are older and underwent more deformation during the tectonic history of the area. General trend of axes of the folds in the units is along NE-SW. But sometimes axes are curved gradually towards NNE-SSW direction.

The northern part of the study area - at the northwest of Çırpan village - is composed of successive major fold structures (Plate 2). The series of folds, FL-1, at the north of Çırpan village extend through out of the study area but lengths of their fold axes are not more than 1 km. An anticline located along the Öteyüz creek has a fold axis with NE trend and dip amounts around 40^0 to 44^0 displays a major structure within this series of folds. The folds have a trend in NE-SW direction. Dip amount at the northwestern limb of the northern anticline is 35^0. The syncline at its south has a northwestern limb (southeastern limb of the anticline) dipping at 25^0 to 35^0 while the dip amount is 32^0 at its southeastern limb. The fold structures at the NW of Öteyüz creek have a NE-SW trend with a plunge direction towards SW. Their lengths are not more than 1 km. They have dip amounts ranging from 24^0 to 72^0. Thus most of these structures are asymmetric with SE and NW-directed vergence.

There are three major fold structures in the NE-SW trending elongate outcrop that embraces Çalta village in the middle of the study area (Plate 2). First one, FL-2, is an anticline in the center of a narrow outcrop at south of İnönü hill. Its fold axis runs around 1 km towards NE and ends at southeast of Çalta village. The anticline is plunging towards NE and there is a monocline structure at its northeastern end (Figure 4.6). Northwestern limb of the anticline is more inclined, at 37^0 to 60^0, than its southeastern limb, which dips at 29^0 to 45^0. So this structure is asymmetric with a vergence in NW direction. Second one, FL-3, is also an anticline, whose fold axis starts at south of Çalta village. It trends in NE-SW direction and curves about 10^0 towards N (i.e. the axis becomes NNE-SSW-trending) at its northern end, which is located at the east of the village. Dip amount at its northwestern limb is 40^0 while it is quite steep, about 80^0, at its southeastern limb. So FL-3 is asymmetric with a vergence in SE direction. The third fold structure, FL-4, is composed of one syncline and one anticline at the north and northwest of Çalta village. The syncline is concealed under the overlying Plio-Quaternary units but by looking at the bedding attitudes, it can be deduced that the

Figure 4.6. A monoclinal structure developed within Miocene units observed at ~750 m SE of Çalta village (photo towards ENE).

Miocene units form a syncline. Beddings in the northwestern limb have dips between 15^0 and 21^0 and between 23^0 and 53^0 at the southeastern limb.

The spatially extensive Miocene outcrop trending NE-SW at the eastern part of the study area contains two major fold structures. First one, FL-5, consists of a broad anticline and syncline couple at the northeast of Sarılar village (Plate 2). The anticline has a fold axis trending in NE direction. It has a slight curvature towards north. It plunges towards SW. Beddings in its northern limb have dips from 10^0 to 27^0. Its southeasterly dipping southern limb hosts a monocline structure (Figure 4.7). Axis of the monocline has also NE-SW trend. It has a length of about 1 km. The horizontal distance (i.e. its width) between its upper hinge and its lower hinge reaches up to 250 m. Beddings in this structure have dip amounts varying from 05^0 to 53^0. Fold axis of a gentle syncline at the south of the monocline is recorded. Dip amounts at both its northern and southern limbs are gentle, changing from 10^0 to 12^0.

Second structure, FL-6, in this area is composed of a couple of successive NE-SW trending anticline and syncline situated at NNW of Karalar village. The syncline at north has a steep northwestern limb with a dip reaching up to 57^0. And the anticline at south has limb angles ranging from 24^0 to 45^0.

Fold structures in the other parts of the Miocene outcrops (e.g., between Evci and İneköy villages) remain unclear due to lack of sufficient dip-strike measurements and intense deformation due to faulting.

Fold analysis by using the dip-strike measurements from the Miocene units is performed with the help of RockWorks 2002 software. When the resultant contoured stereonet diagram obtained is examined (Figure 4.8) , it can be confidently said that the bedding plane measurements of Miocene units are quite consistent throughout the study area with two prominent bedding planes as indicated by two maximum concentrations in the diagram. First one is $N45^0E/27^0SE$ having about 7% abundance. And the other one is $N60^0E/16^0NW$ with about 6% abundance. When those results are compared with the ones obtained by rose diagrams in the previous section, it is seen that there is a great conformity. The above calculated measurements fall into the interval of dominant strike trends found by using the simple rose diagrams. Presence of two dominant bedding plane trends, which are more or less parallel, with two opposing dip directions (i.e. NW and SE) suggests that there are large scale asymmetrical folds (or successive anticlines and synclines), whose axes have fairly consistent trends all over the region. That common fold axis can be found by using the best fit circle (or girdle, the thick blue line in the Figure 4.8) calculated by the program. The axis of the folding is perpendicular to the direction of the girdle. Fold axis is found to be in $N46^0E$ direction.

Figure 4.7. The monoclinal structure in the Miocene Pazar Formation, FL-5, at ~1.2 km northeast of Sarılar village (view to NE).

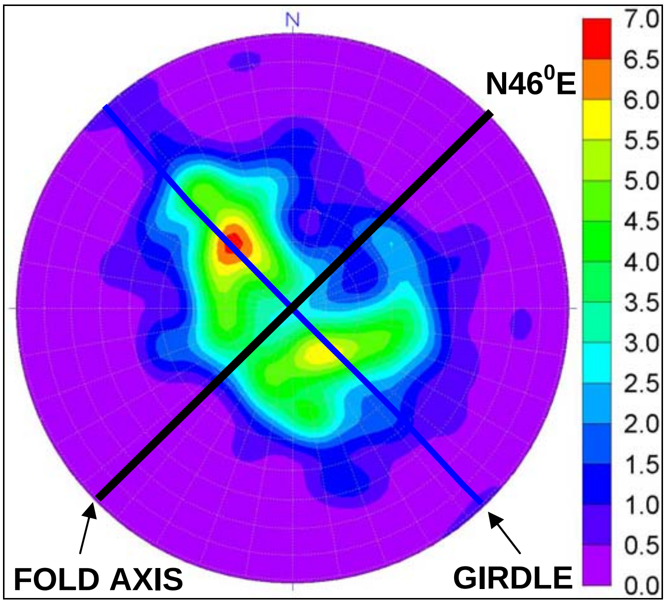

Figure 4.8. Stereographic contoured plot of the bedding plane measurements taken from Miocene units (n=157).

4.2.2. Plio-Quaternary Units

Plio-Quaternary units are also commonly folded in the study area. However folding in these units is much less intense and folds are broader having gentler limb angles with respect to the Miocene units. General trend of fold axes in the units is along NE-SW. But, in some places axes are curved towards NNE-SSW direction.

The area at the northeast of Evci village is a type locality for the folding in the Plio-Quaternary units. There are two main combinations of fold structures in that area (Plate 2). First group, FL-7, is located at 500 m northeast of the village and composed of a pair of anticline-syncline. Trend of their axes is approximately NE-SW. Core of the anticline structure is eroded so that the Miocene units are exposed. The probable anticline axis is located in the center of this Miocene outcrop. The syncline is present at the southeast of this anticline. Dip amounts on both limbs of the anticline and the syncline are quite uniform ranging from 20^0 to 29^0. Second group, FL-8, is also positioned between Çalta and Evci villages and composed of syncline-anticline-syncline structures, respectively, from northwest to southeast. Axis of the syncline continues roughly in NNE direction (Plate 2). It becomes abruptly curved to roughly NE direction at its northern end. Southern edge of the syncline has steep dips on both its northwestern and southeastern limbs, ranging from 37^0 to 69^0 while its NE-trending northern continuation has dip amounts ranging from 15^0 to 40^0 at its limbs. The core of the anticline in the middle is eroded so that the Miocene units are exposed. The probable anticline axis, which trends NE-SW, is at the center of this Miocene outcrop. However the anticline in Plio-Quaternary units has shallower dip angles around 20^0. NE-SW trending southeastern syncline has limb angles close to the ones in the anticline, around 24^0.

The largest Plio-Quaternary outcrop, which extends NE-SW in the middle of the study area between Çalta and Sarılar villages, hosts an outcrop scale gentle folded structure, FL-9, composed of successive syncline-anticline-syncline structures from northwest to southeast respectively (Plate 2). Although their axes have smooth curvatures along their courses, they all

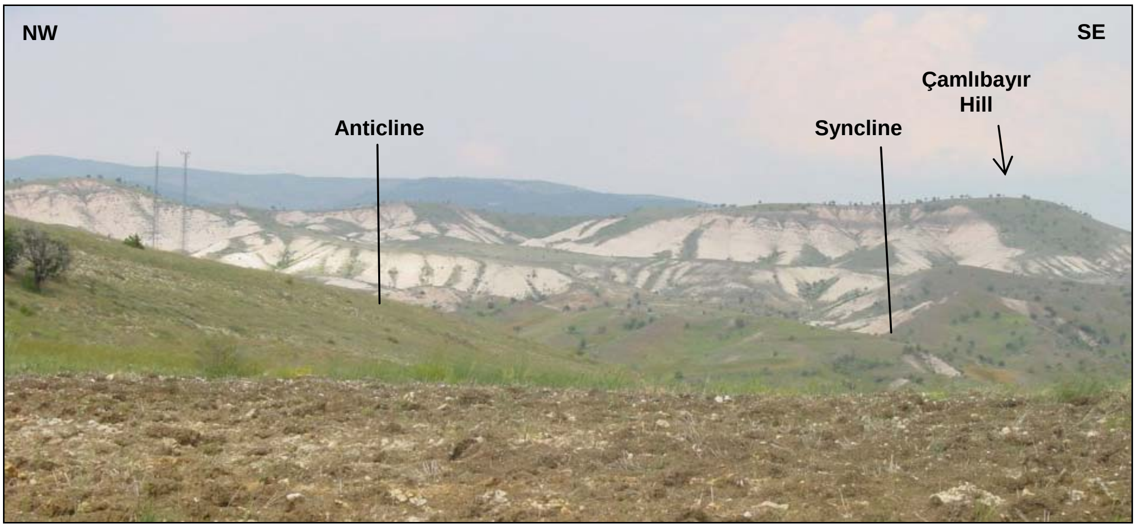

Figure 4.9. A broad anticline and a syncline (FL-9) in the Plio-Quaternary Sinap Formation, NW of Sarılar village.

have roughly NE-SW trends. The longest of all, the syncline at the north, has a length of about 4 km. Since the available dip-strike measurements in this specific area are scarce, the structures are not very well defined.

When the contoured stereographic plot of dip-strike measurements is examined, it is clearly seen that the bedding planes of Plio-Quaternary units are quite consistent over the study area (Figure 4.10). The diagram is not scattered at all and there are two maximum concentrations of beddings. First one is N45^{0}E/17^{0}SE having 11% abundance and the second one is N35^{0}E/19^{0}NW with 14% abundance. Just by looking at the above results, which give two parallel strike trends with opposite dip directions, it can be easily said the folds are almost symmetric. Common fold axis of those structures is located perpendicular to the best fit circle calculated by the program (thick blue line in the Figure 4.10). It gives N40^{0}E direction. Moreover, the concentration of data points pretty close to the center in the stereographic plot and absence of scattering of the points suggest that the

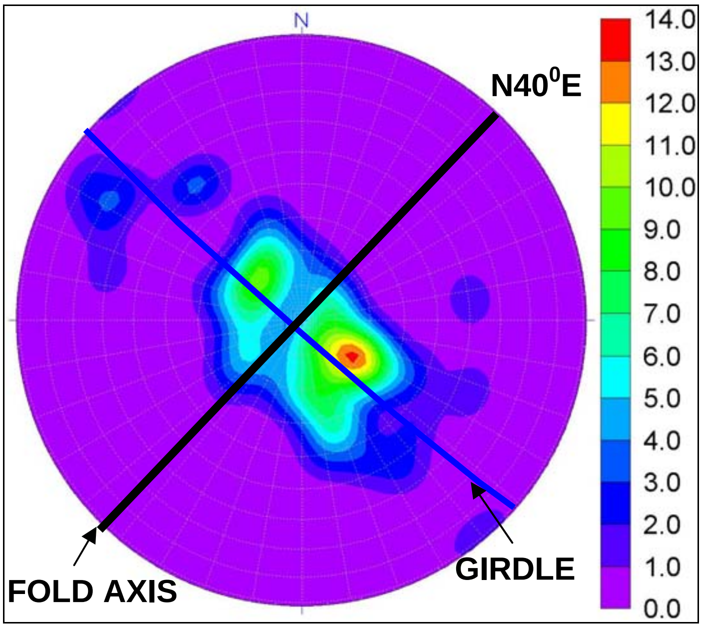

Figure 4.10. Stereographic contoured plot of the bedding plane measurements taken from Plio-Quaternary units (n=55).

inter-limb angles of the fold structures in the units are not steep and the structures are broad and gentle. This interpretation is fairly consistent with the field observations on fold structures in the Plio-Quaternary units.

4.3. Unconformities

There are four unconformities observed in the study area. The first one is the one between the Miocene units and underlying pre-Miocene basement rocks. This unconformity is non-conformity where the units overlie crystalline rocks (i.e. schist) and angular where they overlie bedded rocks (e.g. Eocene conglomerates). It is observed only in the southeastern corner of the study area. Best places observed are between Karalar and İneköy villages and the north of İneköy village (Plate 1). The second unconformity is the one between Plio-Quaternary units and pre-Pliocene rocks. This unconformity is non-conformity where the units overlie crystalline rocks (i.e. schist) and angular where they overlie other rocks (e.g. the Miocene units). This is the most widespread unconformity observed throughout the study area (Figure 4.11). The boundary between those units is always an unconformity otherwise it is faulted contact. In some places, the angular difference between the dips of the Plio-Quaternary units and the Miocene units is so small that angular relationship is not well-pronounced. The third unconformity is between the Quaternary terrace deposit and the underlying pre-Quatarnary units. Gently dipping Quaternary terrace deposits have an angular relationship with the underlying more steeply dipping post-Miocene units (Figure 4.12). It is clearly observable in places: (i) 1 km southwest of Çalta village in İnönü hill where terrace units overlie Plio-Quaternary units (Plate 1), and (ii) 1.2 km northwest of Çırpan village where the terrace deposits clearly overlie the Miocene units. The last unconformity is the youngest one between the Quaternary deposits and older units in the study area.

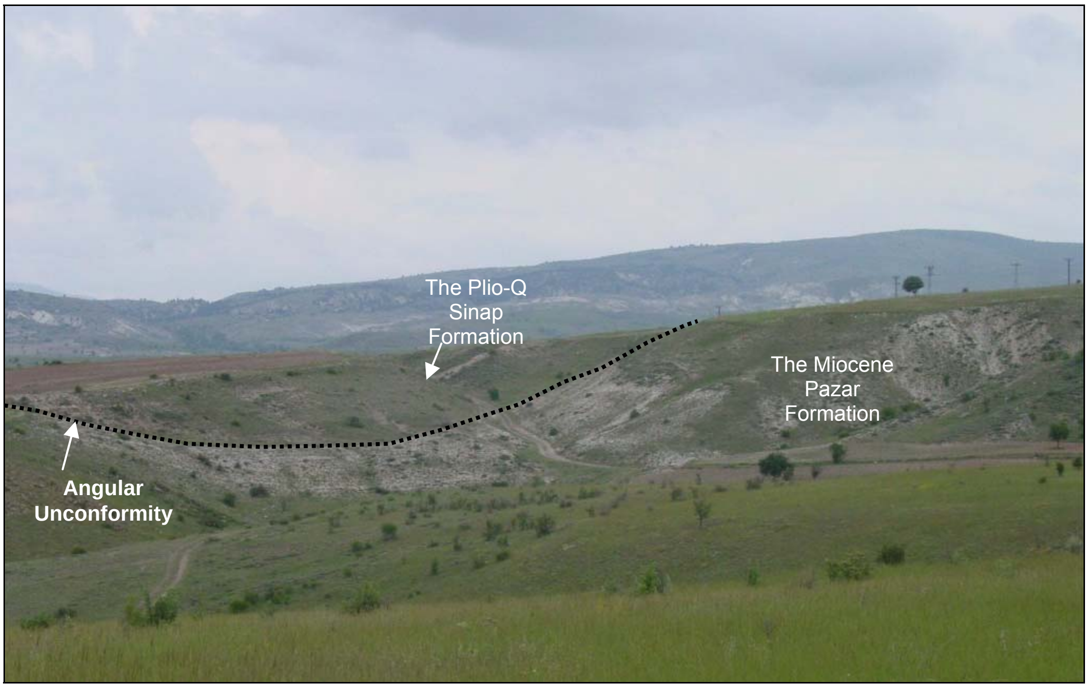

Figure 4.11. The angular unconformity between the Miocene Pazar Formation and the Plio-Quaternary Sinap Formation. Location is ~1.5 km soutwest of Çalta village, view to NNE.

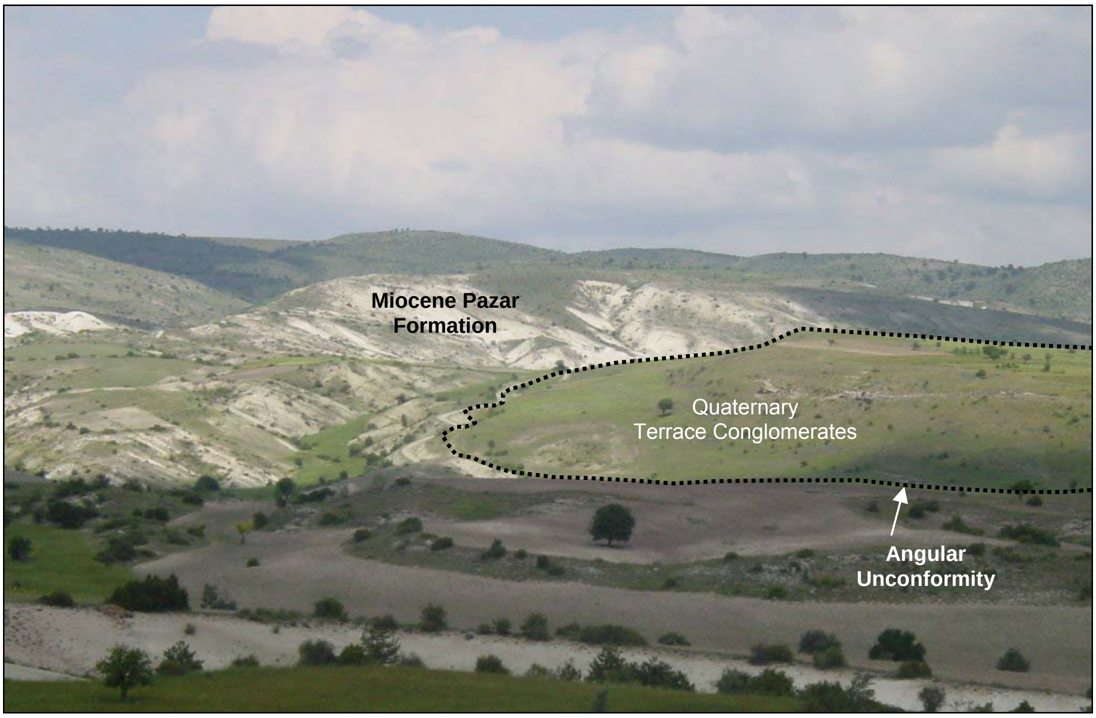

Figure 4.12. The angular relation between the Quaternary terrace deposits and the mudstones of the Miocene Pazar Formation. Location is at ~2.5km NW of Çırpan village (view is towards NE).

4.4. Faults

In this section, the major faults in the study area will be explained. The information given in this section will help to better evaluate slip analysis, which will contribute to understand the tectonic evolution of the study area.

During the field studies, faults are mapped at 1:25,000 scale. The faults recognized in the aerial photos prior to the field studies were also checked in the field. Numerous slip data measurements (where available) from the faults were taken for slip data analysis. There are many small- to large-scale faults developed in the Miocene and the Plio-Quaternary units. Some of them form the boundary between the Miocene and the Plio-Quaternary units. Some are confined to one of these units and yet some others cut both the Miocene and the Plio-Quaternary units. Possible estimated age of faulting is based on the cross-cutting relations. Age of the youngest unit in which the fault is developed was taken as the oldest age of the faulting. Types of the individual faults were determined either by using the slickenlines, where available, or other field observations (drags, offsets, juxtaposition, cross-cutting or shear sense indicators).

On the structural map of the area (Plate 2), it is easily seen that most of the structures strike in NE-SW direction with additional NW-SE- and N-S-trending features. According to their trends, the post-Miocene faults are grouped into three sets; (1) NE-SW-trending faults; (2) NW-SE-trending faults; and (3) N-S-trending faults. Syn-depositional faults observed in Plio-Quaternary units will also be examined in a separete section.

The faults are named by giving numbers to the twenty-four faults named from Fault-1 to Fault-24.

4.4.1. NE-SW-Trending Faults

The Fault-1 is located at around 750 m northeast of İneköy village (Plate 2). It is developed mainly in the Miocene Pazar Formation but also observed to cut through the Sinap Formation. It initiates in Miocene units at ~500m ENE of İneköy village and goes through NE-SW direction. Fault plane dips at 30^0 towards N. Character of the fault is dominated by left-lateral movement with a reverse dip-slip component. There are 5 slip measurements on this fault (Site-19, Site-25, Site-27 and Site-29).

The Fault-2 is located close to Fault-1 at NNE of İneköy village (Plate 2). It is observed only in the Miocene Pazar Formation. A part of the fault forms the boundary between Miocene units and the basement rocks. The curvilinear fault trends from NNE at its southern tip to more or less N-S at its northern edge. Fault plane dips steeply close to 90^0 towards N. It is right-lateral strike-slip fault with a reverse dip-slip component. There are 5 slip measurements taken from the fault plane (Site-22 and Site-23).

The Fault-3 is one of the most important major faults in the study area. It is situated at the southeastern part of the study area at around 1.75 km southeast of Sarılar village (Plate 2). It extends for about 3 km in the study area starting at around 1.5 km SE of Sarılar village. It mainly strikes through NE-SW but it makes a slight curvature to NNE direction near the main road from İymir village to Sarılar village (Plates 1 & 2). The fault is developed in tuffaceous sandstones, claystones of the Pazar Formation. The plane of the main fault dips towards N with dip amounts varying from 65^0 to 87^0 (Figure 4.13). Character of the fault also varies from left-lateral fault with reverse component to reverse fault with left-lateral component. There are 67 slip measurements from this fault (Site-44, Site-44/2, Site-224 and Site-225). These sites are among the rarest places in the study area where the relation between the older reverse movement and the younger normal movement is clearly observed. As seen in the slip data, there are normal faults cutting Fault-3 at these localities.

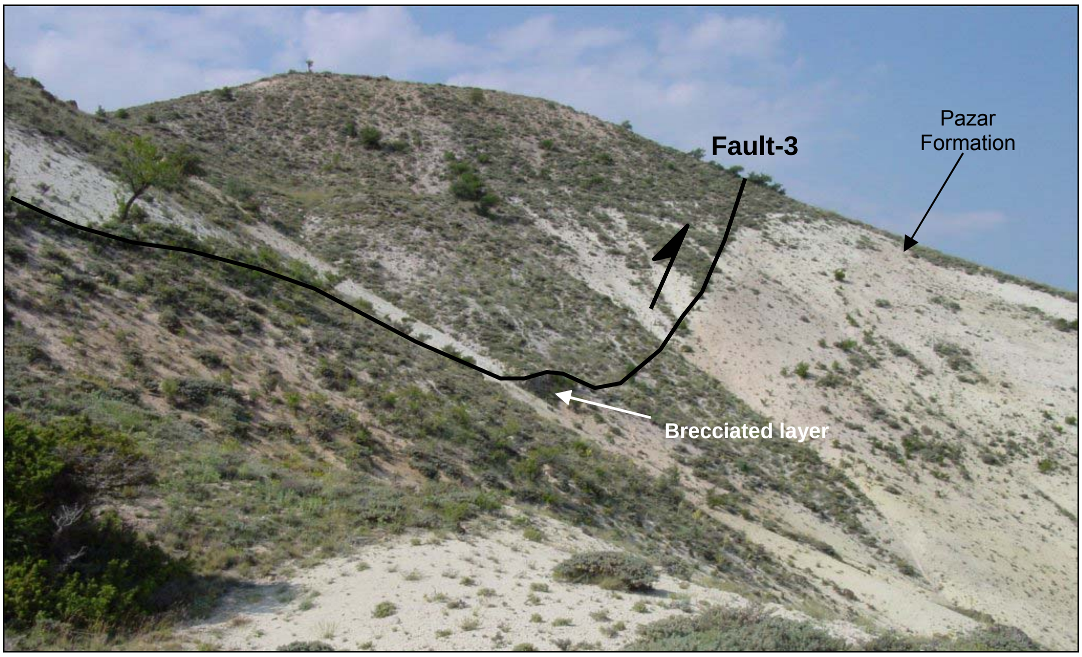

Figure 4.13. A reverse fault, Fault-3, observed in the Pazar Formation (see Site-44, Site-44/2 and Site-223 for the slip data). View is towards NE.

The Fault-4 is the reverse fault that passes through Sarılar village. It starts at ~300 m SW of Sarılar village and goes through NE-SW direction for some 1.25 km (Plate 2). The fault is hosted by the cherts and clayey/silicified limestones of the Miocene Pazar Formation. Fault plane dips at around 60^0 to 67^0 towards N. Character of the fault is oblique-slip with dominant right-lateral and minor reverse movement. The fault continues towards the monocline observed near the fold structure, FL-5 (Figure 4.7), which may suggest that the monocline is formed due to the reverse movement along this fault. There are 6 slip data measurements collected from this particular fault (Site-49 and Site-226).

The Fault-5 is located at around 1 km southeast of Sarılar village (Plate 2) between Fault-3 and Fault-4. It also follows their trends, NE-SW, but its southern end is bended to ENE direction. The fault could be followed in the field for about 1.75 km. However no slip data could be extracted from that fault. It is interpreted as a reverse fault with a fault plane dipping towards N.

The Fault-6 is situated at approximately 1.5 km WSW of Sarılar village (Plate 2). It is a reverse fault developed within the cherts of the Miocene Pazar Formation. It brings two different stratigraphic levels side by side. Trend of the fault, which extends for some 1.5 km, is WSW to ENE. Plane of the fault dips towards north with steep dip amounts between 70^0 and 80^0. There is no slip data collected on this fault but the closest site, Site-227, has slip planes trending NW-SE (e.g., $N45^0W/47^0N/55^0W$ - reverse fault).

The Fault-7 is located at around 1 km east of Çalta village. It is situated in the middle of the Miocene outcrop trending NE-SW around Çalta village (Plate 2). It is developed in cherts and clayey/silicified limestones of the Miocene Pazar Formation. The fault is easily distinguished in the field by the steeply dipping (45^0) chert beds along its course, which is in ENE direction. Although no slip data could be obtained from this fault, this fault has normal character and a fault plane dipping at ~75^0 towards south. Dip amount of the chert beds in the up-thrown block reaches up to 80^0.

The Fault-8, located at 750 m southeast of Evci village, at the southwestern corner of the area (Plate 2). The fault is hosted by volcaniclastics / tuffaceous sandstones of the Miocene Pazar Formation. It makes a slight bend but it mainly trends NE-SW. Its fault plane dips towards south at steep dip amounts (~75^0). Dip of the units in the up-thrown block reaches up to 60^0 due to faulting. No slip data could be collected from this fault.

The Fault-9 is located between Alibey village and Çırpan village, at around 2 km east of Alibey village. It starts at the north of Ağa hill and runs towards ENE direction for about 1.5 km. It diminishes close to the northern boundary of the study area (Plates 1 & 2). It is formed within white colored silicified mudstones of the Pazar Formation. Well-preserved slickensides on those competent rock units suggest that the fault is a right-lateral oblique fault with normal dip-slip component. Dip of the fault plane is steep reaching up to 80^0 to south. Since it forms the northern boundary of the Quaternary terrace deposits at this particular locality, it is speculated that their deposition was controlled by the faulting. There are 7 slip measurements from this fault (Site-206 and Site-207).

The Fault-10 is located very close to Çırpan village, at 250 m northwest of the village. This normal fault has a trend in NE-SW direction and a length of some 1.2 km. It is developed in NE-SW trending outcrop of Plio-Quaternary units. It cuts and displaces the units in the normal sense so that a small outcrop (hardly mappable) of Miocene units is exposed in the footwall of the fault (Plates 1 & 2). In that outcrop, there are chert beds having well-preserved slickensides from which the slip data of the fault were collected (Figure 4.14). The fault plane dips gently towards south at dips ranging from 20^0 to 40^0. There are 13 slip measurements taken from this fault (Site-200 and Site-211).

The Fault-11 (Çalta fault) runs across most of the study area in NE-SW direction with a curvilinear trend. The fault is called as Çalta fault. It forms a faulted contact between the Miocene Pazar Formation and the Plio-Quaternary Sinap Formation. The observable length is about 4 km (Plates 1 & 2). Although no slickenside data could be obtained due to brittle and unresistant nature of the units it cuts, it is suggested, based on morphological features and juxtaposition that the fault has a normal sense. The fault plane dips towards north at steep dip amounts ranging from 75^0 to 85^0. Steeply dipping chert beds along the fault can be observed in and around Çalta village.

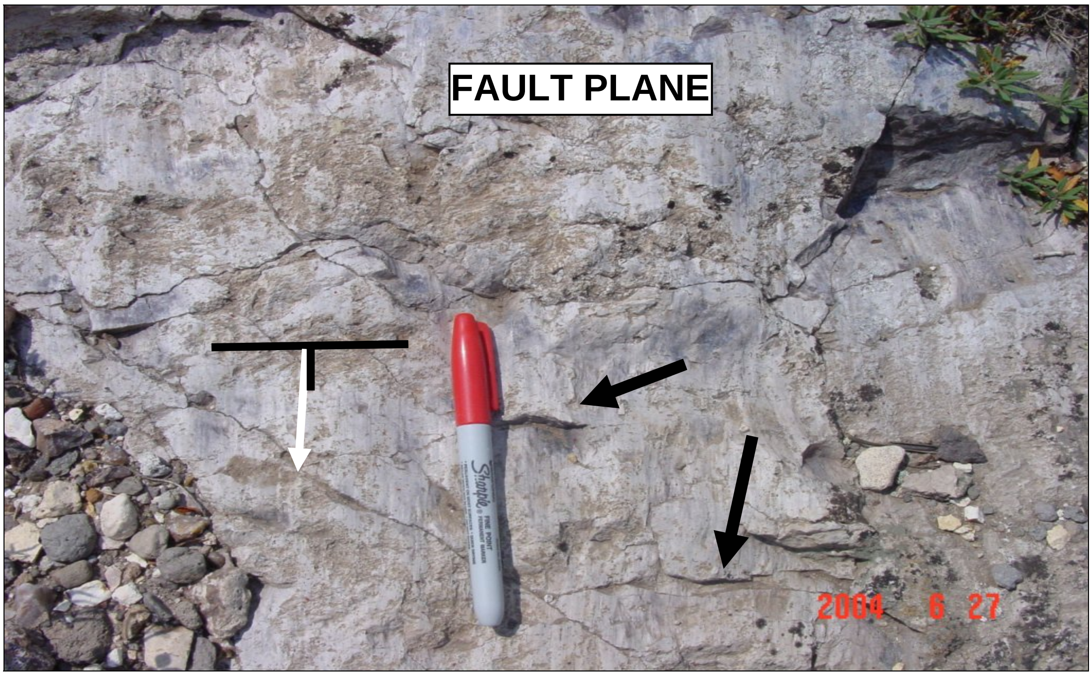

Figure 4.14. Well preserved slickenside of the Fault-10. White arrow shows the slip direction. Black arrows show the chatter marks indicating that the hanging-wall is downthrown (Site-211).

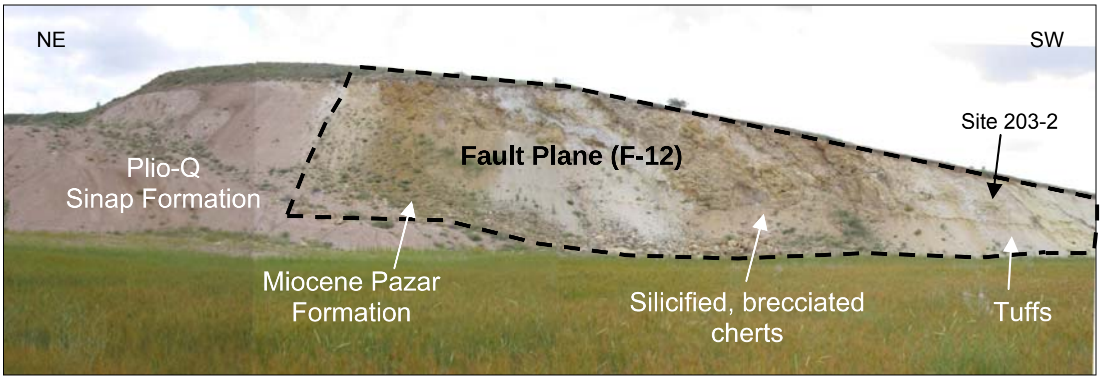

Figure 4.15. The normal faulting between the Plio-Quaternary Sinap and Miocene Pazar formations, Fault-12.

The Fault-12 is one of the best exposed faults in the study area. It is located at 2 km northeast of Evci village (near Beşpınar hill). It is a NE-SW trending normal fault with a length of 500 m. It juxtaposes the altered tuff and cherts of the Miocene Pazar Formation with the pinkish colored clastics of the Plio-Quaternary Sinap Formation (Plates 1 & 2). A brecciated zone in cherts and tuffs is noted along the fault (Figure 4.15). The fault has a plane dipping towards north with dips varying from 40^0 to 60^0. There are only two slip data taken from this fault (Site 203-2).

The Fault-13 is situated near Evci village. It is a normal fault juxtaposing cherts and silicified limestones of the Miocene Pazar Formation with sandstones and conglomerates of the Plio-Quaternary Sinap Formation. Its concave southward curvilinear trend is about 1.2 km long. Its southern portion trends NE-SW near Evci village while it's northern portion trends almost E-W near İstanbul highway (Plates 1 & 2). The fault plane dips towards south. No slip data could be obtained from this fault.

The Fault-14 is located near Sarılar village. It runs in NE-SW direction. Its western continuation could not be followed due to poor outcrops so it was mapped as probable structure. The fault is a boundary fault juxtaposing the Miocene silicified limestones and pinkish colored clastics of the Plio-Quaternary units (Plates 1 & 2). By using that relation the fault is interpreted as southward dipping normal fault. Ther is no record of any slickenside due to soft and unresistant lithologies.

The Fault-15 is located at the southeastern corner of the study area, at 1.25 km north of Karalar village. It has a NE-SW trend and a length of 2 km. It forms a faulted contact between silicified silty limestones of the Plio-Quaternary Sinap Formation and the underlying basement rocks. It is a northward dipping normal fault. No slip data could be obtained from this fault.

The Fault-16 is another fault running across most of the area in NE-SW direction. It is situated between Sarılar and Çalta villages. It has three more or less parallel segments which cut both the Miocene Pazar and Plio-Quaternary Sinap formations, in places, forming their boundary. Its observable length within the study area is about 3 km (Plates 1 & 2). It is chiefly a normal fault with very trivial strike-slip component. Its southeasterly dipping fault plane has steep dip angles reaching up to 85^0. In an outcrop (Site-238) where it cuts the chert beds, 8 slip measurements were collected from well-preserved slickensides.

The Fault-17 is the fault passing through İneköy village in NE-SW direction. It is developed in the Miocene Pazar Formation but cuts through the basement rocks as well (Plates 1 & 2). Even though no slickenline data could be obtained from this fault, it is determined by using field observations.that it is a northwest dipping normal fault with 65^0 dip amounts. Its course extends out of the study area but a length of 1 km was measured within the limits of the study area.

The Fault-18 is a small NE-SW-trending fault at just southeast of İneköy village. It is developed between the Miocene Pazar Formation and the basement rocks. Its length is not more than 500 m. No slip data could be extracted due to the insuitability of the rock units but field relations show that it is a northwesterly dipping normal fault. Dip amount of the fault plane is around 75^0. A brecciated zone in chert beds, which are also steeply dipping due to faulting, was noted.

Fault-19 constitutes the products of the latest tectonic event. It must be the youngest fault in the area since it is developed in Quaternary alluvium exposed at the northwestern part of the study area. It sometimes forms a faulted contact between the alluvium and the Plio-Quaternary Sinap Formation (Plates 1 & 2). Its NE-SW trend could hardly be traced due to the unconsolidated nature of the alluvium. No slip data could be gathered from this fault but it is obvious that the northern block was downthrown as indicated morphologically.

4.4.2. NW-SE-Trending Faults

There are a number of NW-SE-trending faults in the northwestern half of the study area (Plates 1 & 2). Their trends are usually perpendicular to the strikes of the units. They are either oblique-slip (having both strike-slip and dip-slip components) or strike-slip structures. They cut through both the Miocene units (Pazar Formation) and the Plio-Quaternary units (Sinap Formation) laterally displacing some of their boundaries. This suggests that the age of the faulting must be post-Plio-Quaternary.

The Fault-20 is found at just S of Çırpan village. It is trending in NW-SE direction. It could be followed in the field for 800 m. The fault is developed in both the Miocene units and the Plio-Quaternary units cutting and displacing them (Plates 1 & 2). The right-lateral offset of the fault calculated by using the displaced boundaries is around 100 m. There is no slip data from this fault. So the exact character of the fault can not be determined.

The Fault-21 is located at 1.5 km southeast of Çalta village, through the valley between Beşpınar hill and İnönü hill (Plate 2). Similar to Fault-20, this fault also trends in NW-SE and it cuts through the Miocene and the Plio-Quaternary units. Its observable length is around 1.25 km. There is no slip data obtained from this fault.

The Fault-22 was mapped at 500 m north of Evci village (Plate 2). It is developed both in the Miocene and the Plio-Quaternary units, cutting through them nearly at right angles to their strikes. It extends in NNW-SSE direction for about 750 m. Although there is also a left-lateral strike-slip movement, dip-slip movement, which is of normal-type, is more dominated in this fault. It vertically displaces these units more than 5 m, juxtaposing the Plio-Quaternary units with the Miocene units in the outcrop-scale. The fault plane dips towards northeast at 67^0. There is only one slip measurement taken from this fault (Site-220).

The Fault-23 is also located at the Evci area, southwestern corner of the research area (Plate 2). It initiates at ~1 km E of Evci village within the volcaniclastics and cherts of the Miocene Pazar Formation and runs in NNW-SSE direction (i.e. its trend makes 25^0 from the W) cutting through the Plio-Quaternary and the Miocene units nearly at right angles to their strikes. It terminates somewhere at 100 m north of Evci village (Plates 1 & 2). Like Fault-22, this fault also possesses oblique character. Similarly, normal faulting is more dominated over the right-lateral strike-slip movement along this fault. Fault plane is inclined towards southeast with a 70^0 dip. There is only one slip measurement taken from this fault (Site-217 and Site-219). Normal drags observed on the fault cutting across sandstones and conglomerates of the Plio-Quaternary units further confirm the normal character of the structure.

4.4.3. N-S-Trending Faults

Indeed there is only one fault (Fault-24) identified in the study area belonging to this group. It is situated at 2 km northeast of Evci village, close to the highway. It has a trend of N-S to NNE-SSW. It is developed within the Plio-Quaternary pinkish to reddish clayey sandstones and conglomerates (Sinap Formation). Its observable length is around 1 km (Plates 1 & 2). In an outcrop near the highway where the fault is very well exposed, it was observed that the fault cuts through the soil (Figure 4.16 and Figure 4.17). This indicates that it is a Quaternary fault. In this outcrop, it was also observed that the fault plane, which dips towards north, has a listric character with dip amounts changing from 50^0 to 30^0. Vertical offset along this fault was measured as 216 cm. There are 20 slip measurements taken from this fault (Site-204).

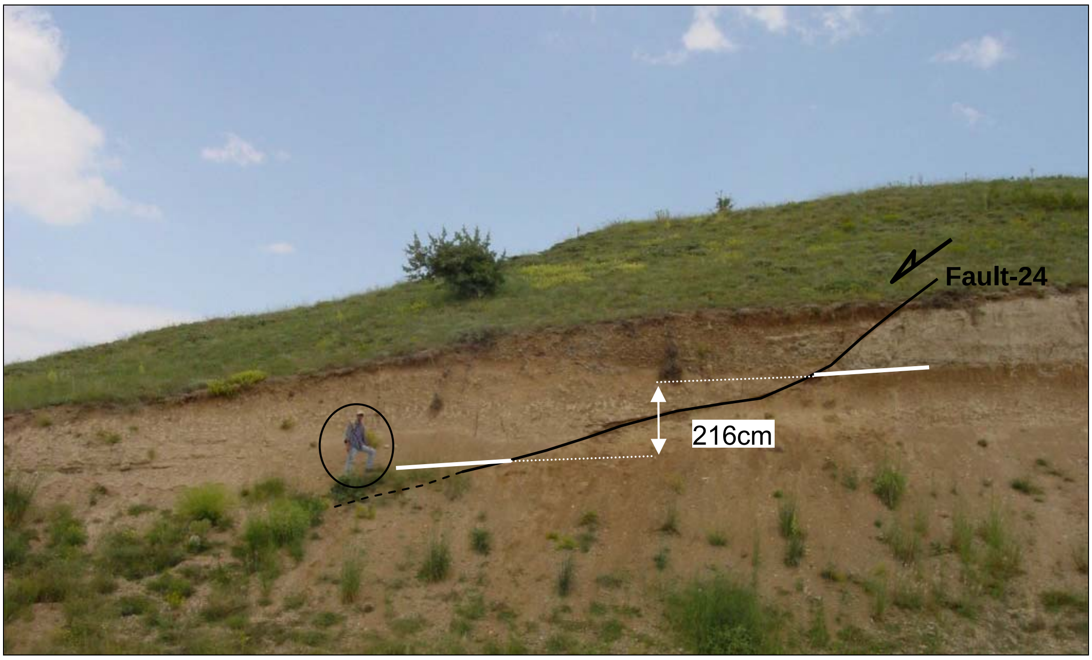

Figure 4.16. The normal fault, Fault-24, having a listric profile in the Sinap Formation. Photo is towards NNE. Note the person (circled) for scale.

Figure 4.17. Close-up view of the Fault-24. Note that it cuts through the soil (hammer at left of the photo for scale, 33-cm long).

4.4.4. Syn-depositional Faults

In a well-exposed outcrop of the Plio-Quaternary units at around 2.5 km northeast of Evci village, a fault set of small- to medium–scale (i.e. outcrop scale) syn-depositional faults was identified (Site-191). Syn-depositional development of those faults is indicated by termination of the faults within sediments, thickness variations in reverse drags and disturbance in the sedimentary bedding planes. So age of the faulting must be coeval with the age of the units, which is Plio-Quaternary. The fault set is composed of N-S to NNW-SS-trending steeply dipping normal faults (60^0 to 85^0). Their profiles usually have an undulating appearance. Dip direction changes from N to S since there are conjugates. As no slip data could be read from the fault surfaces because of the soft and non-clayey nature of the sediments, the exact character of the faults is not clear. But as shown by the normal offsets, the faults interpreted as normal faults (faults with dip-slip components). Offset amounts measured ranges from 6 cm to 23 cm (Figure **4.18** and Figure **4.19**). Some of the syn-depositional faults are re-activated (Figure 4.18).

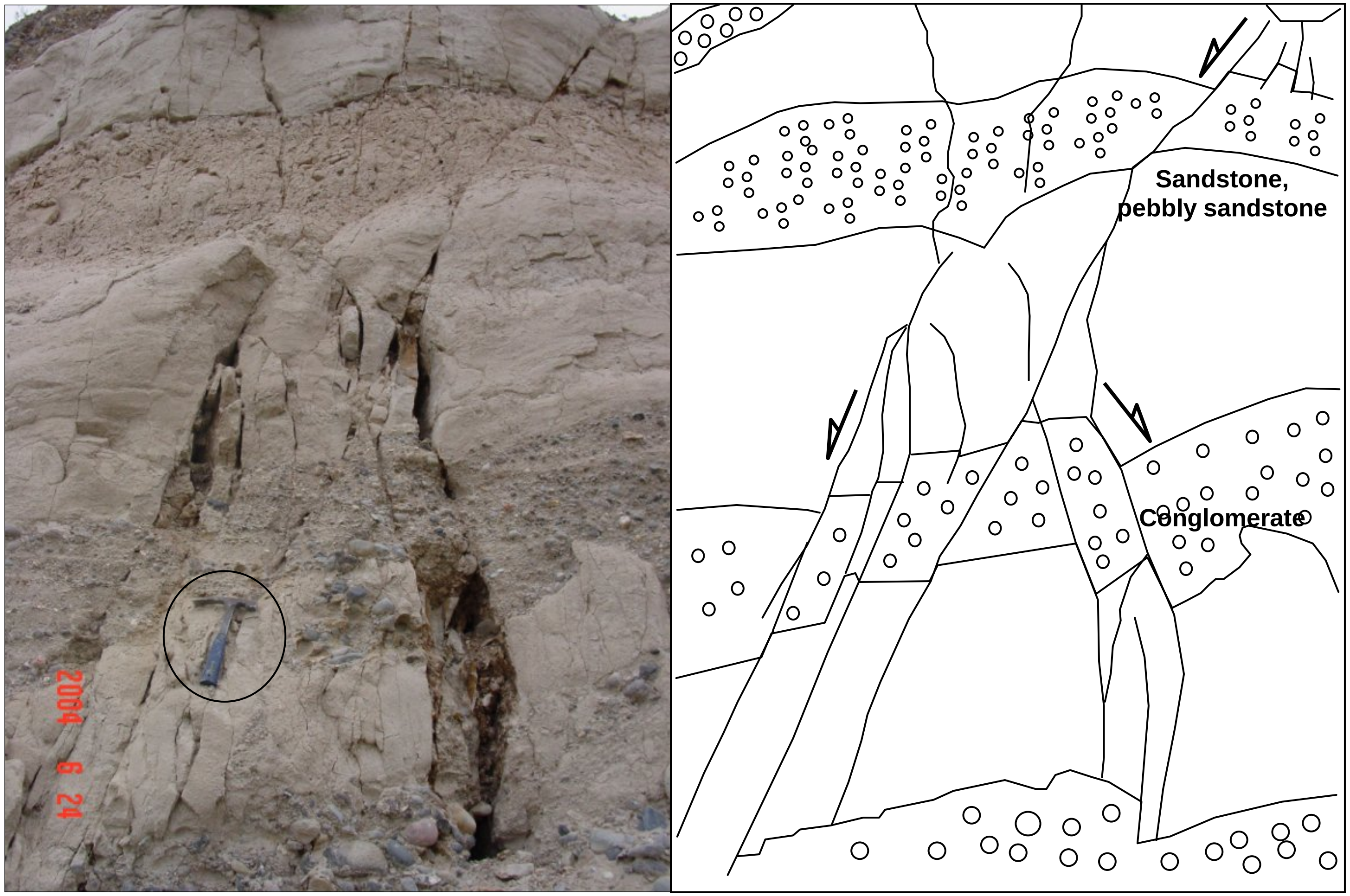

Figure 4.18. Re-activated syn-depositional normal faulting in the Sinap Formation. Location:~2.5 km NE of Evci village (Site-191). Note hammer for scale (33-cm-long).

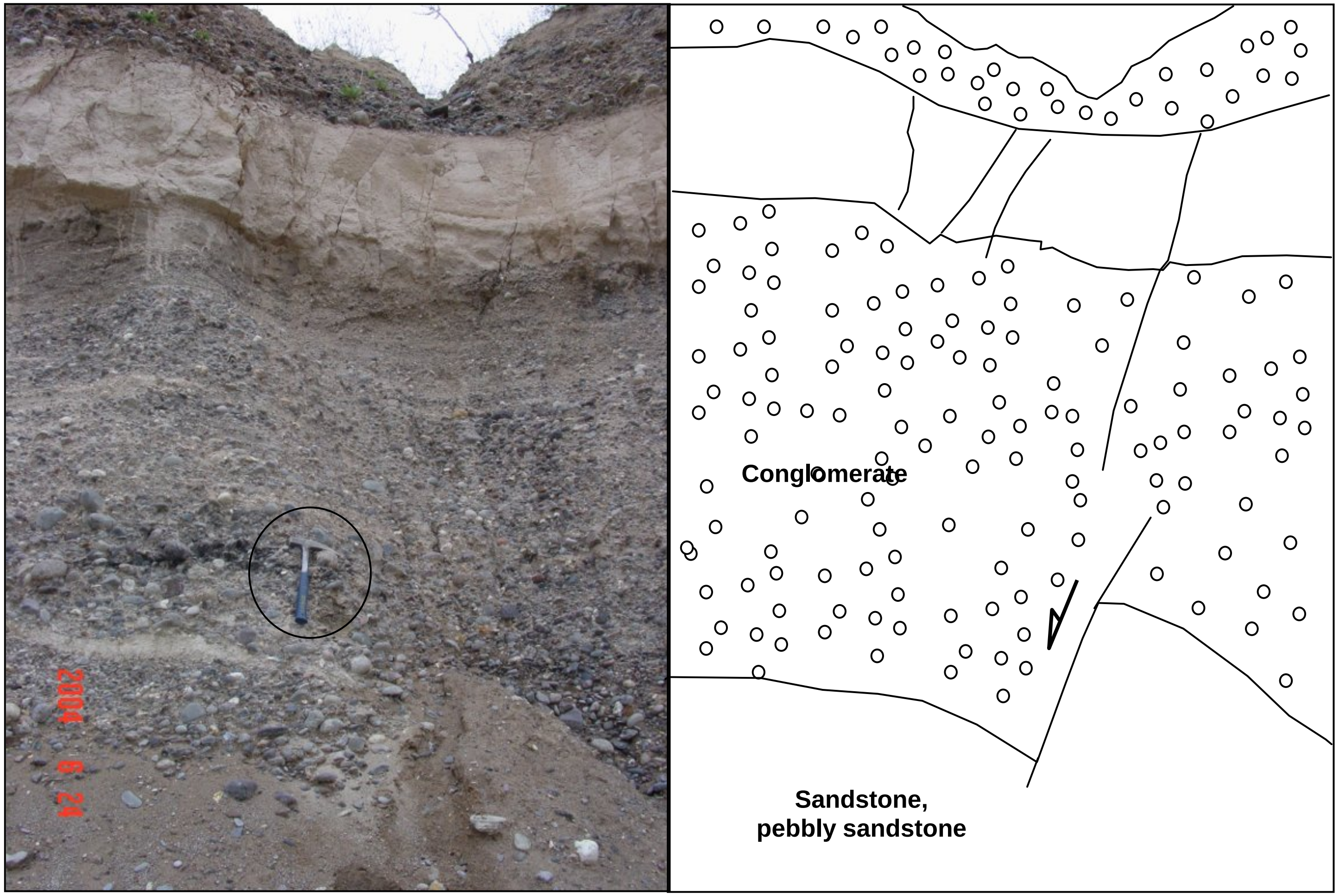

Figure 4.19. Syn-depositional normal faults pinching-out within the sedimentary layers. Location is ~2.5 km NE of Evci village (Site-191).Note hammer for scale (33-cm-long).

4.5. Slip Data Analysis

To be able to differentiate the deformational phases and to calculate the directions of principle stresses acted in the area, 204 slip lineation data were measured at 39 locations (Table 4.2). 24 of those locations are situated on the major faults mapped in the area. Other locations are located on the minor faults in the post-Miocene outcrops. In the places where slip lineation is obscured or not present, only the fault planes were measured (e.g., the site-191). Fault planes together with the slip lineations taken from those sites were drawn on stereonets in order to better visualize variable behaviour of the faults at the sites visited (Figure 4.20). 17 of the fault data are utilized in the determination of deformation history.

Overprinting relations of the slip lines on fault planes are not very common throughout the study area. However prior to running of the data during the collection of slip lineations, it was clearly observed that normal faults cut reverse ones in a number of locations. That means that the normal faulting post-dates the reverse faulting in the research area. Moreover, no compressional movement was observed in any of the faults developed in the Plio-Quaternary outcrops. On the other hand, other faults (N-S-trending faults, NE-SW-trending normal faults) are developed both in the Miocene and the Plio-Quaternary units.

Bearing in mind those geological considerations, the slip data were made ready to run the analysis by using direct inversion method in Angelier's "TENSOR" software (Angelier, 1979; 1984; 1991). Sites with less than 4 slip data were not included in the analysis. The data were grouped so that the populations do not have less than 20 data or more than 60. At the end of the analysis, unfortunately no reliable result for the post-Miocene compressional phase could be obtained as observed in the field. But the results found for

Table 4.2. Table showing the information on the faults having slip data.
M: Miocene; P: Plio-Quaternary; Q: Quaternary.

Site #	Easting	Northing	Lithology	Age of Units	# of Slip Data	Field Observations
1	465750	4452375	Mudstone	M	12	Normal drags on the fault
3	465380	4454538	Mudstone	M	3	Bed parallel slip ($N71^0E/36^0S$)
16	464250	4450750	Mudstone	M	9	1st reverse, 2nd right-lat, 3rd left-lat and 4th is normal faulting
19	464264	4450763	Sandstone	M	1	Northern block is downthrown
22	464123	4450689	Sandstone/ Siltstone	M	4	Monoclinal structure is present
23	464064	4450670	Sandstone/ Siltstone	M	1	Right lateral reverse fault
25	464582	4450832	Cherty Limestone	M	2	Left-lateral strike-slip fault
27	464356	4450818	Cherty Limestone	M	1	Left-lateral strike-slip fault
29	464622	4450848	Chert	M	1	$N42^0W/75\,^0S$ fissures with 27cm aperture
33	466600	4451050	Conglomerate	P	1	Right-lateral strike-slip fault
44	465769	4453146	Tuffaceous Sandstone	M	37	Normal faults offset reverse faults
44/2	465769	4453146	Tuffaceous Sandstone	M	27	Normal faults offset reverse faults
49	464555	4453863	Cherty Limestone	M	5	Monoclinal structure is present
60	460810	4453092	Conglomerate	P	1	Left-lateral strike-slip fault
63	459675	4453825	Chert	M	4	$N60^0W/66^0S$ calcite veins
65	459354	4453882	Conglomerate	P	2	Left-normal oblique fault
66	459392	4453949		P	2	Conjugate faults
68	459303	4454073	Conglomerate	P	1	The fault offsets the soil
80	460605	4457160	Silicified Limestone	M	4	Right-reverse oblique fault
90	460700	4456950	Silicified Limestone	M	10	Left-normal oblique fault
174	465993	4451327	White Limestone	P	2	Left-lateral strike-slip fault
182	460155	4454878	Terrace Conglomerate	Q	1	Southern block is downthrown

Table 4.2 (continued).

Site #	Easting	Northing	Lithology	Age of Units	# of Slip Data	Field Observations
191	460334	4453793	Sandstone	P	10	Syn-depositional faulting, offset ranges from 6 cm to 27 cm
196	462215	4455187	Clayey Limestone	M	4	Left-reverse oblique fault
200	461379	4456827	Chert	M	2	Left-reverse oblique fault
203-2	459675	4453825	Tuff	M	2	A brecciated zone in chert
204	459315	4454066	Conglomerate	P	18	The fault offsets the soil, same as the site-68
206	460551	4457740	Limestone	M	4	Right-normal oblique fault
207	460882	4457758	Silicified Mudstone	M	3	Right-normal oblique fault
211	461382	4456825	Chert	M	10	Faults cut bedding
215	458735	4452588	Siltstone	P	1	Bed-slip normal faulting ($N30^0E/29^0N$)
217	458697	4452690	Sandstone	P	1	Normal drags on the fault
219	458628	4452831	Sandstone	P	1	Southern block is downthrown z-structures are present
220	458476	4452897	Sandstone	P	1	Northern block is downthrown
223	465868	4453281	Tuffaceous Sandstone	M	1	A brecciated layer with sulphur coatings
224	465894	4453306	Claystone	M	2	Left-reverse oblique fault
226	464343	4453795	Chert	M	1	No-slip data
227	462989	4453423	Chert	M	4	The fault forms the boundary between the Miocene & Jurassic limestones
238	464244	4456569	Chert	M	8	Normal faulting

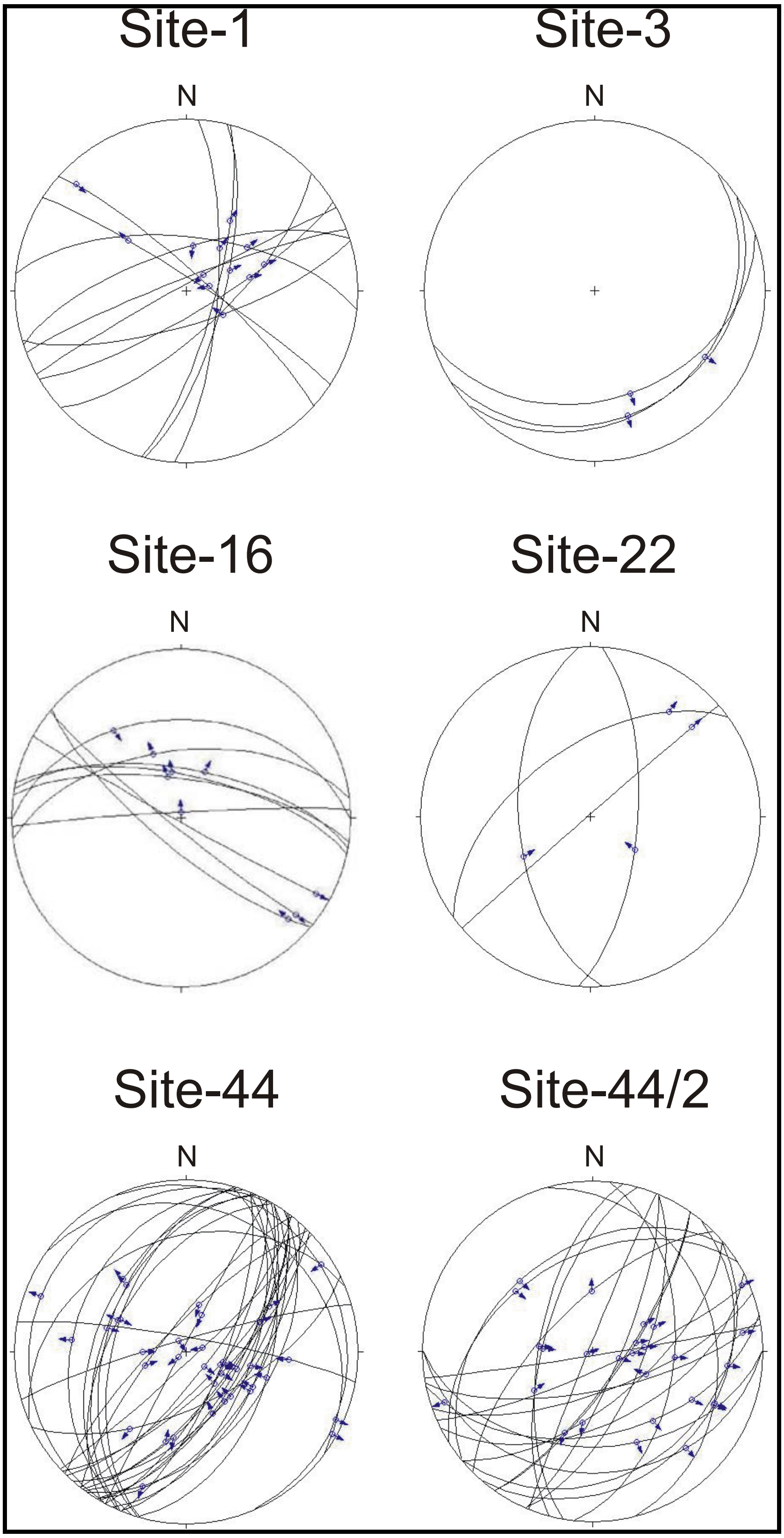

Figure 4.20. Stereonet plots of the faults from which the slip data were gathered. Small arrows on the great circles show movement direction of the hangingwalls.

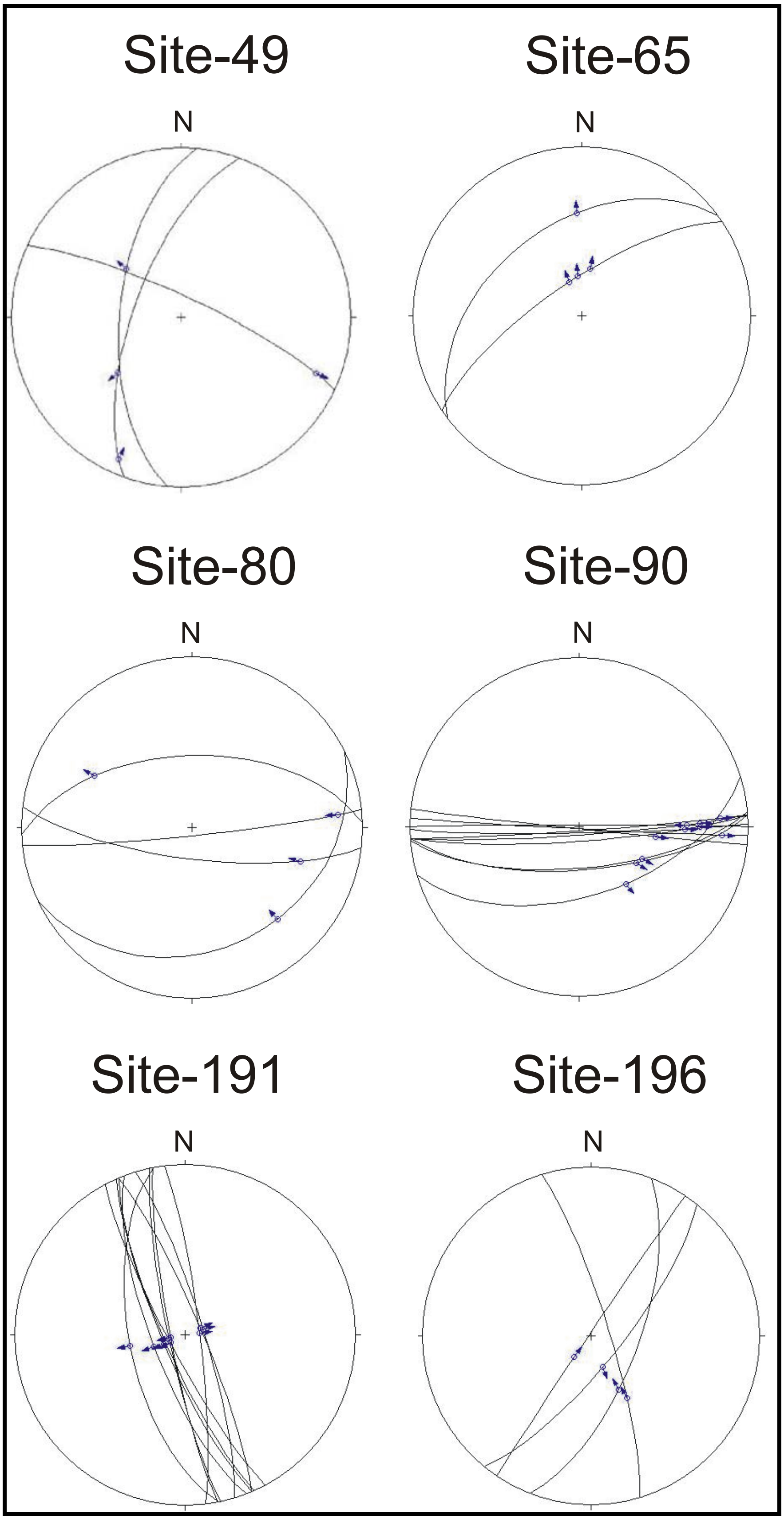

Figure 4.20 (Continued).

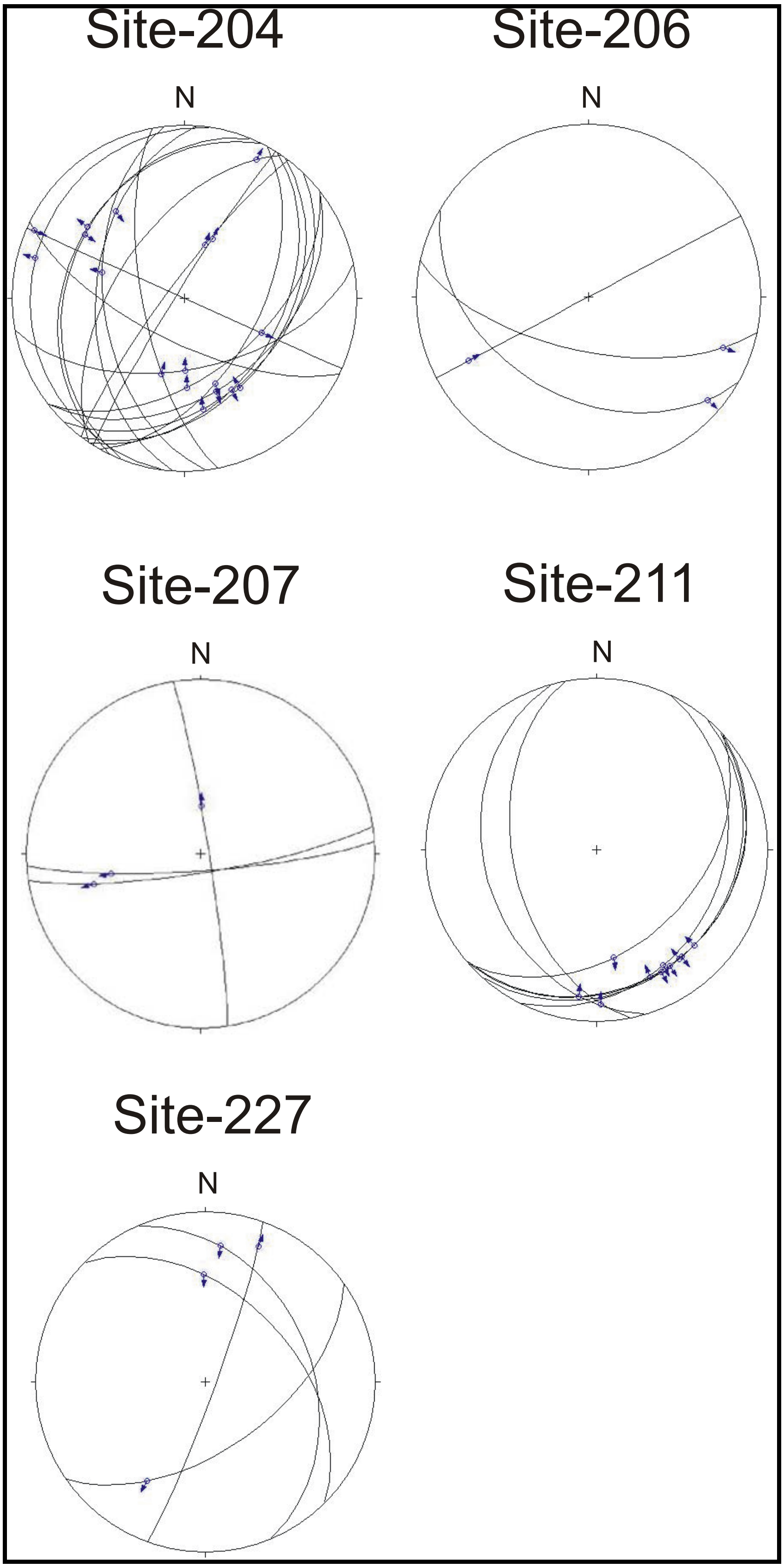

Figure 4.20 (Continued).

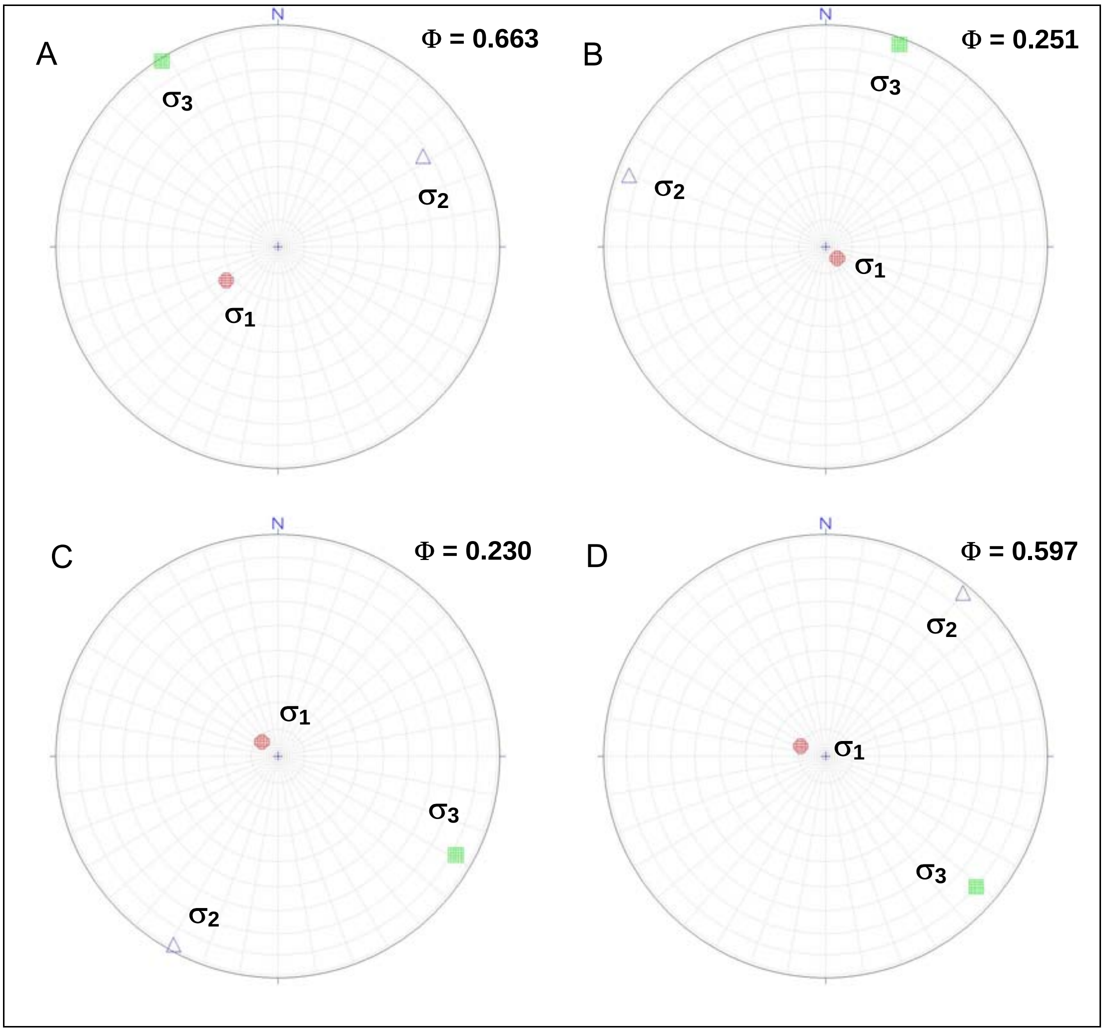

Figure 4.21. Figure showing the stereo-plots of the principle stress directions obtained by analysis of the slip data for the post-Plio-Quaternary extensional phase.

Table 4.3. The table summarizing the slip analysis results

Solution	Φ	σ_1		σ_2		σ_3	
		Trend	Plunge	Trend	Plunge	Trend	Plunge
A	0.663	237^0N	67^0	058^0N	23^0	328^0N	0^0
B	0.251	135^0N	84^0	290^0N	05^0	20^0N	02^0
C	0.230	312^0N	82^0	209^0N	02^0	119^0N	08^0
D	0.597	292^0N	80^0	40^0N	03^0	131^0N	10^0

the post-Pliocene extensional regime are quite reliable. It clearly gives an extension in NW-SE direction. It yielded 4 reliable solutions (Figure 4.21 and Table 4.3).

It is so clear that there is a deformational difference in the intensity and style of deformation. The Miocene Pazar Formation rock units are intensely folded and faulted (Figure 4.22). However, the Plio-Quaternary Sinap Formation rock units are less folded, -where folded, broad open folding is characteristic (Figure 4.9) -, and faulted with well-preserved slickensided fault planes. NW-SE to NNW-SSE compressional regimes acted on the Miocene units during post-Miocene-Pliocene period. This is well-manifested with NE-SW trending, asymmetric-close folds and NE-SW striking reverse faults (Figure 4.13).

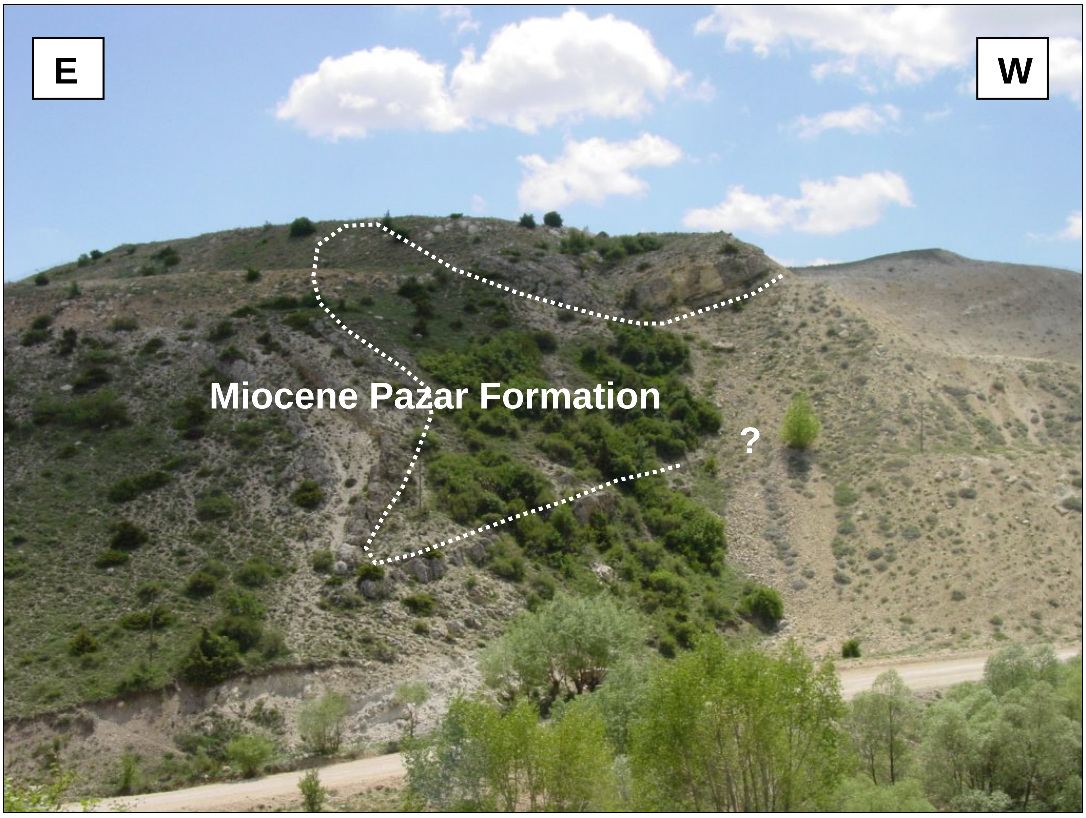

Figure 4.22. Overturned, intensely folded clayey-silicified limestones of the Miocene Pazar Formation indicating post-Late Miocene deformation. (Location: N: 4450847, E:464321)

4.6. Seismicity

In order to understand geologically recent tectonic activities in the study area and its vicinity, some seismic data were obtained from Kandilli Observatory and USGS web sites ("neic.usgs.gov/neis/epic/epic.html"; "www.koeri.boun.edu.tr/depremmuh/default.htm"). They were plotted on the regional map (Figure 1.2) to see the earthquakes falling into the region.

Most of the Ankara province falls into the third and fourth order seismic zone in the seismic map of Turkey. It is generally believed that Ankara is seismically not active and no major earthquake can happen in Ankara. Indeed in the records there are three major earthquakes happened in the close vicinity of Ankara (Orta-Çankırı, 06/06/2000, Mw=6.0; Çerkeş-Gerede, 01/02/1944, Ms=7.4; Ladik-Ilgaz, 26/11/1943, Ms=7.3). Last two earthquakes are located on the major strands of North Anatolian Fault Zone running E-W at the north of the study area. First one is on a major fault bifurcating from North Anatolian Fault Zone in N-S direction. Other past eartquakes are generally small to medium ones ranging in magnitude from Md=2.5 to Md=4.3. Three important ones are; Başbereket-Ayaş, 04/04/1995, Md=4.0, Uruş, 22/08/2000, Md=4.3, and Çamlıdere, 27/02/2003, Md=4.0. The earthquake happened in 1995 near Ayaş, at the SW of the study area, has a focal mechanism solution suggesting normal faulting with a right-lateral strike-slip component (Baran, 1996). The focal mechanism solution It gives a normal faulting with a left-lateral strike-slip component that occurred on a NW-trending NE-dipping fault segment in Peçenek Fault Zone (Kaplan, 2004). However, unlike the other two, Uruş earthquake has a focal solution showing a left-lateral faulting with a reverse component along a NE-striking NW-dipping fault (Kaplan, 2004).

When the regional map (Figure 1.2) surrounding the study area is examined, it is seen that there is one earthquake (1992) of unknown magnitude falling into the study area. It is situated near Evci village. It is important to note the recent seismic activity going on in the study area might be related to the Quaternary normal faulting along the normal faults (Fault-19 and Fault-24) located in southern margin of the İlhan stream.

There are some other small earthquakes (occurred in 1987 and 1992) whose epicenters are located in the middle of the Kazan depression showing a recent activity in the faults bounding the Kazan depression. There is also one earthquake located near Çeltikçi town indicating the recent faulting in the Çeltikçi depression.

CHAPTER 5

DISCUSSION

The results of the thesis are summarized below with discussions on them. The results are categorized as stratigraphy results, structural geology results, slip analysis results and geodynamic evolution.

5.1. Results of the Stratigraphy

1) Two main Neogene rock formations extensively cropping out were distinguished; the Late Miocene Pazar Formation and unconformably overlying the Plio-Quaternary Sinap Formation.
2) The Late Miocene Pazar Formation is mainly composed of bedded cherts, silicified clayey limestones, silicified marls and volcaniclastics. The formation represents a deposition in a stagnant, fresh water lacustrine environment.
3) A mammalian fossil was found in the stratigraphically lower levels of the Pazar formation. Age of the sample is determined by lithostratigraphically correlating with the nearby type locality to be in MN-9 to MN-13 time interval in the mammalian time scale for Europe (11.1 Ma to 6.8 Ma; Agusti et al., 2001). However, documented paleontological data reveals an age of Late Miocene (Ozansoy 1961; Tekkaya et al., 1973; 1974; Şen and Rage, 1979).
4) Volcanism in the area coeval with the deposition of the Pazar Formation especially at the lower parts of the Miocene succession. Hydrothermal activity, which may have a close relation with the

Miocene volcanism, has affected the units of Pazar Formation and Sinap Formation.

5) The Plio-Quaternary Sinap Formation is mainly composed of sandstones/siltstones/conglomerates, and clayey limestones and kaolinites. They all possess features depicting a fluvio-lacustrine environment.
6) There are four unconformities identified in the study area in the interval of Late Miocene to Quaternary.

5.2. Results of the Structural Geology Analysis

Results on the structural geology analysis based on the analysis carried out on bedding planes and faults.

Results of the analysis carried out on bedding planes:

1) The analysis of 157 dip-strike measurements from the Late Miocene Pazar Formation shows that the units have a general strike varying from $N40^0E$ to $N60^0E$.
2) The analysis of 55 dip-strike measurements from the Plio-Quaternary Sinap Formation shows that the units have a wide range of bedding attitudes ($N40^0E$ to $N50^0E$) with average attitude of $N45^0E$.
3) The Pazar Formation is observed to be relatively more folded than the Sinap Formation. There is no preferred vergence of the folds but they tend to be asymmetrical with vergences either in NW or SE direction. Fold analysis on the dip-strike measurements indicates two dominant bedding planes; $N45^0E/27^0SE$ and $N60^0E/16^0NW$. Common trend of the fold axes in the formation was calculated as striking in $N46^0E$ direction.
4) The Sinap Formation has more gently dipping symmetrical open folds. Fold analysis on the dip-strike measurements indicates two dominant

bedding planes; N45^{0}E/17^{0}SE and N35^{0}E/19^{0}NW. Common trend of the fold axes is N40^{0}E direction.

Results of the analysis carried out on faults:

1) Most of the fault structures strike in NE-SW direction with other NW-SE and N-S trending ones. There are four groups of faults; 1) NE-SW trending faults, 2) NW-SE trending faults, 3) N-S trending normal faults, and 4) syn-depositional faults.
2) It was clearly observed that normal faults cut reverse ones. The normal faulting post-dates the reverse faulting in the research area. On the other hand, other faults (N-S trending faults, NE-SW trending normal faults) cross-cuts both Miocene and Plio-Quaternary units.
3) Moreover no reverse faulting was observed in the Plio-Quaternary rock units.
4) Syn-depositional faults with trends in N-S to NNW-SSE directions were discovered in the Sinap Formation. Syn-sedimentary development of those faults is indicated by termination of the faults within sediments, thickness variations in beds along reverse drags and disturbance in the sedimentary beds. Therefore the age of N-S to NNW-SSE trending normal faulting must be coeval with the age of the units, which is Plio-Quaternary.
5) One very young fault with fault striae data (Fault-24) was identified within the limits of the research area. Since the fault cuts the soil or Quaternary alluvium, they are thought to be products of recent tectonic activity, which might be still going on in the study area where created earthquakes.

5.3. Results on the Slip Analysis:

Taking geological considerations and field observations into account, it can be said that the compressional regime that affected only Miocene units has been most probably caused by almost N-S-directed compressional forces. It is reflected by NE-SW-trending reverse faults with left lateral strike slip components (e.g. Fault-3). Although there are open folds observed within the Plio-Quaternary units, no compressional features were noted in them. Extensional regime onsets firstly in E-W direction during the Plio-Quaternary as reflected by almost N-S-directed syn-depositional normal faults in the Plio-Quaternary units. Then the extension direction changes to NW-SE in the post-Plio-Quaternary as indicated by NE-SW-trending normal faults cutting the Plio-Quaternary units. Analysis of slip measurements related to this phase yielded reliable stress directions. Later on, during post-Plio-Quaternary, the extension direction becomes WNW-ESE. And the last extensional period, which might be still going on, is represented by NW-SE-directed extension, which caused the formation of youngest NE-SW-trending normal faults cross-cutting N-S directed normal faults.

The slip and field survey analysis partially conformable with the previous workers approaches. The NW-SE to N-S compression during the post-Late Miocene – Early Pliocene is well-recorded by various workers and it is linked to the initiation on the North Anatolian Fault at north (Yağmurlu et al., 1988; Toprak et al., 1996; Gökten et al., 1988; 1996; Yürür et al. 2002) or to the stress regime changes due to progressive collision (Koçyiğit, 1991; 1992; Koçyiğit et al., 1995). The post-Late Miocene – Early Pliocene NW-SE compression is well-recorded in the study area too. However, there is no record of compression during the post-Plio-Quaternary period (post-Pliocene N-S compressional period) in the study area as proposed (Gökten et al., 1988; Koçyiğit, 1991; 1992; Koçyiğit et al., 1995; Yürür et al 2002). This period is the time of almost NW-SE extensional period in the study area.

5.4. Discussion on the post-Miocene Deformation (Post-Miocene Geodynamic Evolution of the Region)**:**

The accreted İzmir-Ankara-Erzincan suture belt and Galatian Volcanic Province resulted in the uplift of the northern Central Anatolian terrain during post-Eocene (Şengör and Yılmaz, 1981).

The Miocene basins developed on this complex where Eocene marine basins, imbricate piles of various tectonic slices of Cretaceous North Anatolian ophiolitic mélange, Paleozoic-Triassic metamorphics and Triassic Karakaya complex are amalgamated into a single mass.

During Miocene, the Pazar Formation began to deposit in a fresh water lacustrine environment over the accreted mass with coeval Neogene Galatian volcanism. The Galatian volcanism took place in two distinct phases during Early to Late Miocene (Keller et al., 1992; Wilson et al., 1997; Tankut et al., 1998; Adıyaman et al., 2001; Koçyiğit et al., 2003). The volcaniclastic products from the nearby vents have been deposited intermittently with clastics in the lake environment during Miocene (Türkecan et al., 1991; Gökten et al., 1996; Toprak et al., 1996). Moreover, hydrothermal activity that may be related with the volcanism has caused the deposition of widespread cherts and travertines.

Under the affect of NW-SE-directed compressional forces acted during post-Miocene (Gökten et al., 1988; Koçyiğit, 1992; Koçyiğit et al., 1995) before the deposition of the Sinap Formation, the units of Pazar Formation were tilted and folded. The NE-SW folding, NE-SW-striking low-angle reverse faults and high-angle strike-slip faults with reverse dip-slip component are the fingerprints of the NW-SE compressional regime in the area.

The Neogene sequence evolution within the GVP basins is somehow different than the study area where the Miocene to Pliocene sedimentation is continuous in the GVP Neogene basins (Toprak et al., 1996).

During Pliocene times, the units of Sinap Formation started to deposit in an alluvial-fluvial to fresh water lacustrine environments. The Pliocene units unconformably overlie the pre-existing rock units under almost E-W directed extension. The area has undergone subsequent uplift and erosion during post-Pliocene. By the onset of extensional tectonics in the area, NE-SW trending normal faults has been developed cross-cutting and displacing both the Pazar and Sinap Formations under NW-SE to N-S directed extension. Upthrown blocks were eroded and Quaternary terrace deposits covering some of today's hill tops extensively covers the area and lately uplifted with normal faulting resulting from NW-SE to N-S directed extension. Consequently, most of the today's configuration of the area has been established during this period.

CHAPTER 6

CONCLUSIONS

Under the light of above mentioned results obtained by this study and the evaluations performed, following conclusions can be reached;

1) Study area is located at the southeast of Galatian Volcanic Province and north of İzmir-Ankara-Erzincan Suture belt, a place where fluvial to fresh water lacustrine systems covered large areas with coeval volcanic activity during the Miocene-Pliocene. It might be possible that this lake system was somehow connected with the coexisting Beypazarı – Çayırhan – Ayaş basins during Miocene-Pliocene.
2) Two main Neogene rock formations extensively cropping out were distinguished; the Late Miocene Pazar Formation and unconformably overlying the Plio-Quaternary Sinap Formation
3) There are four unconformities identified in the study area in the interval of Late Miocene to Quaternary.
4) The Pazar Formation is observed to be relatively more folded than the Sinap Formation. There is no preferred vergence of the folds but they tend to be asymmetrical with vergences either in NW or SE direction.
5) There are four groups of faults; 1) NE-SW trending faults, 2) NW-SE trending faults, 3) N-S trending normal faults, and 4) syn-depositional faults.
6) It was clearly observed that normal faults cut the reverse ones. The normal faulting post-dates the reverse faulting in the research area.
7) Moreover no reverse faulting was observed in the Plio-Quaternary rock units.

8) Syn-depositional faults with trends in N-S to NNW-SSE directions were discovered in the Sinap Formation. Syn-sedimentary development of those faults is indicated by termination of the faults within sediments, thickness variations in beds along reverse drags and disturbance in the sedimentary beds. Therefore the age of N-S to NNW-SSE-trending normal faulting must be coeval with the age of the units, which is Plio-Quaternary.
9) One very young fault with fault striae data cross-cuts the soil or Quaternary alluvium, they are thought to be products of recent tectonic activity, which might be still going on in the study area where earthquakes created.
10) Basically three tectonic phases are differentiated as ;
    a. almost N-S-directed compression during post-Miocene,
    b. E-W-directed extension during Pliocene, and
    c. NW-SE to WNW-ESE-directed extension during post-Plio-Quaternary.

Collectively, post-Miocene compression is followed by a regionally continuous extension from Pliocene to Quaternary. The Plio-Quaternary is the time of initiation of continuous extension operating in the region.

REFERENCES

Ach J. A., 1982, The Petrochemistry of the Ankara Volcanics, Central Turkey, MSc Thesis, State University of New York at Albany, USA, 148 pages.

Adıyaman, Ö., Chorowich, J., Arnaud, O. N., Gündoğdu, M. N, and Gourgaud, A., 2001, Late Cenozoic tectonics and volcanism along the North Anatolian Fault: new structural and geochemical data, Tectonophysics, 338, 135-165.

Agusti, J., Cabrera, L., Garces, M., Krijgsman, W., Oms, O., and Pares, J. M., 2001, A calibrated mammal scale for the Neogene of Western Europe. State of the art, Earth-Science Reviews, 52, 247-260.

Akyol, E., 1968, Ankara-Kızılcahamam, Çeltikçi civarında bulunan kömür zuhurlarının 1/25000 ölçekli detay jeolojik etüdü hakkında rapor, MTA, Report no. 4405, 14 pages.

Akyürek, B., Bilginer, E., Akbaş, B., Hepşen, N., Pehlivan, S., Sunu D., Soysal Y., Değer, Z., Çatal E., Sözen, B., Yıldırım, H., and Hakyemez, Y., 1984, Ankara-Elmadağ-Kalecik dolayının temel jeolojik özellikleri, Jeoloji Mühendisliği Bulletin, 20, 21-46.

Angelier, J., 1979, Determination of the mean principal directions of stresses for a given fault population, Tectonophysics, 56, T17-T26.

Angelier, J., 1984. Tectonic analysis of fault slip data sets. Journal of Geophysical Research, 80, 5835–48.

Angelier, J., 1991. Inversion of field data in fault tectonics to obtain regional stress. III: A new rapid direct inversion method by analytical means. Geophysical Journal International, 103, 363–76.

Baran, B., 1996, The Seismotectonics of the western part of Ankara, MSc Thesis, Ankara University, Ankara (Turkey), 52 pages.

Boggs, S. Jr., 1995, Principles of Sedimentology and Stratigraphy, 2nd edition, Printice Hall, 328-340.

Bozkurt, E., 2001, Neotectonics of Turkey – a synthesis, Geodinamica Acta, 14, 3-30.

Burtman, V. S., 1994, Meso-Tethyan oceanic sutures and their development, Tectonophysics, 234, 305-327.

Demirci C. Y., 2000, Structural Analysis in Beypazarı-Ayaş-Kazan-Peçenek Area, NW of Ankara (Turkey), PhD Thesis, Middle East Technical University, Ankara, 178 pages.

Erdoğan, B., 1990, Tectonic Relations Between İzmir-Ankara Zone and Karaburun Belt, MTA Bulletin, 110, 1-15.

Erol, O., 1951, Ayaş Dağları ve Mürted Ovasının Kuzey Bölümü Hakkında rapor, MTA, Report no. 2456, 28 pages.

Erol, O., 1954, Ankara ve Civarının Jeolojisi Hakkında rapor, General Directorate for Mineral Research and Exploration (MTA), Report no. 2491, 238 pages.

Erol, O., 1955, Köroğlu-Işık dağları volkanik kütlesinin orta bölümleri ile Beypazarı-Ayaş arasındaki Neojen havzasının jeolojisi hakkında rapor, MTA, Report no. 2279, 43 pages.

Erol, O., 1961, Orogenic phases of the Ankara region, T.J.K. Bulletin, 7, 57-85.

Erol, O., 1993, Ankara yöresinin jeomorfolojik gelişimi: A. Suat Erk Jeoloji Simpozyumu Bildirileri, 25-35.

Gökten, E., Kazancı, N., and Acar, Ş., 1988, Ankara kuzeybatısında (Bağlum-Kazan arası) geç Kretase-Pliyosen serilerinin stratigrafisi ve tektoniği, MTA Bulletin, 108, 69-81.

Gökten, E., Özarksoy, V., and Karakuş, K., 1996, Tertiary volcanic and tectonic evolution of the Ayaş-Güdül-Çeltikçi region, Turkey, International Geology Review, 38, 926-934.

Göncüoğlu, M. C., Turhan, N., Şentürk, K., Özcan, A., Uysal, Ş., and Yalınız, M. K., 2000, A geotraverse across northwestern Turkey: tectonic units of the Central Sakarya region and their tectonic evolution: Tectonics and Magmatism in Turkey and the Surrounding Area, Geological Society, London, Special Publications No.173, Bozkurt, E., Winchester, J. A., and Piper J. D. A. (eds), 173, 139-161

Gürbüz, M., 1981, İnönü (KB Ankara) Orta Miosendeki Hemicyon sansaniensis (Ursidae) türünün tanımlanması ve stratigrafik yayılımı, T.J.K. Bulletin, 24, 2, 85-90.

Kaplan, T., 2004, Seismicity of the Ankara Region and a Case Study in Uruş Area, MSc Thesis, Middle East Technical University, Ankara (Turkey), 84 pages.

Kazancı, N., and Gökten, E., 1988, Lithofacies features and tectonic environments of the continental Paleocene volcaniclastics in Ankara region, Middle East Technical University Journal of Pure and Applied Sci., 21, 1-3, 271-282.

Keller, J., Jung, D., Eckhard, F., J., and Kreuzer, H., 1992, Radiometric ages and chemical characterization of the Galatean andesite massif, Pontus, Turkey, Acta Vulcanologica, 2, 267-276.

Ketin, İ., 1966, Tectonic units of Anatolia: MTA Bulletin, 66, 23-34.

Koçyiğit, A., 1991a, Changing Stress Orientation in Progressive Intracontinental Deformation as Indicated by the Neotectonics of the Ankara Region (NW Central Anatolia), TAPG Bulletin, 3/1, 43-55.

Koçyiğit, A., 1991b, An example of an accretionary forearc basin from northern Central Anatolia and its implications for the history of subduction of Neo-Tethys in Turkey: Geol. Soc. of America Bulletin, 103, 22-36.

Koçyiğit, A., 1992, Southward-vergent imbricate thrust zone in Yuvaköy: A record of the latest compressional event related to the collisional tectonic regime in Ankara-Erzincan Suture Zone, TAPG Bulletin, 4/1, 111-118.

Koçyiğit, A., Özkan, S. and Rojay, B., 1988, Examples from the Forearc Basin Remnants at the active Margin of Northern Neo-Tethys; Development and Emplacement Ages of the Anatolian Nappe, Turkey, Middle East Technical University Journal of Pure and Applied Sci., 21, 1-3, 183-210.

Koçyiğit A., Türkmenoğlu A., Beyhan, A., Kaymakçı, N., and Akyol, E., 1995, Post-Collisional Tectonics of Eskişehir-Ankara-Çankırı Segment of İzmir-Ankara-Erzincan Suture Zone (IAESZ): Ankara Orogenic Phase, TAPG Bulletin, 6/1, 69-86.

Koçyiğit, A., Winchester, J. A., Bozkurt, E., and Holland, G., 2003, Saraçköy Volcanic Suite: implications for the subductional phase or arc evolution in the Galatean Arc Complex, Ankara, Turkey, Geological Journal, 38, 1-14.

Ozansoy, F., 1961, Ankara Bölgesi Fauna Teakubu Etüdünün Esaslı Sonuçları, M.T.A Bulletin, 56, 86-95.

Öngür, T., 1976, Kızılcahamam, Çamlıdere, Çeltikçi, Kazan dolayının jeoloji durumu ve jeotermal enerji olanakları, MTA, Report no. 3273, 34 pages.

Platzman, E. S., Tabirdamaz, C., and Sanver, M., 1998, Neogene anticlockwise rotation of central Anatolia (Turkey): preliminary paleomagnetic and geochronological results, Tectophysics, 299, 175

Piper, J. D. A., Tatar, O., and Gürsoy, H., 1997, Deformational behaviour of continental lithosphere deduced form block rotations across the North Anatolian fault zone in Turkey, Earth and Planetary Science Letters, 150, 191-203.

Sickenberg, O., and Tobien, H., 1971, New and lower Quaternary vertabrate faunas in Turkey, Newsl. Stratigr., 1, 3, 51-61.

Stchepinsky V., and Lahn E., 1941, Ankara-Çankırı-Gerede Arasındaki Mıntıka Hakkında Rapor, MTA, Report no. 1312.

Süzen, M. L., 1996, Lacustrine mineral facies of the Neogene Pelitçik Basin (Galatean Volcanic Province), MSc Thesis, Middle East Technical University, Ankara, 106 pages.

Şen, Ş., and Rage, J. C., 1979, Çalta (Ankara) Pliyosen Omurgalı Faunası, T.J.K. Bulletin, 22, 1, 155-160.

Şengör, A. M. C., 1979, Mid-Mesozoic closure of Permo-Triassic Tethys and its implications: Nature, 279, 590-593.

Şengör, A. M. C., and Yılmaz, Y., 1981, Tethyan evolution of Turkey: a plate tectonic approach: Tectonophysics, 75, 181-241.

Şengör, A. M. C., Görür, N., and Şaroğlu, F., 1985, Strike-slip Deformation, Basin Formation and Sedimentation: The Society of Economic Paleontologists and Mineralogists, Special Publication No.37

Tankut, A., Wilson, M., and Yihunie, T., 1998, Geochemistry and tectonic setting of Tertiary volcanism in the Güvem area, Anatolia, Turkey: Journal of Volcanology and Geothermal Research, 85, 285-301.

Tankut, A., Akiman, O., Türkmenoğlu, A., Güleç, N., Göker, T. T., 1990, Tertiary volcanic rocks in Northwest-Central Anatolia, In IESCA 1990 Proceedings 2, Savaşçın, Y., Eronat, A.H., (eds)., 450–466.

Tatlı, S., 1975, Kızılcahamam Doğu Alanının Jeolojisi ve Jeotermal Enerji Olanakları, MTA, Report no. 5749, 42 pages.

Tekkaya, İ., 1973, Orta Sinaptaki Yeni Bir Gazella Türü, MTA Bulletin, 80, 113-136.

Tekkaya, İ., 1974a, The Bovidae fauna of middle Sinap of Turkey, T.J.K. Bulletin, 17, 1, 173-186.

Tekkaya, İ., 1974b, A new species of Tortonian Anthropoid (primate, mammalia) from Anatolia, MTA Bulletin, 83, 148-165.

Toprak, V., Savaşçın Y., Güleç, N., and Tankut, A., 1996, Structure of the Galatean volcanic province. International Geology Review, 38, 747-758.

Turgut, T., 1978, Kızılcahamam (Ankara) – Çeltikçi ve Çamlıdere Neojen havzalarının linyit olanakları, MTA, Report no. 6173, 20 pages.

Türkecan, A., Hepşen, N., Papak, İ., Akbaş, B., Dinçel, A., Karataş, S., Özgür, İ.B., Akay, E., Bedi, Y., Sevin, M., Mutlu, G., Sevin, D., Ünay, E., ve Saraç, G., 1991, Seben-Gerede (Bolu)- Güdül- Beypazarı (Ankara) ve Çerkeş- Orta-Kurşunlu (Çankırı) yörelerinin (Köroğlu Dağları) jeolojisi ve volkanik kayaçların petrolojisi, MTA, Report no. 9193, 118 pages.

Türkünal, M., 1958, Note on some lower Cretaceous ammonites from Karalar köyü, northwest of Ankara, MTA Bulletin, 50, 75-79.

Wilson, M., Tankut, A., and Güleç, N., 1997, Tertiary volcanism of the Galatia province, north-west Central Anatolia, Turkey, Lithos, 42, 105-121.

Yağmurlu, F., Helvacı, C., İnci, U., and Önal, M., 1988, Tectonic characteristics and structural evolution of the Beypazarı and Nallıhan Neogene basin, Central Anatolia, METU Journal of Pure and Applied Sciences, 21, 1-3, 127-143.

Yürür, M. T., Temel, A., and Köse, O., 2002, Evidences of Extensional Tectonics at the Southern Boundary of the Galatean Volcanic Province, NW Central Anatolia, Geological Bulletin of Turkey, 45, 1, 85-98.

PLATE 1

GEOLOGICAL MAP OF THE AREA BETWEEN KARALAR AND ALIBEY VILLAGES (KAZAN-ANKARA)

by
Aykut KARACA

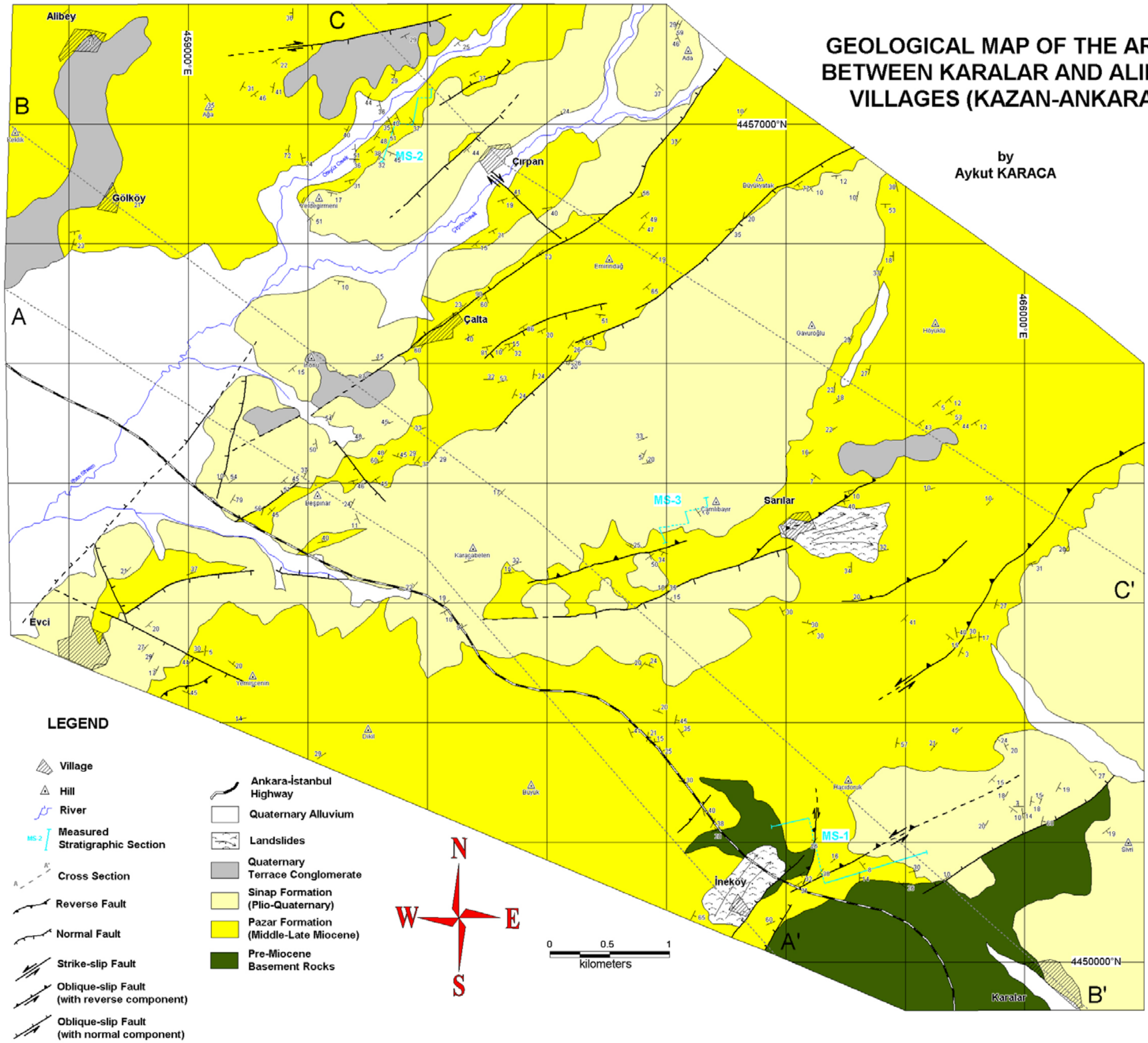

PLATE 2

STRUCTURAL MAP OF THE AREA BETWEEN KARALAR AND ALIBEY VILLAGES (KAZAN-ANKARA)

by
Aykut KARACA

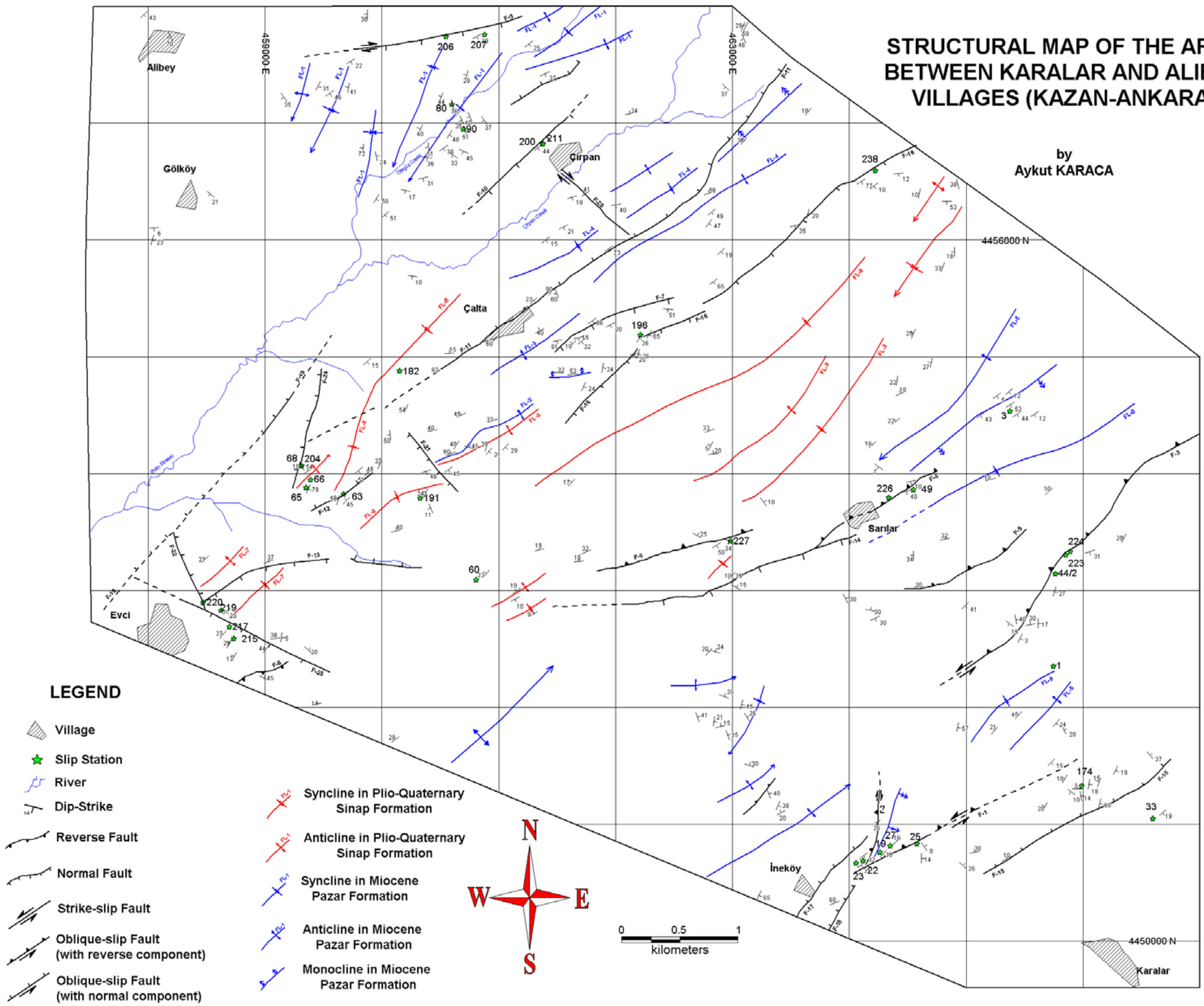

LEGEND

Plate 3. Cross Sections